# Innovative Coal Solids-Flow Monitoring and Measurement Using Phase-Doppler and Mie Scattering Techniques

**Type of Report: Final Technical Report**

**Report Period End Date: 01/19/2010**

**Principal Author(s): Dr. Stephen Seong Lee**

**Date Report was issued: 01/19/2010**

**DOE Grant Number: DE-FG26-06NT42743**

**Name and Address of Submitting Organization:**
**Morgan State University**
**School of Engineering**
**1700 East Cold Spring Lane**
**Baltimore, MD 21251**

## DISCLAIMER

## ABSTRACT

Fuel flow to individual burners is complicated and difficult to determine on coal fired boilers, since coal solids were transported in a gas suspension that is governed by the complex physics of two-phase flow. The objectives of the project were the measurements of suspended coal solids-flows in the simulated test conditions. Various extractive methods were performed manually and can give only a snapshot result of fuel distribution. In order to measure particle diameter & velocity, laser based phase-Doppler particle analyzer (PDPA) and particle image velocimetry (PIV) were carefully applied. Statistical methods were used to analyze particle characteristics to see which factors have significant effect. The transparent duct model was carefully designed and fabricated for the laser-based-instrumentation of solids-flow monitoring (LISM).

The experiments were conducted with two different kinds of particles with four different particle diameters. The particle types were organic particles and saw dust particles with the diameter range of 75~150 micron, 150~250 micron, 250~355 micron and 355~425 micron. The densities of the particles were measured to see how the densities affected the test results.

Also the experiment was conducted with humid particles and fog particles. To generate humid particles, the humidifier was used. A pipe was connected to the humidifier to lead the particle flow to the intersection of the laser beam. The test results of the particle diameter indicated that, the mean diameter of humid particles was between 6.1703 microns and 6.6947 microns when the humid particle flow was low. When the humid particle flow was high, the mean diameter was between 6.6728 microns and 7.1872 microns. The test results of the particle mean velocity indicated that the mean velocity was between 1.3394 m/sec and 1.4556 m/sec at low humid particle flow. When the humid particle flow was high, the mean velocity was between 1.5694 m/sec and 1.7856 m/sec.

The Air Flow Module, TQ AF 17 and shell ondina oil were used to generate fog particles. After the oil was heated inside the fog generator, the blower was used to generate the fog. The fog flew

along the pipe to the intersection of the laser beam. The mean diameter of the fog particles was 5.765 microns. Compared with the humid particle diameter, we observed that the mean diameter of the fog particles was smaller than the humid particles. The test results of particle mean velocity was about 3.76 m/sec. Compared with the mean velocity of the humid particles, we can observed the mean velocity of fog particles were greater than humid particles.

The experiments were conducted with four different kinds of particles with five different particle diameters. The particle types were organic particles, coal particles, potato particles and wheat particles with the diameter range of 63~75 micron, less than 150 micron, 150~250 micron, 250~355 micron and 355~425 micron.

To control the flow rate, the control gate of the particle dispensing hopper was adjusted to 1/16 open rate, 1/8 open rate and 1/4 open rate. The captured image range was 0 cm to 5 cm from the control gate, 5 cm to10 cm from the control gate and 10 cm to 15 cm from the control gate. Some of these experiments were conducted under both open environment conditions and closed environment conditions. Thus these experiments had a total of five parameters which were type of particles, diameter of particles, flow rate, observation range, and environment conditions.

The coal particles (diameter between 63 and 75 microns) tested under the closed environment condition had three factors that were considered as the affecting factors. They were open rate, observation range, and environment conditions. In this experiment, the interaction of open rate and observation range had a significant effect on the lower limit. On the upper limit, the open rate and environment conditions had a significant effect. In addition, the interaction of open rate and environment conditions had a significant effect. The coal particles tested (diameter between 63 and 75 microns) under open environment, two factors were that considered as the affecting factors. They were the open rate and observation ranges. In this experiment, there was no significant effect on the lower limit. On the upper limit, the observation range had a significant effect. In addition, the interaction of open rate and observation range had a significant effect for the source of variation with 95% of confidence based on analysis of variance (ANOVA) results.

## Table of Contents

## LIST OF GRAPHICAL MATERIALS

### List of Figures

## List of Tables

# 1 INTRODUCTION

Fuel flow to individual burners is complicated and difficult to determine on coal fired boilers, since coal solids are transported in a gas suspension that is governed by the complex physics of two-phase flow. This difficulty leads to the following problems in coal-fired boilers including poor emission performance, increased unburned carbon in the fly ash, distorted oxygen profile at boiler outlet, uneven steam temperature profiles, flame impingement, increased slagging, and water wall wastages.

A particle is the smallest discrete portion of something. Particles covered in this article range from a few nanometers to a few millimeters, even though the upper end of particle diameter in many industrial applications may extend into the range of centimeters.

The definition of a particle is a 3D object for which three parameters are required in order to provide a complete description.[1] The three parameters that are needed are length, breadth, and height. For this reason it is not possible to describe a particle using a single number that equates to particle diameter. Most sizing techniques assume that the particle being measured is spherical. As an example a technique can measure the mass or volume of the particle. It will lead to the diameter of the sphere that has the same volume as the measured particle being reported as particle diameter.

Laser diffraction has become the most widely used technique for particle diameter analysis. In laser diffraction measurements one obtains information about particle diameter distribution through measurements of scattering intensity as a function of the scattering angle and the wavelength. Laser diffraction has become a popular and important physical means for sizing industrial particles. Particle sizing by laser diffraction is restricted to the use of only the Fraunhofer diffraction theory. New laser diffraction analyzers are no longer limited to just simple diffraction effects. More general approaches based on the Mie theory and the measurement of

scattering intensity over a wide scattering angular range can be employed. Secondly, some light source of continuous wavelength is often used to complement the main laser source in order to gain additional characteristic information about submicron-size particles based on wavelength and polarization dependencies of scattering intensity. The whole process starts with a light source that generates a monochromatic.[1] After passing through several optical components, the raw beam is conditioned to create an expanded, collimated beam having a smooth radial intensity distribution which illuminates the particles in the scattering patterns. These patterns are then Fourier transformed into another intensity pattern, which is detected by a multi-element detector array. The photocurrent from the detectors is subsequently accessed and digitized creating an intensity flux pattern. Computer software sizing appropriate scattering theories then converts the set of flux values into particle diameter distribution.

### 1.1 PDPA System

The phase Doppler measurements allow for the sizing of spherical particles. Along with size information, the velocity of the particle was also obtained. So in this sense, the phase Doppler technique [2] was an extension of Laser Doppler Velocimetry (LDV). The phase Doppler method was based upon the principles of light scattering interferometry. Measurements were made at a small, non-intrusive optical probe volume defined by the intersection of two laser beams. The intersection of the two beams creates a fringe pattern within the probe volume. As a particle passes through the probe volume, it scatters light from the beams and projects the fringe pattern. A receiving lens strategically located at an off-axis collection angle projects a portion of this fringe pattern onto several detectors. Each detector produces a Doppler burst signal with a frequency proportional to the particle velocity. The phase shift between the Doppler burst signals from two different detectors was proportional to the size of the spherical particles. [3]

The Phase Doppler Particle Analyzer (PDPA) measurements were not based upon the scattered light intensity, and consequently, were not subject to errors from beam attenuation or deflection

which occur in dense particle and combustion environments. Hence, PDPA is a perfect tool to measure the coal solids-flow in coal-fired boilers.[4] Laser light from the laser generator splits into two equal intensity beams. When the two beams focus, they interfere and generate a fringe pattern. As a droplet flows through the fringe pattern, it scatters the Doppler signal. Three detectors collect the different phase Doppler signals and present them as one sample point. All the droplets passing through the sample volume contribute to the measurements. The area of the probe volume is the cross-sectional area of the intersection of the two laser beams. The particle scattering method using the PDPA was used in the preliminary particle scattering test. PDPA systems were used in a wide variety of disciplines around the world. A few examples of where PDPA systems have been used include: [5]

1. Combustion research: Measurement of fuel droplets.
2. Aircraft icing research: Measurement of water and ice drops and their effect on the aircraft
3. Ink-jet printer development: Improve performance of ink-jet printers. Both size of drops and the trajectories of drops being fired were measured.
4. Basic industrial sprays research: PDPA is used to characterize various chemicals that were atomized (pesticides, petrochemicals, etc.).
5. Spray drying: Used in pharmaceutical and food applications.
6. Characterization of Metered Dose Inhalers (MDI's): Characterize the size and velocity of droplets produced by medical inhalers.
7. Nasal sprays: Drop size and velocity measurements of medical nasal sprays

Fire sprinklers, fixed nozzles and water mist nozzles have been characterized using the PDPA technique. Any liquid spray with transparent/semitransparent droplets can be characterized with this equipment. [6]

The hydrodynamic effects of varying operating parameters in the fluidized bed combustor (FBC) have been of great interest to the FBC design and manufacturing process. Some

experiments to investigate the gas/particle flows in the gaseous fluidized bed were performed with the laser-based PDPA. In the experiments, the PDPA was used to measure the vertical component of fluidizing particle velocity at one specific position point. [7, 8] The recent results of the particle characteristics and analysis using PDPA were presented along with statistical methods. [9]

A PDPA, also referred to as phase Doppler interferometer (PDI), is used to serve the research needs of several ongoing research programs dealing with droplet- based processes of metals and composites at University of California, Davis. Spray forming (also referred to as spray atomization and deposition) is a state-of-the-art technology for manufacturing droplet-based advanced materials that exhibit superior mechanical properties. It provides a unique opportunity for achieving combinations of properties that were otherwise unachievable with equilibrium materials and near-net- shape control of products. [10] During this reporting period, the transparent duct model was carefully designed and fabricated for the laser-based-instrumentation of solids-flow monitoring (LISM).

## 1.2 PIV System

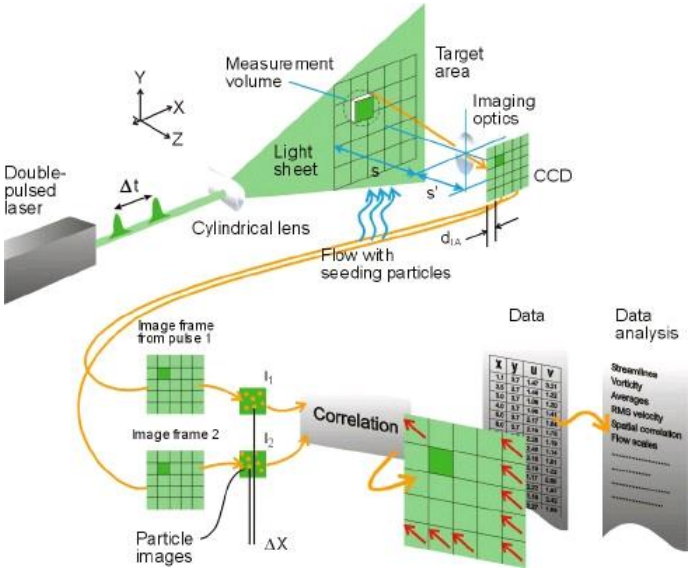


Figure 1 Pictorial View of PIV System

Particle Image Velocimetry (PIV) system components include Imaging Subsystem (Laser, Beam delivery system, light optics), Image Capture Subsystem (Charge Coupled Device (CCD) Camera, Camera Interface, Synchronizer-Master control unit), Analysis and Display Subsystem. Figure 1 shows pictorial view of PIV system. Particle Image Velocimetry (PIV) systems measure velocity by determining particle displacement (ΔX, ΔY) in a flow over a known time Δt. A pulsed laser sheet illuminates a plane in the flow, and the positions of the particles were recorded. A second laser pulse Δt later illuminates the same plane, creating the second set of particle images. If the particles in the flow field move by an amount ΔX in the x-direction an ΔY in the y-direction in the time Δt, the velocities of the particles in the x and y direction were u = ΔX / Δt and v = ΔY / Δt. [1, 11]

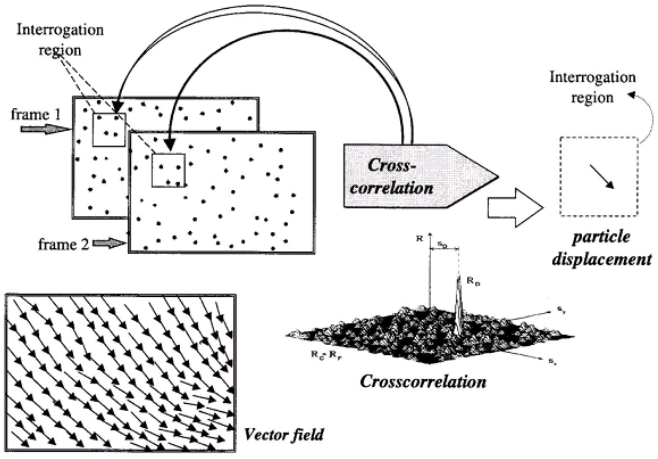


Figure 2 Cross Correlation Processing

Figure 2 shows cross correlation processing. Typically, the particle images obtained from the two laser pulses were recorded on separate camera frames. The images in each of these frames were subdivided in to a large number of interrogation regions, each small enough that the velocity within the region is uniform. Spatial cross correlation of the image intensities in one interrogation region in the first frame with the image intensities in the corresponding interrogation region in the second frame provides a statistical estimate of ΔX and ΔY for that region – given by the peak of the correlation function R. since particle images were in separate frames, cross correlation

analysis also gives the direction of image displacement, and hence the velocity vector. PIV is particularly useful for the measurement in unsteady flows. However, the PIV application on solid particle turbulent flow has been rarely done so far. But according to its design principle and algorithm, the PIV system should be qualified to measure the combustion test flow and solid particle turbulent flow successfully without disturbing the flow field. [12, 13]

The principle layout of a modern PIV system is shown in Figure 1. The PIV measurement includes illuminating a cross section of the seeded flow field, typically by a pulsing light sheet, recoding multiple images of the seeding particles in the flow using a camera located perpendicular to the light sheet, and analyzing the images for displacement information. The recorded images were divided into small sub-regions called interrogation regions, which the dimensions determine the spatial resolution of the measurement. The interrogation regions can be adjacent to each other, or more commonly, have partial overlap with their neighbors. The shape of the interrogation regions can deviate from square to better accommodate flow gradients. In addition, interrogation area A and B, corresponding to two different exposures, may be shifted by several pixels to remove a mean dominant flow direction and thus improve the evaluation of small fluctuating velocity components about the mean. The peak of the correlation function gives the displacement information. For double or multiple exposed single images, an auto-correlation analysis is performed. For single exposed double images, a cross-correlation analysis gives the displacement information. [14]

If multiple images of the seeding particles were captured on a single frame, then the displacements can be calculated by auto-correlation analysis. This analysis technique has been developed for photography based PIV, since it is not possible to advance the film fast enough between the two exposures. The auto-correlation function of a double exposed image has a central peak, and two symmetric side peaks. This poses two problems: (1) although the particle displacement is known, there is an ambiguity in the flow direction, (2) for very small

displacements, the side peaks can partially overlap with the central peak, limiting the measurable velocity range.[15, 16]

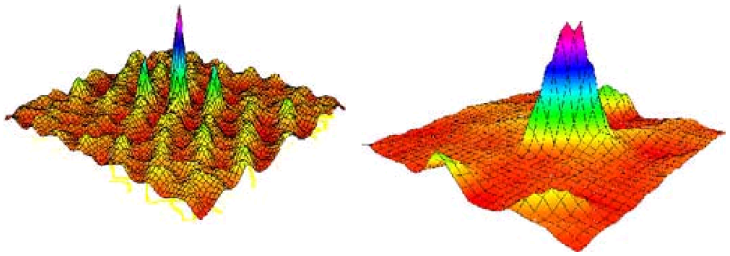

Figure 3 Auto-correlation (left) versus Cross-correlation (right) Analysis Result

The preferred method in PIV is to capture two images on two separate frames, and perform cross-correlation analysis. This cross-correlation function has a single peak as shown in Figure 3, which provides the magnitude and direction of the flow without ambiguity. The common particles need to exist in the interrogation regions, which were being correlated, otherwise only random correlation, or noise will exist. The PIV measurement accuracy and dynamic range increase with increasing time difference $\Delta t$ between the pulses. However, as $\Delta t$ increases, the likelihood of having common particles in the interrogation region decreases and the measurement noise goes up. A good rule of thumb is to insure that within time $\Delta t$, the in-plane components of velocity *Vx* and *Vy* carry the particles no more than a third of the interrogation region dimensions, and the out-of-plane component of velocity *Vz* carries the particles no more than a third of the light sheet thickness. [17, 18]

In the following the different methods for the evaluation of PIV recordings by means of correlation and Fourier techniques will be summarized.

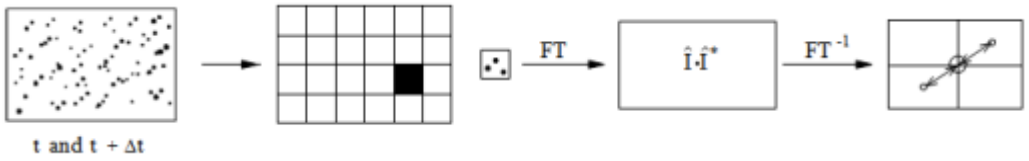


Figure 4 The Fully Digital Autocorrelation Method

Figure 4 presents a flow chart of the fully digital autocorrelation method. The PIV recording is sampled with comparatively small interrogation windows (typically 20 - 50 samples in each dimension). For each window the autocorrelation function is calculated and the position of the displacement peak is determined. The calculation of the autocorrelation function is carried out either in the spatial domain or in most cases – via the bypass over the frequency plane through the use of Fast Fourier Transformation (FFT) algorithms.[19-22]

If the PIV recording system allows the employment of the double frame/single exposure recording technique the evaluation of the PIV recordings is performed by cross-correlation shows in Figure 5. In this case, the cross-correlation between two interrogation windows sampled from the two recordings is calculated. It is advantageous to offset both these samples according to the mean displacement of the tracer particles between the two illuminations. This reduces the in plane loss of correlation and therefore increases the correlation peak strength. The calculation of the cross-correlation function is generally computed numerically by means of efficient Fast Fourier Transformation (FFT) algorithms.

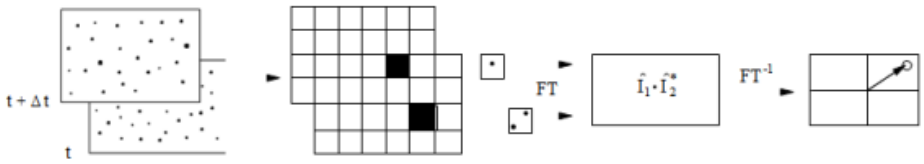


Figure 5 The Digital Cross-correlation Method

Single frame/double exposure recordings may also be evaluated by a cross-correlation approach instead of autocorrelation shows in Figure 6. In this case the interrogation windows can be chosen of different size and/or slightly displaced with respect to each other in order to compensate for the in-plane loss of correlation due to the mean displacement of particle images. Depending on the different parameters, autocorrelation peaks may also appear in the correlation plane in addition to the cross-correlation peak. This is illustrated in more detail in Figure 6.

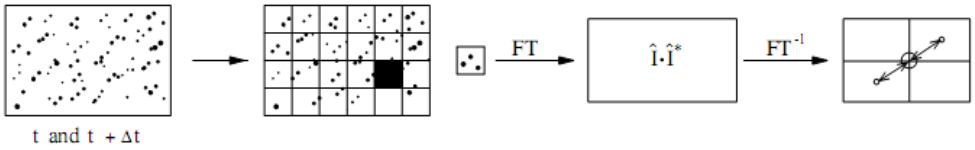


Figure 6 Single Frame/Double Exposure Cross-correlation Method Flow Chart

The counterpart of the fully digital evaluation by means of autocorrelation is a system employing Optical Fourier transform (OFT) for evaluation. In order to obtain the autocorrelation function a setup with two optical Fourier processors has to be implemented, following the bypass through the frequency plane. A spatial light modulator is required to store the output of the first Fourier processor and to serve as input of the second Fourier processor shown in Figure 6.

Figure 7 shows the correlation of the two interrogation areas, $I_1$ and $I_2$. This is a special PIV system, particularly designed for nontransparent fluids such as sand, gravel, quartz, or other granular materials that we can find in geophysical scenarios. In typical PIV, the transparent fluid must be seeded with tracer particles so that the camera and the software can detect some pattern. However, the set-up of the typical PIV differs from the usual PIV in that the optical surface structure which is produced by illumination of the surface of the granular flow is already sufficient to detect the motion. This means one does not need to add tracer particles in the bulk material. [15, 16, 21]

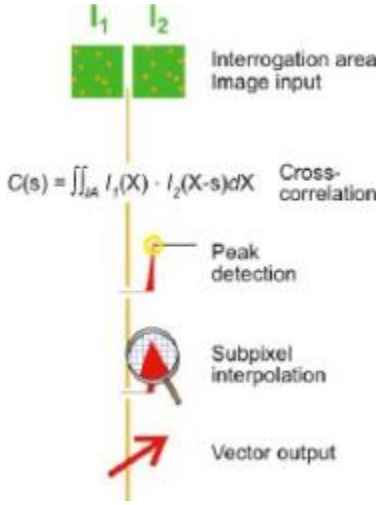


Figure 7 The Correlation of The Two Interrogation Areas, $I_1$ and $I_2$

# 2 LITERATURE SURVEY

## Particle Characterization Technologies Other Than Light scattering methods

### 1.) Sieve Analysis-Fractional and Sizing (5micron-l0cm)

This is one of the oldest sizing technologies. It uses a test sieve or a set of test sieves, which has a screen with many presumably uniform openings to classify materials into different fractions.

### 2.) Sedimentation Methods-Sizing (0.05-100 micron)

This is another classical particle classification and sizing methods for liquid-born particles in a liquid at rest under a gravitational or centrifugal field. Sedimentation methods were based on the rate of settling of particles in a liquid at rest under a gravitational or centrifugal field.

$d_{st} = \sqrt{18nu/(P_S-P_1)g}$

In this equation, $d_{st}$ is the Stokes diameter which is equal to the equivalent diameter of a spherical particle that has the same density and free-falling velocity as the real particle in the same liquid under laminar flow conditions. The quantities n, u, $P_S$, $P_1$ and g were the viscosity of suspension liquid, the particle settling velocity, the effective particle density, the liquid density and the acceleration, respectively.

### 3.) The Electrical Sensing Zone Method (ESZ, The coulter principle) -Counting and Sizing (0.4-1200 micron)

This was invented in the early 1950's and has been so widely accepted in the field of medical technology that presently over 98% of automated cell counters incorporate the Coulter principle. This method can be used to count and size any particulate material that can be suspended in an electrolyte solution. The number of pulses detected during measurement is the number of particles measured, and the amplitude of the pulse is proportional to the volume of the particle:

$U=VP_o$ if/$\pi^2R^4$

In this equation U, V, $P_o$, I, f, and R were the amplitude of the voltage pulse, particle volume, electrolyte resistivity, aperture current, particle "shape" and aperture radius respectively. If a constant particle density is assumed pulse height is proportional to the particle mass.

**4.) Image Analysis:**

*Microscopic Methods-Morphology study and sizing (0.001-200micron)*

In 1827, the English botanist Robert Brown discovered the random thermal motion of flower pollen particles in suspension now knows as "Brownian motion" using an optical microscope. Microscopic analysis has advantages over other methods in that it can provide information on size, shape, surface texture and some optical properties of individual particles in a broad size range and in great detail.

*Holographic Method-Sizing (0.3-1000 micron)*

This is a relatively new imaging technique used in the study of air-borne and liquid-borne particulate systems in their real world environments.

**5.) Holographic Methods:**

The holographic method is a relatively new imaging technique and in a holographic experiment, images were formed in a two-step process. In the first step, a collimated coherent light is used to illuminate the sample. In the second step, the hologram is again illuminated by a coherent light source and a stationary image of all the particles at their original locations in the volume is created.

**6.) Chromatographic Methods:**

In this method, a sample is injected or placed at one location. It is then moved by a carrier, often a type of liquid, and passed through a chromatographic path. Although there were many different devices that can be used to detect effluent materials, based either on their chemical composition or their physical properties, the detectors used in particle characterization were usually some typed of light scattering or UV-vis sensors. Depending on the form of

chromatographic passage and the property of interest, there were several different techniques, which include

- Size Exclusion Chromatography (SEC) - Fractionation and Sizing (0.00 1 ~0.5 micron))
- Hydrodynamic Chromatography (HDC) - Fractionation and sizing (packed column HDC 0.03~2 micron, capillary HDC 0.02-50 micron));
- Field flow fractionation - fractionation and sizing (0.001-500 micron)

**7.) Submicron Aerosol Sizing and counting (0.001 -1 micron)**

The common procedure to characterize sub micron particles has two steps. In the first step, aerosol particles were fractionated according to their size. These fractionated particles then pass through a container of evaporative liquid. In the second scheme, called differential mobility analysis, particles were first charged and then carried by a sheath flow passing through an electric field. Acoustic attenuation spectroscopy is based on the measurement of the attenuation of sound waves as a function of their frequency, typically from 1 to 150 MHz Different from acoustic attenuation spectroscopy, in electro acoustic spectroscopy analysis; sound waves were generated by an applied high frequency electric field across a colloidal suspension and subsequently detected.

**8.) Acoustic Analysis:**

This is used where particle characterization has to be performed in a concentrated phase in which dynamic processes such as aggregation, agglomeration, or flocculation may occur at a much faster rate.

**9.) Gas Sorption -Surface Area and Pore Size Determination:**

Gas sorption (both adsorption and desorption) at the clean surface of dry solid particles is the most popular method for determining the surface area of these particles as well as the pore size distribution of porous materials. There were several adsorption models. The most well known and most widely used is the BET equation for multilayer adsorption:

$$\frac{P}{n(P_0 - P)} = \frac{1}{cn_m} = \frac{c-1}{cn_m}\frac{P}{P_0}$$

In this equation P, $P_0$, c, n, $n_m$ were the adsorption pressure, the saturation vapor pressure, a constant, the amount adsorbed (moles per gram of adsorbent) at the relative pressure $P/P_0$, and the monolayer capacity (moles of molecules needed to make a monolayer coverage on the surface of one gram of adsorbent), respectively. Pore Size Determination In a mercury porosimetry measurement, pressure is used to force mercury into filling the pores and voids of the material. When external pressure forces and electrolyte solution through a capillary, or though a bundle of fibers, or through a plug of porous material, some displacement of charge will take place. In a PFG-NMR measurement, a radio frequency pulse is applied to rotate the magnetization of the nuclear spings of the sample into the transverse plane that is held perpendicular to the main homogeneous magnetic field. When an oscillatory electric field is applied to a colloidal suspension, the electric double layer around the particle will be polarized. The measured distribution can be represented by a histogram. Besides the fractional from q(x), also called differential form, as discussed above, the distribution can also be represented in a cumulative form. There were three was to present a distribution: tabulate, graphic, and functional. The mean is an average over the whole distribution. The median is the x value that divides the population into two equal halves. The mode is the most common value of the distribution, i.e., the highest point of the distribution curve. A measure of distribution broadness defined as, for arithmetic and geometric, respectively:

$$\sigma^2 = \frac{\sum_{i=1}^{N}(x_i - \bar{x})^2}{N-1}$$

$$\sigma_g^2 = \text{anti log}\left(\frac{\sum_{i=1}^{N}\left(\log\left(\frac{x_i}{\bar{x}}\right)\right)^2}{N-1}\right)$$

Standard Deviation (σ) is the square root of the variance. The coefficient of variation (CV) is the standard deviation divided by the mean. Skewness is the degree of distortion from a symmetrical distribution. Kurtosis is a measure of the weight of the tails of a distribution or the peakedness of a distribution. $X_{w\%}$ means the x value at which w% of particles has smaller x values. Precision is the degree of agreement from one measurement to another. In measuring particle size distributions, besides errors introduced due to imperfection in the instrument design and malfunctions of instrument there were several other error sources that should be mentioned. Improper sampling and sample dispersion commonly introduce errors. The volume equivalent diameter (d) of a sphere calculated from cylindrical particle is:

$$d = (6r^2h)^{\frac{1}{3}}$$

Where r is the radius of the cylinder and h is the height. Sampling particles suspended in a liquid medium that is not homogenous requires the use of rotational devices such as rollers, magnetic stirrers, tube rotators, manual inversion, and aspiration with pipettes, etc. in a sample reduction of non-flowing particles, such as fine cohesive solids sticky or moist materials, or fibrous solids. Furthermore, since these materials do not have a tendency to segregate uniformly, it is quite necessary to pass these materials through a mixer or to shake the sample in a container using different modes of shaking.

Liquid sample dispersion occurs when dry Particles are suspended in a liquid medium before analysis. Solid sample dispersion is the attempt to disperse dry particles with the intention of suspending it in air.

## 3 EXECUTIVE SUMMARY

The phase Doppler measurements allow for sizing of spherical particles. The particle scattering method using the phase Doppler particle analyzer (PDPA) was used in the particle scattering test.

The preliminary particle testing with the laser-based phase Doppler particle analyzer (PDPA)[23] was carefully prepared and conducted for humid particles and fog particles.

The mean diameter for humid particles was 6.4325 microns when the humid particles flow was low. When the humid particles flow was high, the mean diameter of humid particle was 6.925 microns. The mean velocity of humid particles was 1.4475 m/sec when the humid particle flow was low. When the humid particle flow was high, the mean velocity was 1.6775 m/sec. The mean diameter for fog particles was 5.765 microns when it's generated by shell ondina oil and the mean velocity for fog particles was 3.76 m/sec.

When the humid particles flow rate was low, the maximum number of particles appeared when the diameter was 8.43 microns and 17.9 microns. When the particle diameter was 18.1 microns, the maximum velocity of 2.8 m/s appeared. When the humid particles flow rate was high, the maximum number of particles appeared when the particle diameter was 8.43 microns, 17.94 microns, and 19.21 microns. When the particle diameter was 5.34 microns, the maximum velocity appeared.

Compared with the mean diameter of humid particles, we observed that the mean diameter of fog particles was smaller than the humid particles. Compared with the mean velocity of the humid particles, we observed that the mean velocity of fog particles was greater than that of humid particles.

The particle testing with laser-based Particle Image Velocimetry (PIV) was carefully prepared and conducted. The experiments were conducted with four different kinds of particles with five different particle diameters. The particle types were organic particles, coal particles, potato particles and wheat particles with a diameter range of 63~75 micron, less than 150 micron, 150~250 micron, 250~355 micron and 355~425 micron.

To control the flow rate, the control gate of the particle dispensing hopper was adjusted to 1/16 open rate, 1/8 open rate and 1/4 open rate. The captured image range was 0 cm to 5 cm from the control gate, 5 cm to10 cm from the control gate and 10 cm to 15 cm from the control gate. Some

of these experiments were conducted under both open environment conditions and closed environment conditions. Thus these experiments had a total of five parameters which were type of particles, diameter of particles, flow rate, observation range, and environment conditions.

The organic particles (diameter between 425 and 500 microns) tested under PIV in the open environment condition, had two factors that were considered as the affecting factors including open rate and observation range. In this experiment, the particles diameter and interaction of the particle's diameter and open rate had significant effect on the lower limit. On the upper limit, none of the parameters had a significant effect on the source of variation with 95% of confidence based on analysis of variance (ANOVA) results.

The potato particles (diameter less than 75 microns) tested using PIV under the open environment condition, had two factors that were considered as the affecting factors including open rate and observation range. In this experiment, the open rate and observation range had a significant effect on lower limit. On the upper limit, the open rate of flow rate control gate and observation range also had significant effect on the source of variation with 95% of confidence based on analysis of variance (ANOVA) results.

The potato particles (diameter between 63 and 75 microns) and wheat particles (diameter between 63 and75 microns) tested using PIV under the open environment condition, had three factors that were considered as the affecting factors including open rate, observation range, and types of particle. In this experiment, the particles type had a significant effect on the lower limit. On the upper limit, the particles type and interaction of open rate and observation range had significant effect on the source of variation with 95% of confidence based on analysis of variance (ANOVA) results.

The coal particles (diameter between 63 and 75 microns) and organic particles (diameter between 63 and75 microns) tested using PIV under the open environment condition, had three factors that were considered as the affecting factors including open rate, observation range, and particle types. In this experiment, there was no significant effect on the lower limit. On the upper

limit, the interaction of type of particles and observation range had a significant effect on the source of variation with 95% of confidence based on analysis of variance (ANOVA) results.

The organic particles (diameter between 63 and 75 microns) and wheat particles (diameter between 63 and 75 microns) tested using PIV under the closed environment condition, had four factors that were considered as the affecting factors including particle type, open rate, observation range, and environment condition. In this experiment, the type of particles had a significant effect on the lower limit. On the upper limit, the observation range had a significant effect for the source of variation with 95% of confidence based on analysis of variance (ANOVA) results.

The potato particles (diameter between 63 and 75 microns) tested under the closed environment condition, three factors that were considered as the affecting factors including open rate, observation range, and environment condition. In this experiment, the environment condition had a significant effect on the lower limit. On the upper limit, the interaction of observation range, open rate and environment condition had a significant effect for the source of variation with 95% of confidence based on analysis of variance (ANOVA) results.

The coal particles (diameter between 63 and 75 microns) tested under closed environment condition, three factors that were considered as the affecting factors including open rate, observation range, and environment condition. In this experiment, the interaction of open rate and observation range had a significant effect on the lower limit. On the upper limit, the open rate and environment condition had a significant effect. In addition, the interaction of open rate and environment condition had a significant effect on the source of variation with 95% of confidence based on analysis of variance (ANOVA) results.

The coal particles test (diameter between 63 and 75 microns) under the open environment condition, two factors that were considered as the affecting factors including the open rate, observation ranges. In this experiment, there was no significant effect on the lower limit. On the upper limit, the observation range had a significant effect. In addition, the interaction of open rate

and observation range had a significant effect on the source of variation with 95% of confidence based on analysis of variance (ANOVA) results.

# 4 EXPERIMENTAL FACILITY AND PROCEDURE

## 4.1 The Design and Fabrication of the Transparent Duct Model

The transparent duct model for the laser-based instrumentation solids-flow monitoring was carefully designed and fabricated. In order to enhance an accurate measurement of the diameter and velocity of our particle specimens, we designed and fabricated a container around the laser beams to reduce any external interference. The materials used in our fabrication included a Plexiglas, a cutting machine with a rotating band saw, a hacksaw and a file to smooth the edges of the Plexiglas. In choosing the material for the duct model, we decided to use Plexiglas for the following reasons:

- It is transparent, so we could see the laser beams striking the particles
- It is lighter: its density (1190 kg/m3) is about half that of glass. It did not shatter.
- It transmits more light (92% of visible light) than glass.

First cut the Plexiglas with four sides having the following dimensions:

Side 1: 36” by 18”, Side 2: 18” by 18”, Side 3: 36” by 18”, Side 4: 18” by 18”. Thereafter, we modified each side to give room for each of the laser beams.

For side 1, the cut was 6” by 14”, Side 2, the cut was 8” by 14”, Side 3, the cut was 7” by 14” and side 4 did not need any alterations. In addition, we put two partitioning in the duct model each with dimensions 18” by 18”. After cutting the four sides of the Plexiglas and altering them, we glued the sides together to make our model in the shape of a rectangle as shown in Figure 8 For the gluing process, we used 100% Silicone Sealant for Lexan sheet and other plastics. This glue enabled us to firmly glue the sides of the model securely and permanently.

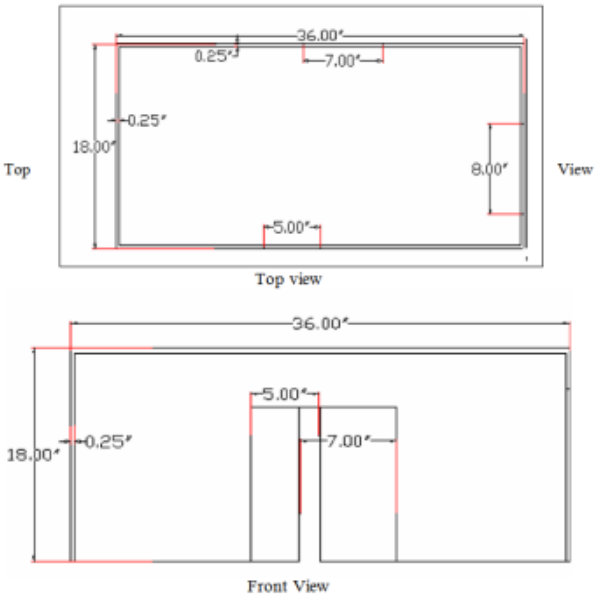


Figure 8 Schematic Diagram of the Transparent Duct for LISM

## 4.2 Experimental Procedure

To measure the particle diameter, the screen was set in the proper position so that the image of particle flow was caught. In order to catch the images, the PDPA system was turned on for Data Acquire. The Phase Doppler Method is based upon the principles of light scattering interferometry. Measurements were made at a small, non-intrusive optical probe volume defined by the intersection of two laser beams. As a particle passes through the probe volume, it scatters light from the beams into a multi-detector receiving probe, strategically located at an off-axis collection angle as shown in Figure 9. The phase shift between the Doppler burst signals from different detectors is proportional to the diameter of the spherical particles. [24]

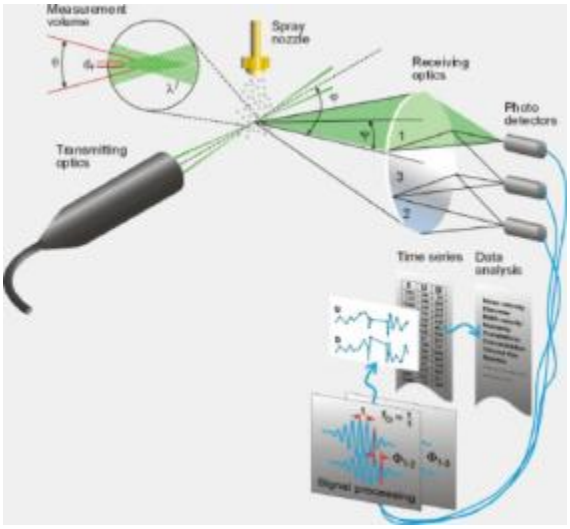


Figure 9 Working Principle of PDPA System

The particle velocity U is calculated from the Doppler frequency $f_D$ of the signal from any one of the detectors:

$$U = \frac{\lambda}{2 \sin(\theta/2)} f_D$$

The particle diameter D is derived from the phase difference F between the signals from two detectors.

If light scattering is dominated by reflection:

$$\Phi = \frac{2\pi D}{\lambda} \frac{\sin\theta \sin\psi}{\sqrt{2(1-\cos\theta\cos\Psi\cos\varphi)}}$$

If light scattering is dominated by refraction:

$$\Phi = \frac{-2\pi D}{\lambda} \frac{n_{rel} \sin\theta \sin\psi}{\sqrt{2(1+\cos\theta\cos\Psi\cos\varphi)}(1+n_{rel}^2-n_{rel}\sqrt{2(1+\cos\theta\cos\Psi\cos\varphi)})}$$

In order to get the continuous flow of the particles, the particles were stirred as they drop down. After the image is caught, the data acquisition is stopped and the data is saved. A typical PDPA measurement contains a large number of sample points and the information is evaluated statistically to yield the mean droplet diameter, diameter distribution, standard deviation, and velocity distribution.[25]

### 4.3 Design and Fabrication of Enclosure Testing Model:

The Plexiglas material was used for design and fabrication the enclosure testing model, which will be used for the particle testing along with the laser based PIV system. Figure 10 shows the pictorial view of the enclosure testing model.

Figure 10 Pictorial View of Enclosure Testing Model

Top lid dimension was 24 inches of width and 26 inches of length, the side dimension was 23 inches of width, 25 inches of length and 37 inches of height, the bottom dimension was 24 inches of width and 26 inches of length. Figure 11 shows the mockup design of enclosure testing model along with all dimensions for different views.

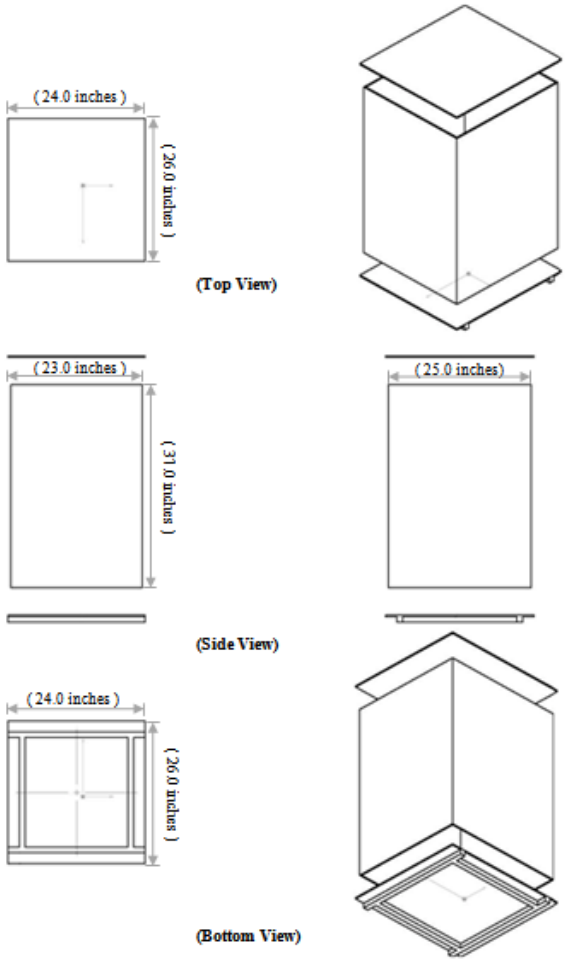


Figure 11 Mockup Design of Enclosure Testing Model

### 4.4 The Preliminary Particles Testing with the Particles Image Velocimetry (PIV)

The particle testing with the particle image velocimetry (PIV) was carefully prepared and conducted. In this report period different diameter potato particle, coal particle, organic particle and wheat particle were used to measure the velocity, which was on-going instrumentation on particles characteristics. The potato Particles density was 0.9959 g/cm$^3$, the wheat power density was 0.997 g/cm$^3$ determined by PAAR Digital Density Meter Model DMA 35. The coal Particles density was 0.7173 g/cm$^3$, the organic Particles density was 0.53 g/cm$^3$. Figure 12, Figure 13, Figure 14 and Figure 15 shows the potato, coal, wheat and organic particles used in experiments.

Figure 12 Pictorial View of Potato Particles

Figure 14 Pictorial View of Coal Particles

Figure 13 Pictorial View of Wheat Particles

Figure 15 Pictorial View of Organic Particles

### 4.5 Design & Working Principle of the Particles Flow & Hopper System

The PDPA system[23] was used to measure the particle diameter and velocity. The phase Doppler particle analyzer (PDPA) consists of a laser-based optical transmitter, an optical receiver, an electronic signal processor and the software for data acquisitions and analysis.[25] To fit the measurement capacity, the organic particles were grinded and sieved to get the particle sample. The diameters of sample particles were greater than 810 microns.

To measure the particle diameter, the screen was set in the proper position so that the image of particle flow was caught. In order to catch the images, the PDPA system was turned on for the software, Data Acquire. In order to get the continuous flow of the particles, the particles were stirred as they drop down. After the image was caught, the data acquisition was stopped and the data were saved.

To control the amount and rate of particles crossing the beams, we designed the hopper system. We then sent our hopper design to Particles Engineering Systems who manufactured the hopper for us to fit our dimensions.

The designed hopper was a simple, non-mechanical device using semi-transparent plastic material that offered an inexpensive, reliable Particles dispensing solution. Particles were dispensed reliably and accurately. The flow rate was easily varied from a high rate to a trickle for accurate dispensing.

The hopper can dispense particles in two modes: trickle mode and gates full open. In the trickle mode, the hopper dispenses just a few particles at a time, while when the gates were full open, the hopper dispenses a large amount of particles. The hopper consists of a shaped transition from a circle to a sloped slot. Below the slot were vertical side walls intersecting a curved lower edge. The outlet for the Particles was at the bottom end of the curved lower edge. There was a retainer plate designed to hold a permeable bag along the curved lower edge. The membrane bag had one permeable and one impermeable surface. It was sealed around its edges with a nozzle in one end. When air was blown into the bag it travels up into the particles and did two things:

It removes the Particles' angle of repose at the hopper outlet and it lowers the angle of sliding friction between the Particles and the curved sliding surface. This allows the Particles to flow. The flow rate of Particles can be controlled by the position of the gate and by the amount of air blown into the nozzle. In addition, there was a 5.5" flange, which was an external rim for strength. The flange also connects the top part of the hopper to the cylinder. The flange design was shown in Figure 16.

Moreover, the curvy part accelerates the flow of particles to give them enough speed as they exit the hopper. Also the hopper had a manual tube that helps one adjust the speed at which the particles exit, by regulating the amount of air blown into the nozzle. The manual tube was attached to the hopper. Figure 17 shows a schematic diagram of the Particle flow hopper and cylinder. These parts were made using Plexiglas so that one could see the movement of the particles, as they go through and exit the hopper.

Since we had to leave enough space for the laser to strike the particles, we installed plastic stands for the hopper system. The stand had an allowance of 11.5” from the nozzle of the hopper to the base of the stand. Figure 18 shows a schematic diagram of the hopper and the stand set-up.

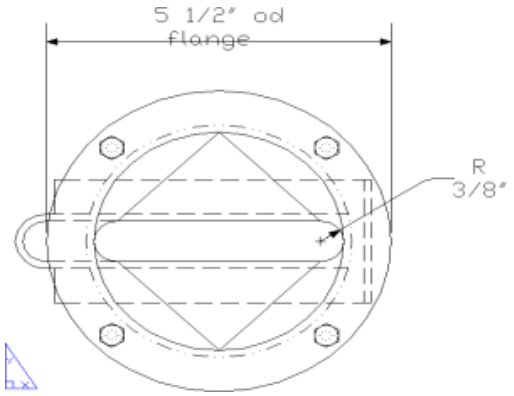


Figure 16 Schematic Diagram of Flange of the Particles Flow & Hopper System

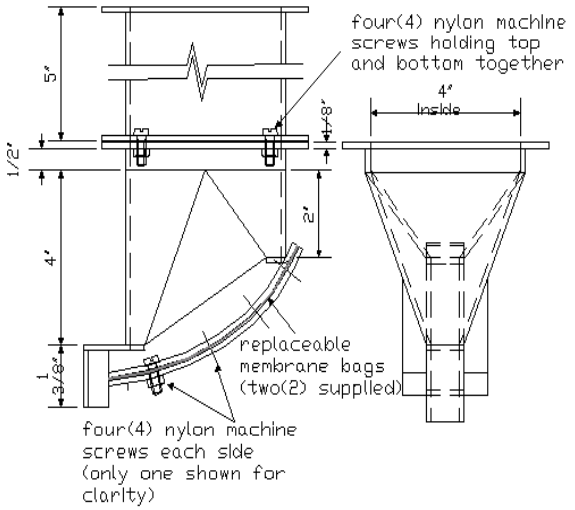


Figure 17 Schematic Diagram of the Particles Flow Hopper and Cylinder

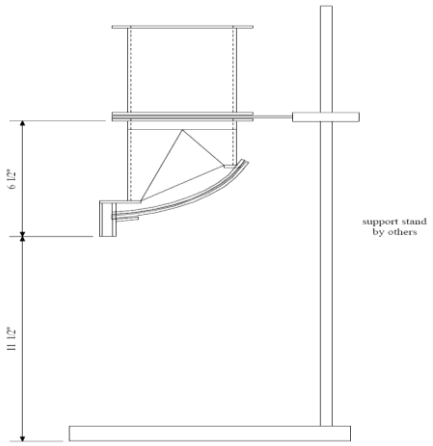


Figure 18 Schematic Diagram of the Hopper and Stand Set-up

### 4.6 Fabrication and Assembling of Transparent Duct model

In order to enhance solid flow measurement and monitoring, the transparent duct model was carefully designed, fabricated and assembled as shown in Figure 19. Figure 20 shows the Schematic Diagram of the Test Facility for the Proposed Laser-based Solids-flow Monitoring (LISM). The prototype LISM was carefully designed and fabricated for testing and demonstration.

In addition, this duct model could reduce any external interference of laser beams around the duct container. The rectangle- shape of the transparent Plexiglas was used to enhance the image and laser-beam diffraction.

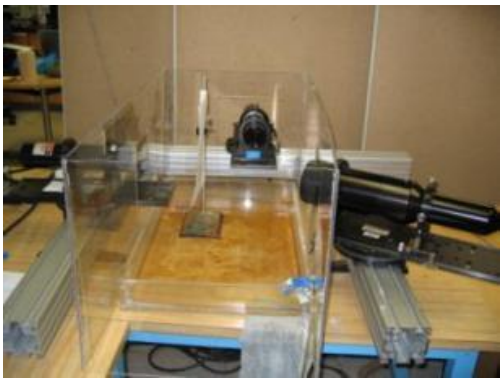

Figure 19 Pictorial View of Transparent Duct Model with Laser-based PDPA System

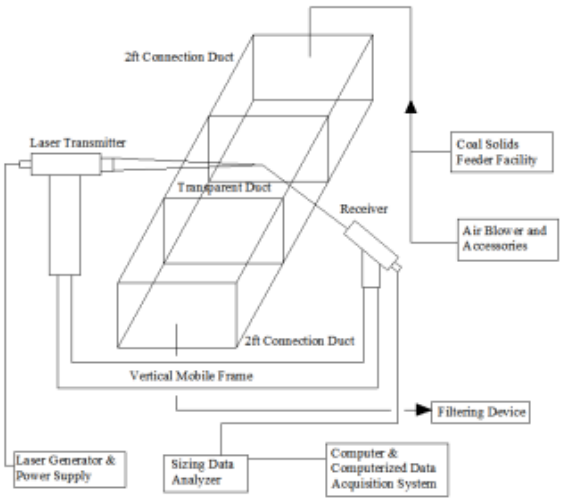


Figure 20 The Schematic Diagram of the Test Facility for the Proposed Laser-based Solids-flow Monitoring (LISM)

The mean diameter was calculated by the equation

$$D_{10} = \frac{\sum_{i=1}^{n} d_i}{n}$$

Where $d_i$ =diameter of particle i

n=number of particles

The experiment showed the mean diameter of 14.46 microns.

Area mean diameter, or the mean surface area based on diameter was calculated by the equation

$$D_{20} = \sqrt{\frac{\sum_{i=1}^{n} d_i^2}{n}}$$

The experiment showed the area mean diameter of 19.5 microns.

The mean velocity was calculated by the following equation

$$\overline{V_1} = \frac{\sum_{i=1}^{n} V_{1i}}{n}$$

Where $V_{1i}$ =velocity for particle i of channel 1.

n=number of particles

The first experiment showed the mean of velocity of 0.2988 m/s.

### 4.7 Particles Testing Using PDPA

The PDPA system [26] was used to measure the particle diameter and velocity. The phase Doppler particle analyzer (PDPA) consists of a laser-based optical transmitter, an optical receiver, an electronic signal processor and the software for data acquisitions and analysis.[25] To fit the measurement capacity, the humid particles and fog particles were used. To generate the humid particles and fog particles, the humidifier and the Air Flow Module, TQ AF17, which were shown in the following Figure 21 and Figure 22 were used.

Figure 21 Pictorial View of Humidifier


Figure 22 Pictorial View of Fog Generator (Part of TQ AF 17)

The humidifier was set to keep the flow rate high and low. The TQ AF17 was turned on to heat the oil for 3 minutes and blow it with the blower. The fog then flows along the tube. For humid particles, the strength of the flow was adjusted for low flow rate and high flow rate to see if it had an effect on the mean diameter and maximum velocity. For fog particles, shell ondina oil and olive oils were used to see if different oil types would affect the mean diameter and maximum velocity.

To measure the particle diameter, the tube was set in the proper position so that the image of particle flow was caught. In order to catch the images, the PDPA system was turned on for the software, Data Acquire. In order to get the continuous flow of the particles, the particles were stirred as they drop down. After the image was caught, the data acquisition was stopped and the data were saved.

### 4.8 Particles Testing Using PIV

The laser based phase Doppler particle analyzer (PDPA) system was used to measure the particle diameter and velocity of the fog particles. The PDPA consists of a laser-based optical transmitter, an optical receiver, an electronic signal processor and software for data acquisitions and analysis. The TQ AF 17 [27] was turned on to heat the oil for 3 minutes and then blown with the blower. The fog then flows along the tube. To measure the particle diameter, the tube was set in the proper position so that the image of particle flow was caught. In order to catch the image, the PDPA system was turned on for the software.

The PIV laser head and camera were positioned perpendicular near to the test section to capture the image of organic particles and coal particles. Then all the electric connections, including power supply, synchronizer, and computer were checked. The key on the power box was turned on and it was confirmed that the knot on the small control boxes on the synchronizer pointed to the start up status. The green buttons was pressed and the power of the synchronizer was turned on from the back. The knot on the small boxes was rotated to remote control. The “insight-NT” icon on the desktop computer was double clicked and the brightness was adjusted between ranges 4.5-6.7. The

run icon on the menu was clicked and it was confirmed that the laser was shooting out from the laser head. The camera on the desktop was clicked and the program was switched to focus mode. On the right side of the camera menu, the system options was selected and then clicked to start. The camera was adjusted to an appropriate distance to acquire the best image on the computer screen. The focus mode was stopped and the program was switched to sequence mode and started. The best images were selected to be analyzed. The quality of each image was checked by creating the vector file until the errors were visually acceptable. At last the vector file was saved to be analyzed. The vector file was opened and the errors were replaced by 0, 0, 1. [28] The vector file was then opened in software Tecplot [29] to create vector images to be analyzed and printed [30].

Figure 23 Pictorial View of Laser-based PIV Experimental Set Up and Instrumentation

Figure 23 shows the set up of laser based PIV system including charge-coupled camera (CCD), laser power supply, 2 Yag lasers, a laser pulse synchronizer and a computer monitoring system. It also shows the hopper system, which was specially designed for particle flow and dispensing. [31]

Figure 24 Pictorial View of Hopper System

Figure 24 shows the pictorial view of hopper system with the flow rate control gate which can be adjusted.

# 5 RESULTS AND DISCUSSION

## 5.1 Preliminary Particles Test (Saw Dust and Organic Particles diameter 75~150, 150~250, 250~355 and 355~425 microns)

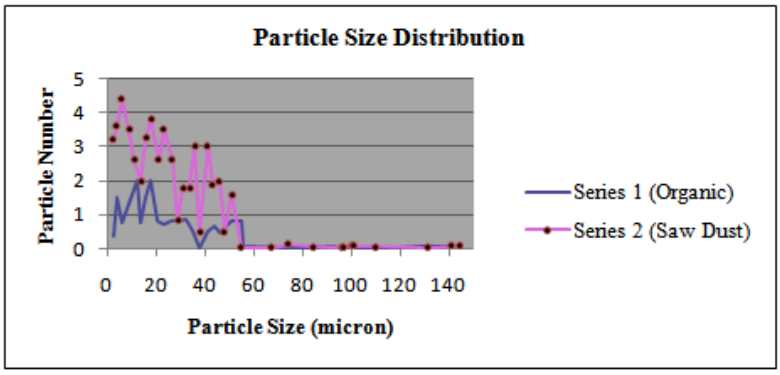


Figure 25 Particles Diameter Distribution for Organic Particles and Saw Dust Particles (diameter 75~150 microns)

The series 1 of Figure 25 shows the test result of organic particles diameter distribution. The particulate size (max) for this PDPA model is less than 200 microns. And also because of the limitation of the feeding system, the flow rate of the particles seemed relatively unstable. So this

might be caused that most data appeared between the sizes of 0 to 50 microns. Few particles appeared between 50 to 150 microns as shown in Figure 25. The maximum particles number appeared when the particles diameter was 17.5 microns. The first peak appeared at the particles diameter of 2.5 microns and the second one appeared at 10 microns. The third peak, which was the maximum number, appeared at the diameter of 17.5 microns. After the particles diameter of 17.5 microns, the number decreased rapidly to 0.8. From diameter 32.5 microns, the number decreased rapidly again. For the diameter 37.5 microns, the number increased again.

The series 2 of Figure 25 shows the test result of saw dust particles diameter distribution. The maximum particles number appeared when the particles diameter was 5 microns. The first peak appeared at the particles diameter of 5 microns and the second one appeared when the particles diameter was 17.5 microns. The first one showed the maximum number of particles. Then some other peaks appeared at the particles diameter of 12.5 microns, 35 microns and 40 microns.

In comparing the particles for the diameter of 75~150 microns, the particles number of saw dust particles were larger than organic particles. In comparing the particles number for which the maximum number appeared, the organic particles diameter was larger than the saw dust particles diameter. Organic particles density was 0.535 $kg$/d $m^3$and sawdust particles density was 0.235 $kg$/d $m^3$ respectively.

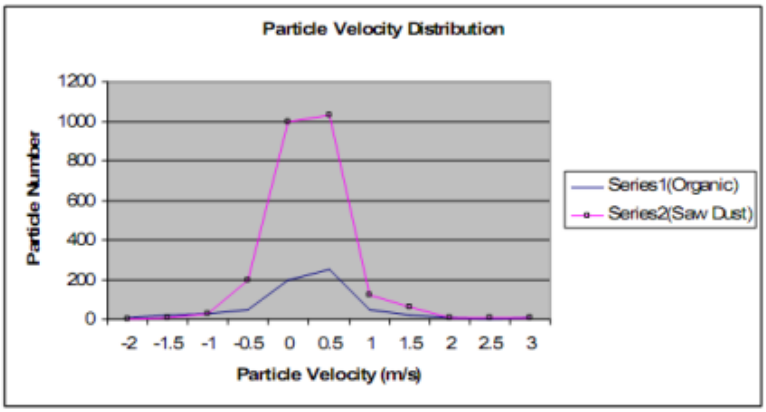


Figure 26 Particles Velocity Distribution for Organic Particles and Saw Dust Particles (diameter 75~150 microns)

The series 1 of Figure 26 shows the test result of organic particles velocity distribution. The velocity range was from -2~3 m/s. The maximum particles number appeared when the velocity was 0.5 m/s. Because the particles were so small, it went up sometimes so the velocity appeared to be a negative value.

The series 2 of Figure 26 shows the test result of saw dust particles velocity distribution test for particles diameter of 75~150 microns. The velocity range was from -1.5~3 m/s as shown in the series 2. The maximum particles number appeared when the velocity was 0.5 m/s. Because the particles were so small sized, it went up quickly such that the velocity appeared to be a negative value.

In comparing the particles for the diameter of 75~150 microns, the particles velocity range for organic particles was larger than saw dust particles. In comparing the velocity for the maximum number of particles, organic particles and saw dust particles were the same.

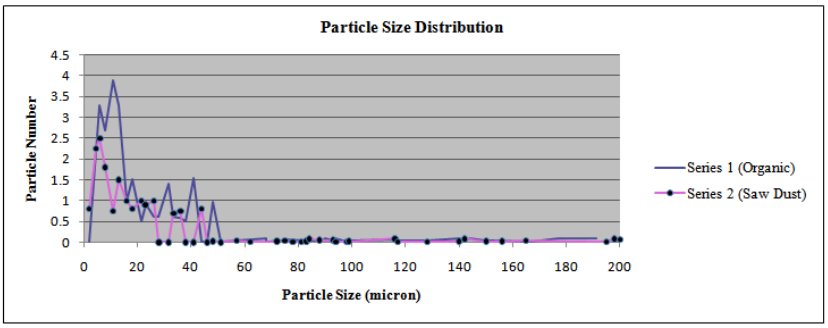


Figure 27 Particles Diameter Distribution for Organic Particles and Saw Dust Particles (diameter 150~250 microns)

The series 1 of Figure 27 shows the test result of organic particles diameter distribution. The maximum particles number appeared when the particles diameter was 10 microns. When the particles diameter was larger than 20 microns, the number was about 1. The first peak appeared at the particles diameter of 5 microns and the second one appeared when the particles diameter was 10 microns. The second peak showed the maximum number of particles. The particles number decreased rapidly after the second peak. Then, some small peaks appeared at the particles diameter of 17.5 microns, 22.5 microns, 30 microns, 40 microns and 47.5 microns.

The series 2 of Figure 27 shows the test result of saw dust particles diameter distribution. The maximum particles number appeared when the particles diameter was 5 micron. The first peak appeared at the particles diameter of 5 microns and the second one appeared when the particles diameter was 12.5 microns. The first one showed the maximum number of particles. The particles number decreased rapidly from the particles diameter of 25 microns.

In comparing the particles for the diameter of 150~250 microns, the particles number of organic particles were larger than saw dust particles. In comparing the particles number for which the maximum number appeared, organic particles diameter was larger than saw dust particles diameter. Organic particles density was 0.545 kg/d $m^3$ and saw dust particles density was 0.225 kg/d $m^3$. This might affected the test result.

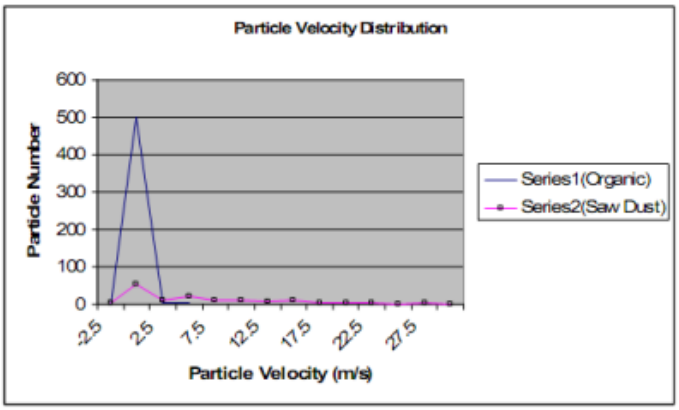


Figure 28 Particles Velocity Distribution for Organic Particles and Saw Dust Particles (diameter 150~250 microns)

The series 1 of Figure 28 shows the test result of organic particles velocity distribution test for particles diameter of 150~250 microns. The velocity range was from -3~3 m/s. The maximum particles number appeared when the velocity was 0.5 m/s. Because the particles were so small sized, the particles number increased quickly. Thus, the velocity appeared to be a negative value.

The series 2 of Figure 28 shows the test result of saw dust particles velocity distribution test for particles diameter of 150~250 microns. The velocity range was from -2.5~30 m/s. The maximum

particles number appeared when the velocity was 0 m/s. Because the particles were so small in diameter, the particles number increased quickly. Thus the velocity appeared to be a negative value.

Comparing the particles for the diameter of 150~250 micron, the particles velocity range for saw dust particles was larger than the organic particles. Comparing the velocity for the maximum number of particles, the organic particles were larger than saw dust particles. It was believed that these particles velocities were affected by their densities. Organic particles density was 0.545 kg/d $m^3$ and saw dust particles density was 0.225 kg/d $m^3$.

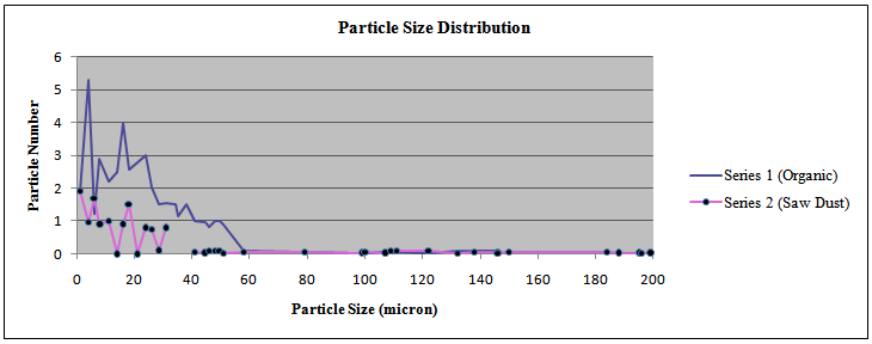


Figure 29 Particles Diameter Distribution for Organic Particles and Saw Dust Particles (diameter 250~355 microns)

The series 1 of Figure 29 shows the test result of organic particles diameter distribution. The maximum particle number appeared when the particles diameter was 2.5 microns. When the particles diameter was larger than 27.5 microns, the number was about 1.5. The first peak appeared at the particles diameter of 2.5 microns and the second one appeared when the particles diameter was 7.5 microns. The third peak and fourth peak appeared at the particles diameter of 15 microns and 22.5 microns. The first peak showed the maximum number of particles. Then the particles number decreased rapidly after the particles diameter of 22.5 microns. After that some small peaks appeared at the particles diameter of 32.5 microns and 47.5 microns.

The series 2 of Figure 29 shows the test result of saw dust particles diameter distribution. The maximum particles number appeared when the particles diameter was 4 microns. The first peak appeared at the particles diameter of 4 microns and the second one appeared when the particles diameter was 10 microns. The first peak showed the maximum number of particles. Then some

small peaks appeared at the particles diameter of 14 microns, 18 microns, 24 microns and 30 microns.

Comparing the particles for the diameter of 250~355 microns, the particles number of organic particles were larger than the saw dust particles. Comparing the particles number, for which the maximum number appeared, saw dust particles diameter was larger than the organic particles diameter.

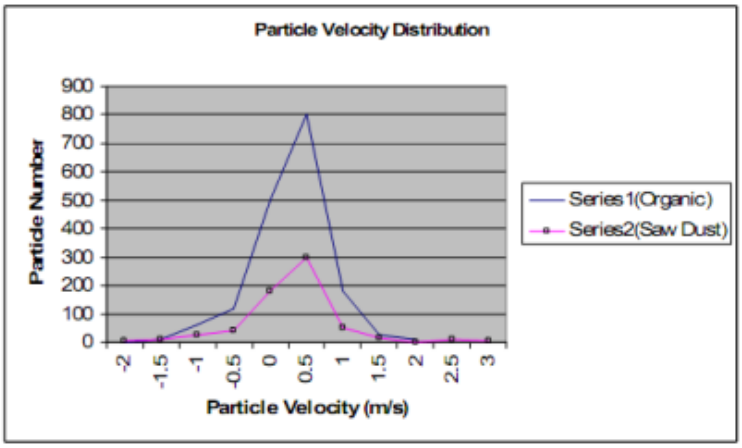


Figure 30 Particles Velocity Distribution for Organic Particles and Saw Dust Particles (diameter 250~355 microns)

The series 1 of Figure 30 shows the test result of organic particles velocity distribution test for particles diameter of 250~355 microns. The velocity range was from -2~2 m/s as shown in the Figure 7. The maximum particles number appeared when the velocity was 0.5 m/s. Because the particles were so small sized, the particles number increased quickly. Thus, the velocity appeared to be a negative value.

The series 2 of Figure 30 shows the test result of saw dust particles velocity distribution. The velocity range was from -2~3.5 m/s. The maximum particles number appeared when the velocity was 1 m/s. A small peak appeared when the particles velocity was 3.25 m/s. Because the particles were so small, the particles number increased sometimes so the velocity appeared to be a negative value.

Comparing the particles for the diameter of 250~355 microns, the particles velocity range for saw dust particles was larger than organic particles. Comparing the velocity for the maximum number of particles saw dust particles was larger than the organic particles.

It was believed that these particles velocities were affected by their densities. The organic density was 0.695 kg/d $m^3$ and saw dust particles density was 0.205 kg/d $m^3$.

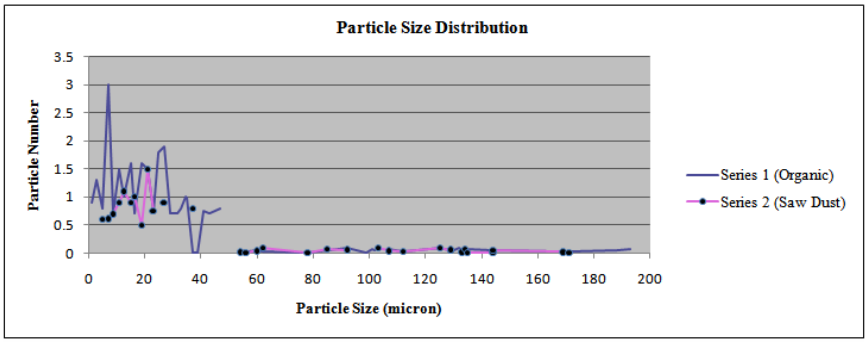


Figure 31 Particles Diameter Distribution for Organic Particles and Saw Dust Particles (diameter 355~425 microns)

The series 1 of Figure 31 shows the test result of organic particles diameter distribution. The maximum particles number appeared when the particles diameter was 6 microns. When the particles diameter was larger than 8 microns, the number was about 1.5. The first peak appeared at the particles diameter of 2 microns and the second one appeared when the particles diameter was 6 microns. The third peak and fourth peak appeared at the particles diameter of 10 microns and 14 microns. The second peak showed the maximum number of particles. Other peaks appeared at the particles diameter of 18 microns and 26 microns.

The series 2 of Figure 31 shows the test result of saw dust particles diameter distribution. The maximum particles number appeared when the particles diameter was 20 microns. The first peak appeared at the particles diameter of 12 microns and the second one appeared when the particles diameter was 16 microns. Then the third peak appeared at the particles diameter of 20 microns. The third one showed the maximum number of particles.

Comparing the particles for the diameter of 355~425 microns, the particles number of organic particles were larger than saw dust particles. Comparing the maximum particles number, saw dust

particles diameter was larger than organic particles diameter. It was believed that the maximum particles number was affected by their particles densities. Organic particles density was 0.71 kg/dm$^3$ and saw dust particles density was 0.175 kg/dm$^3$.

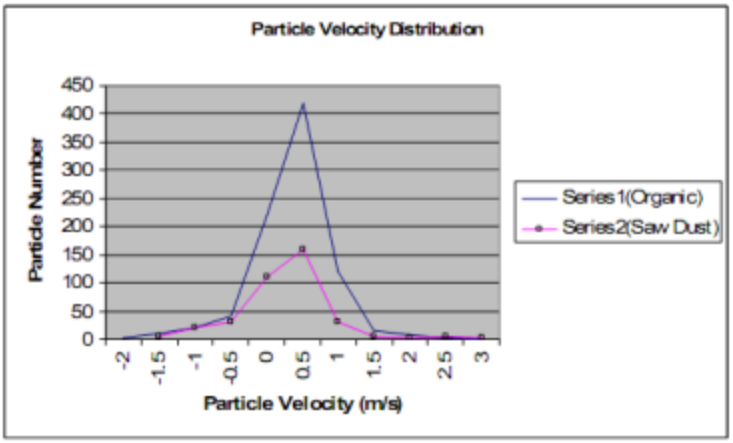


Figure 32 Particles Velocity Distribution for Organic Particles and Saw Dust Particles (diameter 355~425 microns)

The series 1 of Figure 32 shows the test result of organic particles velocity distribution test for particles diameter of 355~425 microns. The velocity range was from -1~3 m/s. The maximum particles number appeared when the velocity was 0.5 m/s. Because the particles were so small in diameter, the particles number increased quickly, such that the velocity appeared to be a negative value.

The series 2 of Figure 32 shows the test result of saw dust particles velocity distribution. The velocity range was from -1~3 m/s. The maximum particles number appeared when the velocity was 0.5 m/s. Because the particles were so small, the particles number increased sometimes so the velocity appeared to be a negative value.

Comparing the particles for the diameter of 355~425 microns, the particles velocity range for saw dust particles was larger than organic particles. Comparing the velocity for the maximum number of particles saw dust particles was larger than organic particles. Organic particles density was 0.71 kg/dm$^3$ and saw dust particles density was 0.175 kg/dm$^3$.

## 5.2 Analysis of Humidifier

The mean diameter was calculated by the equation

$$D_{10} = \frac{\sum_{i=1}^{n} d_i}{n}$$

Where $d_i$ =diameter of particles i

n=number of particles

The mean velocity was calculated by the following equation

$$\overline{V_1} = \frac{\sum_{i=1}^{n} V_{1i}}{n}$$

Where $V_{1i}$ =velocity for particles i of channel 1.

n=number of particles

Table 1 The Analysis of Mean Diameter of Humid Particles

| Particles Flow Rate | Observations (No.s) | | | |
|---|---|---|---|---|
| | 1 | 2 | 3 | 4 |
| low | 6.39 (microns) | 6.73 | 6.35 | 6.26 |
| high | 6.67 (microns) | 6.96 | 7.06 | 7.01 |

Table 1 shows the mean diameter of the humid particles when the humidifier was at the condition of high flow rate and medium flow rate.

$$SS_T = 6.39^2 + 6.73^2 + \ldots\ldots\ldots\ldots + 7.06^2 + 7.01^2 - \frac{(6.39 + 6.73 + \ldots\ldots + 7.06 + 7.01)^2}{8} = 0.5701$$

$$SS_{Strength} = \frac{1}{4}(25.73^2 + 27.7^2) - \frac{(6.39 + 6.73 + \ldots\ldots + 7.06 + 7.01)^2}{8} = 0.351525$$

$$SS_{Error} = SS_T - SS_{Strength} = 0.218575$$

Table 2 Analysis of Humidifier Strength Effect on Particles Mean Diameter

| Source of Variance | Sum of Square | Degree of Freedom | Mean Square | $F_o$ |
|---|---|---|---|---|
| Strength | 0.4851 | 1 | 0.4851 | 13.32 |
| Error | 0.2186 | 6 | 0.0364 | |
| Total | 0.7037 | 7 | | |

Table 2 shows the results of the analysis of the humidifier strength effect on the mean diameter of the humid particles. When the $\alpha$ equal to 90%, the value of $F_{\alpha,1,6}$ was 3.78 which was less than the value of $F_o$. So the strength of the humidifier had a significant effect on the mean diameter of the particles diameter.

Table 3 The Analysis of Mean Velocity of Humid Particles

| Strength | Observations (No.s) | | | |
|---|---|---|---|---|
| | 1 | 2 | 3 | 4 |
| Low Flow Rate | 1.37 (m/sec) | 1.39 | 1.5 | 1.53 |
| High Flow Rate | 1.59 | 1.72 | 1.73 | 1.77 |

Table 3 shows the mean velocity of the humid particles when the humidifier was at the condition of high flow rate and medium.

$$SS_T = 1.37^2 + 1.39^2 + \ldots\ldots\ldots + 1.73^2 + 1.77^2 - \frac{(1.37 + 1.39 + \ldots\ldots\ldots + 1.73 + 1.77)^2}{8}$$

$=0.1672$

$$SS_{Strength} = \frac{1}{4}(5.79^2 + 6.81^2) - \frac{(1.37 + 1.39 + \ldots\ldots\ldots + 1.73 + 1.77)^2}{8}$$

$=0.13005$

$$SS_{Error} = SS_T - SS_{Strength}$$

$=0.03715$

Table 4 Analysis of Humidifier Strength Effect on Particles Mean Velocity

| Source of Variance | Sum of Square | Degree of Freedom | Mean Square | $F_o$ |
|---|---|---|---|---|
| Strength | 0.13005 | 1 | 0.13005 | 21.00 |
| Error | 0.03715 | 6 | 0.00619 | |
| Total | 0.16720 | 7 | | |

Table 4 shows the results of the analysis of the humidifier strength effect on the mean diameter of the humid particles. When the $\alpha$ equal to 90%, the value of $F_{\alpha,1,6}$ was 3.78 which was less than the value of $F_o$. So the strength of the humidifier had a significant effect on the mean velocity of the particles diameter.

$$\overline{y_{i..}} - t_{\alpha/2,N-a}\sqrt{\frac{MS_E}{n}} \le \mu \le \overline{y_{i..}} + t_{\alpha/2,N-a}\sqrt{\frac{MS_E}{n}}$$

$6.1703 \le \mu_1 \le 6.6947$

$6.7628 \leq \mu_2 \leq 7.1872$

$1.3394 \leq V_1 \leq 1.5556$

$1.5694 \leq V_2 \leq 1.7856$

From the result, we can see that with the confidence of 90%, the mean diameter of the low flow was between 6.1703microns and 6.6947 microns, and the mean diameter of the medium flow was between 6.7628microns and 7.1872 microns when the humidifier was set low flow rate. The mean velocity of the low flow was between 1.3394 m/sec and 1.5556 m/sec, and the mean velocity of the high flow was between 1.5694 m/sec and 1.7856 m/sec when the humidifier was set high flow rate.

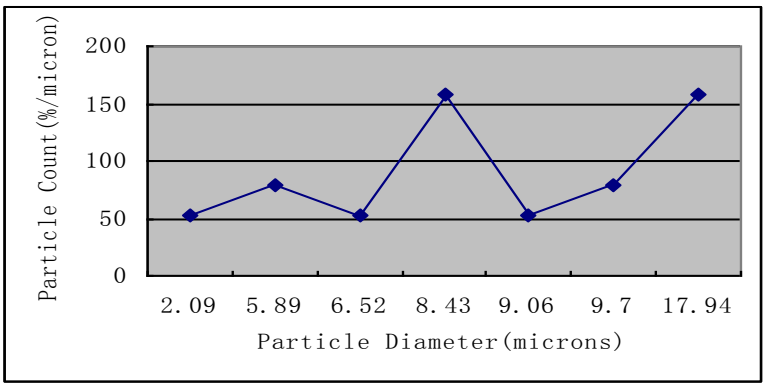


Figure 33 Humid Particles Diameter Distribution (low flow rate))

Figure 33 shows the test results of diameter distribution of humid particles when the flow was set low flow rate. From the figure, when particles diameter was 8.43 microns and 17.9 microns, the maximum particles number appeared.

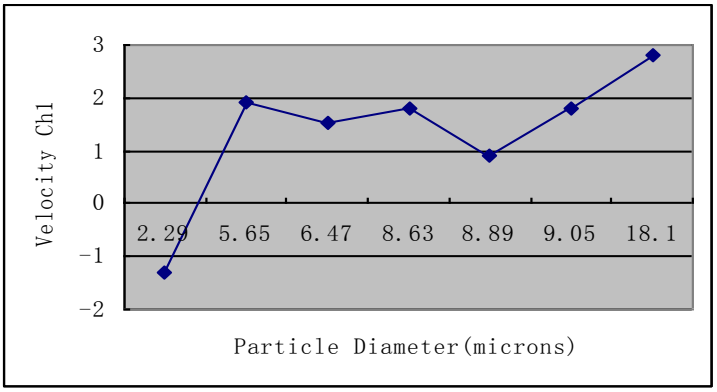


Figure 34 Humid Particles Velocity vs. Particles Diameter (low flow rate)

Figure 34 shows the test results of particles velocity vs. particles diameter. From the figure, at the diameter of 18.1 microns, maximum velocity of 2.8 m/s appeared. At the diameter of 1.29 microns, the velocity was negative. It was because the particles were so small so after it flows down then flow back up.

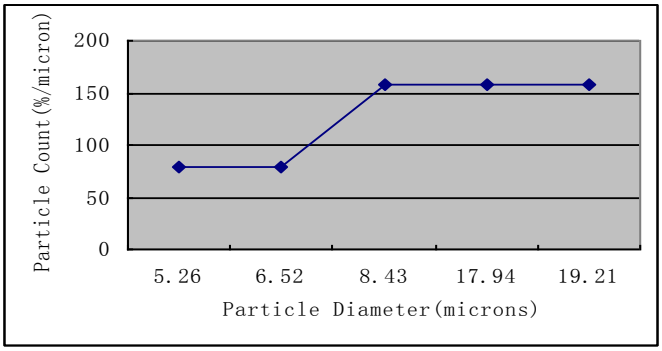


Figure 35 Humid Particles Diameter Distribution (high flow rate)

Figure 35 shows the test results of diameter distribution of humid particles when the flow was high flow rate. From the figure, when particles diameter was 8.43 microns, 17.94 microns and 19.21 microns, the maximum particles number appeared.

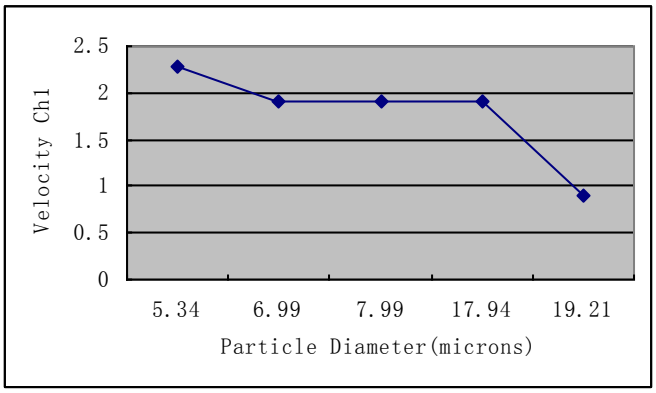


Figure 36 Humid Particles Velocity vs. Particles Diameter (high flow rate)

Figure 36 shows the test results of particles velocity vs. particles diameter. From the figure, at the diameter of 5.34 microns, maximum velocity appeared. And at the diameter of 6.99 microns, 7.949 microns and 17.94 microns, the velocity was also very large. The experiment was conducted using fog particles which were generated by shell ondina oil. The density for the oil was 0.8708kg/m$^3$.

Table 5 Mean Diameter of Fog Particles

| Oil Type | Observations (No.s) | | | |
|---|---|---|---|---|
| | 1 | 2 | 3 | 4 |
| Ondina | 5.80 (microns) | 5.98 | 5.68 | 5.6 |

Table 5 shows the mean diameter of the fog particles. Compared with the humid particles diameter, we observed that the mean diameters of fog particles were smaller than the humid particles.

Table 6 Mean Velocity of Fog Particles

| Oil Type | Observations (No.s) | | | |
|---|---|---|---|---|
| | 1 | 2 | 3 | 4 |
| Ondina | 3.53 (m/sec) | 3.89 | 3.69 | 4.93 |

Table 6 shows the mean velocity of the fog particles. Compared with the mean velocity of the humid particles, we observed the mean velocities of fog particles were greater than humid particles.

### 5.3 Oil Particles (Ondina, Olive) Test Using PDPA

Table 7 Mean Diameter of Fog Particles

| Oil Type | Observation (No.s) | | |
|---|---|---|---|
| | 1 | 2 | 3 |
| Ondina | 5.80 (microns) | 5.98(microns) | 5.68(microns) |
| Olive | 7.37(microns) | 7.29(microns) | 7.25(microns) |

Table 7 shows the mean diameter of particles which were generated by ondina oil and olive oil. From the table, the diameter of fog particles was from 5.68 to 5.98 microns. The mean diameter of fog particles was from 7.25 to 7.37 microns.

The following calculations were prepared for analysis of variance (ANOVA) Table to understand the significant factors. Total sum of square ($SS_T$), sum of square of oil type ($SS_{\text{Oil Type}}$) and sum of square of error ($SS_{\text{Error}}$) was calculated below.

$$SS_T = 5.80^2 + 5.98^2 + \ldots\ldots + 7.25^2 - \frac{(5.80 + \cdots + 7.25^2)}{6} = 3.3535$$

$$SS_{OilType} = \frac{1}{3}(17.46^2 + 21.91^2) - \frac{(5.80 + \cdots + 7.25^2)}{6} = 0.00531$$

$$SS_{Error} = 3.3535 - 0.0531 = 3.3004$$

Table 8 ANOVA Table of Fog Particles Mean Diameter

| Source of Variance | Sum of Square | Degree of Freedom | Mean Square | $F_0$ |
|---|---|---|---|---|
| Oil Type | 3.3004 | 1 | 3.3004 | 248.78 |
| Error | 0.0531 | 4 | 0.0133 | |
| Total | 3.3535 | 5 | | |

Table 8 shows the ANOVA Table of fog particles mean diameter, which was generated by ondina oil and olive oil. When the type one error α equal to 0.1, the degree of freedom equal to the value of test statistics $F_{\alpha,1,4}$ was 4.54 which was less than $F_0$ . So the type of oil been used has a significant effect on the mean diameter of the particles.

Table 9 Mean Velocity of Fog Particles

| Oil Type | Observation(No.) | | |
|---|---|---|---|
| | 1 | 2 | 3 |
| Ondina | 3.53(m/sec) | 3.89(m/sec) | 3.69(m/sec) |
| Olive | 1.32(m/sec) | 1.42(m/sec) | 1.54(m/sec) |

Table 9 shows the mean velocity of fog particles which were generated by the ondina oil and olive oil. The mean velocity of fog particles generated by ondina oil was from 3.53 m/sec to 3.89 m/sec. The mean velocity of fog particles generated by olive oil was from 1.32 m/sec to 1.54 m/sec. The following calculation was prepared for the ANOVA Table. Total sum of square ($SS_T$), sum of square of oil type ($SS_{Oil\ Type}$) and sum of square of error ($SS_{Error}$) was calculated below.

$$SS_T = 3.53^2 + 3.98^2 + \ldots\ldots + 1.54^2 - \frac{(3.53 + \cdots + 1.54^2)}{6} = 7.8642$$

$$SS_{OilType} = \frac{1}{3}(11.11^2 + 4.28^2) - \frac{(3.53 + \cdots + 1.54^2)}{6} = 7.7748$$

$$SS_{Error} = 7.8642 - 7.7748 = 0.089333$$

Table 10 ANOVA Table of Fog Particles Mean Velocity

| Source of Variance | Sum of Square | Degree of Freedom | Mean Square | $F_0$ |
|---|---|---|---|---|
| Oil Type | 7.7748 | 1 | 7.7748 | 348.126 |
| Error | 0.089333 | 4 | 0.022333 | |
| Total | 7.8642 | 5 | | |

Table 10 shows the summary of the ANOVA of fog particles mean velocity which was generated by ondina oil and olive oil. When the type one error α equal to 0.1, the value of test statistics $F_{\alpha,1,4}$ was 4.54 which was less than $F_0$ . So the oil type did have a significant effect on the mean velocity of the particles.

$$\overline{y_{i..}} - t_{\alpha/2,N-a}\sqrt{\frac{MS_E}{n}} \le \mu \le \overline{y_{i..}} + t_{\alpha/2,N-a}\sqrt{\frac{MS_E}{n}}$$

$\overline{y_{i..}}$ for ondina oil is (5.80+5.98+5.68)/3=5.82

$\overline{y_{i..}}$ for olive oil is (7.37+7.29+7.25)/3=7.30

$$t_{\alpha/2,N-a}\sqrt{\frac{MS_E}{n}} = 2.132\sqrt{\frac{0.8251}{3}} = 1.12$$

$$5.82-1.12 \le \mu_{Ondina} \le 5.82+1.12 \quad \Rightarrow \quad 4.7 \le \mu_{Ondina} \le 6.94$$

$$7.30-1.12 \le \mu_{Olive} \le 7.30+1.12 \quad \Rightarrow \quad 6.18 \le \mu_{Olive} \le 8.42$$

So with 90% of confidence, the mean diameter of fog particles generated by ondina oil remained in the range of 4.7 microns to 6.94 microns. And with the same confidence, the mean diameter of fog particles generated by olive oil remained in the range of 6.18 microns to 8.42 microns.

For the solid particles analysis, organic particles with the diameter of less than 150 microns and coal particles with the diameter of less than 74 microns were used to conduct the experiment.

### 5.4 Organic Particles (less than 150 microns) and Coal Particles (less than 74 microns) Test Using PIV

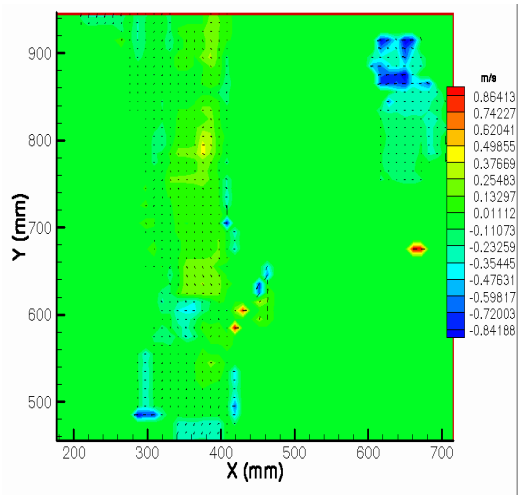


Figure 37 Velocity Profile of Organic Particles (diameter<150microns)

Figure 37 shows the velocity profile of organic particles with the particles diameter of less than 150 microns. The range of particles velocity was between 0.25 m/sec to 0.37 m/sec. The highest velocity was 0.86 m/sec and the minimum velocity was -0.84 m/sec. The negative velocity indicates that the organic particles were so small they sometimes just fly in an upward direction while the velocity was measured.

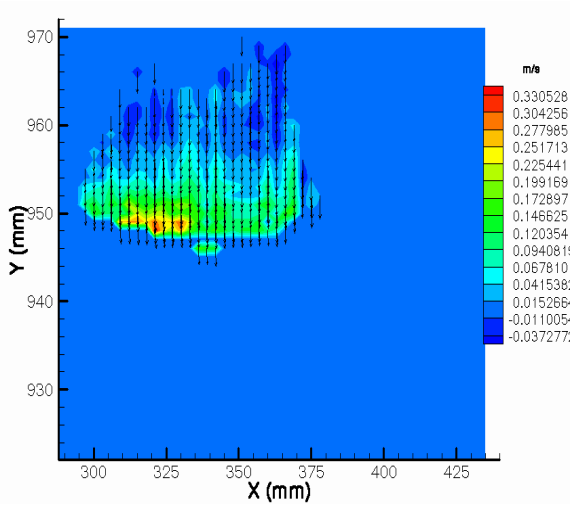


Figure 38 Velocity Profile of Coal Particles (diameter<74 microns)

Figure 38 shows the velocity profile of coal particles with the diameter of less than 74 microns. The range of particles velocity was between 0.12 m/sec to 0.17 m/sec. The highest velocity was 0.33 m/sec and the minimum velocity was -0.03 m/sec.

## 5.5 Organic Particles (less than 150 microns), Organic Particles (between 250 and 355 microns) Test Using PIV

The major PIV test results of organic particles velocity for less than 150 microns and between 250 microns and 355 microns were summarized. The particles were sprayed from the original point of X-axis to increasing point in the particles velocity profile, which indicates the width of particles spray range.

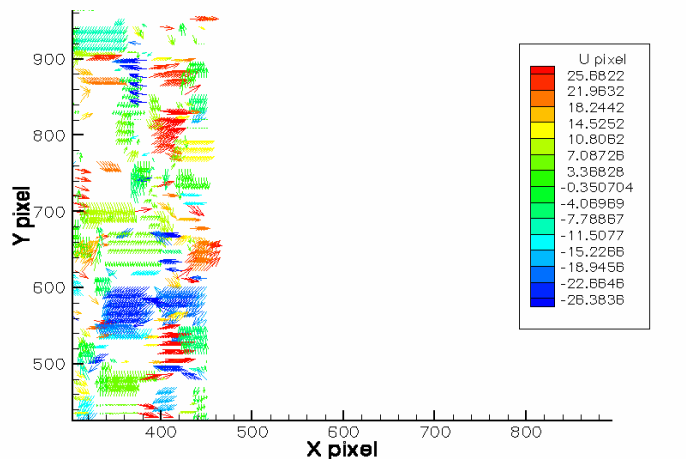


Figure 39 PIV Test Result Using Organic Particles (diameter < 150 microns)

Figure 39 shows the test results under condition of flow rate control gate at 1/8- open and the particles flow section of 0 to 10 cm below the hopper system. The velocity range was between -28.38 cm/sec and 25.68 cm/sec. This was similar with the particles flow section of 0 to 5 cm below the hopper system. At the particles flow section of 0 to 5 cm below the hopper system, most particles have a positive velocity value, but when it goes below, the number of particles with negative velocity increase.

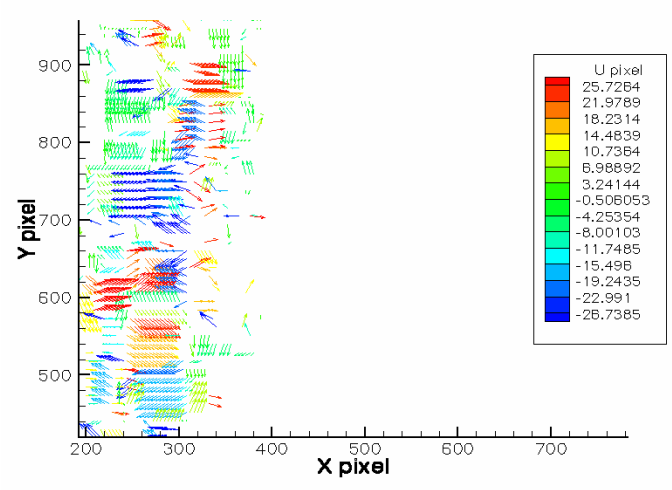


Figure 40 PIV Test Result Using Organic Particles (diameter: 250-355microns)

Figure 40 shows the test result under condition of flow rate control gate at 1/16-open and the section of 0 to 10 cm below the hopper system. Figure 40 shows that the velocity range of the particles was between -26.74 cm/sec and 25.73 cm/sec. Most particles have the velocity between -19.24 cm/sec and 14.48 cm/sec. This particles flow range was wider than the particles flow section of 0 to 5 cm below the hopper system.

## 5.6 Organic Particles (diameter between 150 and 250 microns, between 355 and 425 microns) Test Using PIV in the Open Environment

Two groups of the organic particles were used to conduct the experiment. The particles diameter of the first group was between 355 microns and 425 microns. The particles diameter of the second group was between 150 microns and 250 microns. The flow rate of the hopper control gate was 1/16 and 1/8 open to get different flow rates of the particles. The velocity profile of 5cm and 10cm below the hopper system were captured to see if there was any difference in the velocity range. The major PIV test results of organic particles velocity were summarized. The particles were sprayed from the original point of X-axis to increasing point in the particles velocity profile, which indicated the width of particles spray range.

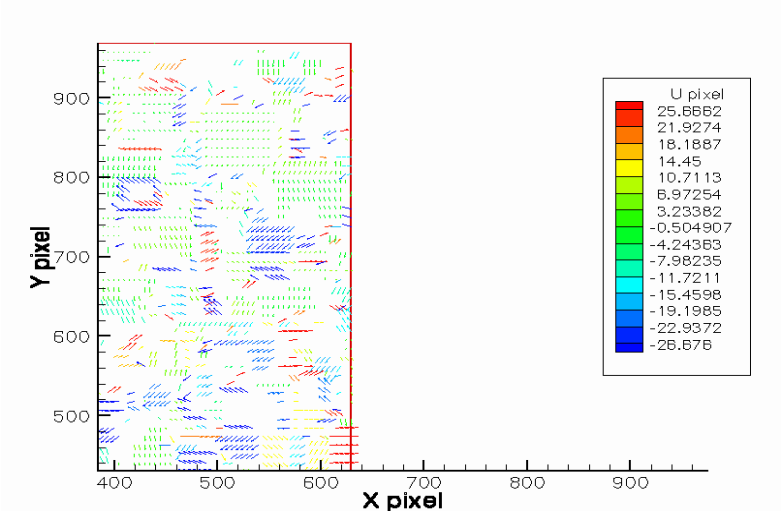


Figure 41 Velocity Profiles of Organic Particles (355 < diameter <425 microns)

Figure 41 shows the test results under condition of flow rate control gate at 1/8- open and the particles flow section of 0 to 10 cm below the hopper system. The velocity range was between -26.68 cm/sec and 25.67 cm/sec. Most of the particles have the velocity between -26.68 cm/sec and 6.98 cm/sec. Most of the particles with low velocity were distributed at the lower section.

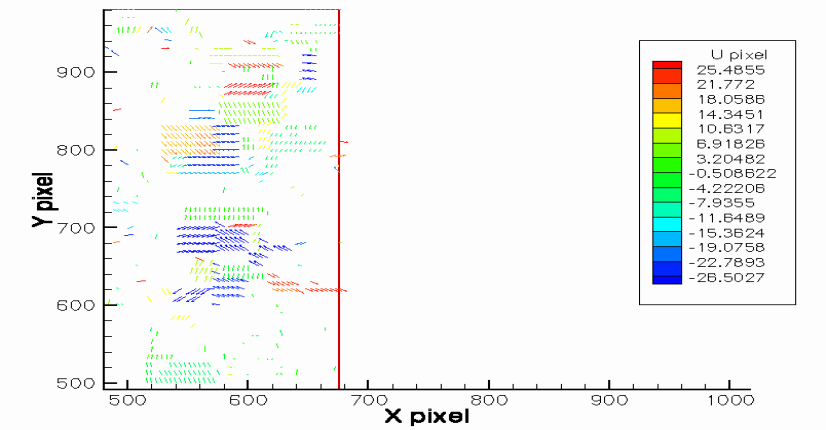


Figure 42 Velocity Profiles of Organic Particles (150 < diameter <250 microns)

Figure 42 shows the test results under condition of flow rate control gate at 1/16- open and the particles flow section of 0 to 10 cm below the hopper system. The velocity range was between -26.50 cm/sec and 25.49 cm/sec. Most of the particles with the velocity of -26.50 cm/sec were distributed at the middle section. At the lower section between 500 and 600 of the Y pixel, the particles velocity was -11.85 cm/sec.

Table 11 Particles Velocity Change for Opening Rate 1/16

| Particles Diameter (microns) | Opening Rate of the Hooper Control Gate (1/16) |
|---|---|
| <150 | -0.26 |
| 150-250 | -0.505 |
| 250-355 | -0.505 |

Table 12 Particles Velocity Change for Opening Rate 1/8

| Particles Diameter (microns) | Opening Rate of the Hooper Control Gate (1/8) |
|---|---|
| <150 | -1.35 |
| 150-250 | -0.49 |
| 250-355 | 0.285 |

The PIV test results were summarized in Table 11 and Table 12. It seems that there was no significant difference of velocity changes between two different diameter ranges of particles. Based on the experimental result, ANOVA (analysis of variance) was applied to analyze data to find the significant factor on particles velocity.

Table 13 Summary of ANOVA for PIV Test Results

| Source of Variation | Sum of Squares | Degree of Freedom | Mean Square | $F_0$ |
|---|---|---|---|---|
| Treatment (Particles Diameter) | 0.4852 | 2 | 0.2426 | 0.543519659 |
| Blocks (Flow Rate) | 0.0135 | 1 | 0.0135 | 0.030245323 |
| Error | 0.8927 | 2 | 0.44635 | |
| Total | 1.3914 | 5 | | |

Table 13 shows the ANOVA table of PIV test. It seems that neither particles diameter nor the particles flow rate have significant effect on the particles velocity because the value of $F_0$ for particles diameter and flow rate were very small.

Table 14 Summary of Particles Velocity Change for Opening Rate 1/16

| Particles Diameter (microns) | Observed Distance | |
|---|---|---|
| | 0-5 cm | 0-10 cm |
| 150-250 | -26.53 ~ 25.57 (cm/sec) | -26.50 ~ 25.49 (cm/sec) |
| 355-425 | -26.59 ~ 25.71 (cm/sec) | -26.49 ~ 25.76 (cm/sec) |

Table 15 Summary of Particles Velocity Change for Opening Rate 1/8

| Particles Diameter (microns) | Observed Distance | |
|---|---|---|
| | 0-5 cm | 0-10 cm |
| 150-250 | -26.75 ~ 25.23 (cm/sec) | -26.36 ~ 25.38 (cm/sec) |
| 355-425 | -26.70 ~ 25.66 (cm/sec) | -26.68 ~ 25.67 (cm/sec) |

Table 14 and Table 15 were the summary of the particles velocity under different experimental condition. When the particles diameter was constant, the particles velocity range increased as the observation range increased. When the opening rates of hopper system and observation range were constant, the velocity range increases as the particles diameter increases. When the observed distance and particles diameter were constant, the lower limit of particles velocity with the hopper system 1/8 open was lower than 1/16 open.

## 5.7 Organic Particles (diameter between 425 and 500 microns) Test Using PIV in the Open Environment

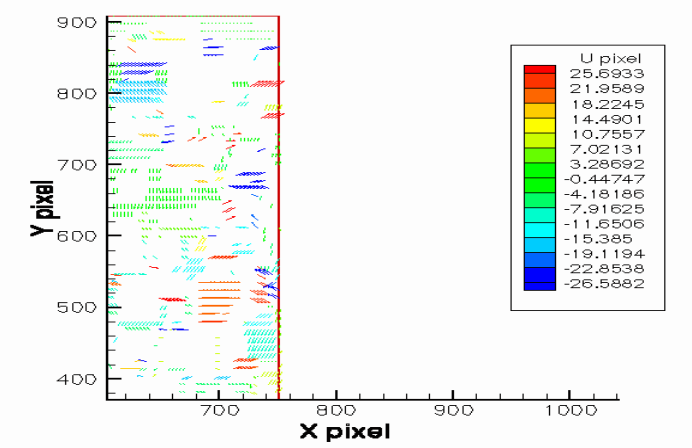


Figure 43 Velocity Profiles of Organic Particles (425 < diameter <500 microns)

Figure 43 shows the test results under condition of flow rate control gate at 1/8- open rate and the particles flow section of 0 cm to 10 cm below the hopper system. The velocity range was between -26.59 cm/sec and 25.69 cm/sec. Particles with high velocity appeared above the area of 500.

Table 16 Summary of Particles Velocity Change under Different Experimental Conditions

| Particles Diameter (microns) | Open Rate of Flow Rate Control Gate | | | |
|---|---|---|---|---|
| | 1/16 | | 1/8 | |
| | Observation Range | | Observation Range | |
| | 5cm | 10cm | 5cm | 10cm |
| <150 | -26.33 – 25.73(cm/s) | -26.30 - 25.78 (cm/s) | -28.77 – 25.53(cm/s) | -28.38 – 25.68(cm/s) |
| 150-250 | -26.53 – 25.57 | -26.50 – 25.49 | -26.75 – 25.23 | -26.36 – 25.38 |
| 250-355 | -26.67 – 25.63 | -26.74 – 25.73 | -25.25 – 25.79 | -25.23 – 25.80 |
| 355-425 | -26.59 – 25.71 | -26.49 – 25.76 | -26.70 – 25.66 | -26.68 – 25.67 |
| 425-500 | -24.48 – 25.89 | -26.77 – 24.57 | -25.99 – 25.67 | -26.59 – 25.69 |

Table 16 shows the summary of the particles velocities under different experimental conditions. There were 5 different groups of particles diameter; below 150 microns, between 150 microns and 250 microns, between 250 microns and 355 microns, between 355 microns and 425 microns; and between 425 microns and 500 microns. The open rate of the flow control gate was 1/16 and 1/8 respectively. The observation range was 5 cm and 10 cm below the hopper system.

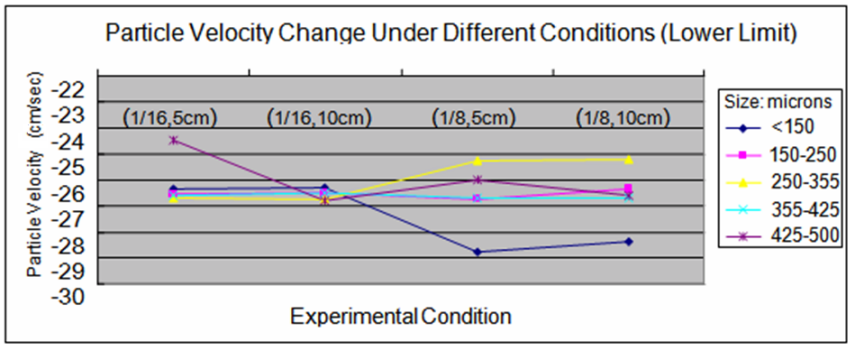


Figure 44 Lower Limit of Particles Velocity Change under Different Experimental Conditions

Figure 44 shows the lower limit of the particles velocity under different experimental conditions. The velocity of the particles sized between 425 microns and 500 microns decreased when the condition changed from (1/16 open rate, observation range: 5cm) to (1/16, 10cm), while others were not changed so much. The velocity of the particles sized between 425 microns and 500 microns decreased when the condition changes from (1/16, 10cm) to (1/8, 5cm), while others increased at that condition.

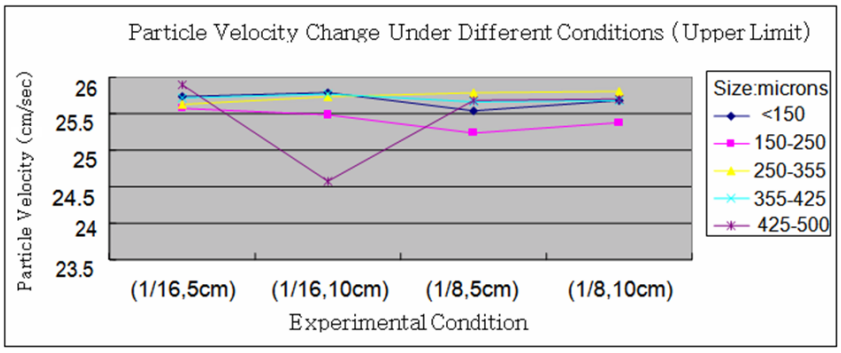


Figure 45 Upper Limit of Particles Velocity Change under Different Experimental Conditions

Figure 45 shows the upper limit of the particles velocity under different experimental conditions. The velocity of the particles sized between 425 microns and 500 microns decreased when the condition changed from (1/16, 5cm) to (1/16, 10cm), while others tend to be increased. The velocity of the particles sized between 425 microns and 500 microns and between 250 microns and 355 microns decreased when the condition changed from (1/16, 10cm) to (1/8, 5cm), while others increased at that condition.

$$SS_{Total} = \sum_i \sum_j \sum_k y_{ijk}^2 - \frac{y_{...}^2}{abn}$$

$$SS_{Size} = \frac{1}{bn} \sum_i y_{i..}^2 - \frac{y_{...}^2}{abn}$$

$$SS_{SubTotale} = \frac{1}{n} \sum_i \sum_j y_{ij.}^2 - \frac{y_{...}^2}{abn}$$

$$SS_{Interaction} = SS_{Total} - SS_{Size} - SS_{FlowRate}$$

$$SS_{Error} = SS_{Total} - SS_{SubTotal}$$

Table 17 ANOVA Table for the Lower Limit of the Particles Velocity

| Source of Variation | Sum of Squares | Degree of Freedom | Mean Square | $F_0$ |
|---|---|---|---|---|
| **Particles Diameter** | 5.91965 | 4 | 1.479912 | 4.99>3.48 |
| **Flow Rate** | 0.5445 | 1 | 0.5445 | 1.84<4.96 |
| **Interaction** | 7.17565 | 4 | 1.793913 | 6.05>3.48 |
| **Error** | 2.9629 | 10 | 0.29629 | |
| **Total** | 16.6027 | 19 | 0.873826 | |

Table 17 was the analysis of variance (ANOVA) table for the lower limit of the particles velocity. As the table shows with 95% of confidence, particles diameter and interaction of particles diameter and flow rate have significant effect on the lower limit of the particles velocity while flow rate had no significant effect on the lower limit of the particles velocity.

Table 18 ANOVA Table for the Upper Limit of the Particles Velocity

| Source of Variation | Sum of Squares | Degree of Freedom | Mean Square | $F_0$ |
|---|---|---|---|---|
| **Particles Diameter** | 0.35847 | 4 | 0.089617 | 0.99<3.48 |
| **Flow Rate** | 0.00288 | 1 | 0.00288 | 0.03<4.96 |

| | | | | |
|---|---|---|---|---|
| **Interaction** | 0.29087 | 4 | 0.072718 | 0.80<3.48 |
| **Error** | 0.9047 | 10 | 0.09047 | |
| **Total** | 1.55692 | 19 | | |

Table 18 was the ANOVA table for the upper limit of the particles velocity. As the table shows, with 95% of confidence, none of the parameters had significant effect on the upper limit of the particles velocity.

## 5.8 Potato Particles (diameter less than 75 microns) Test Using PIV in the Open Environment

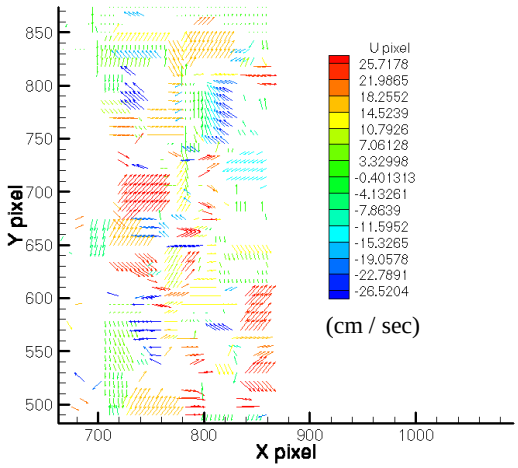


Figure 46 The Particles Velocity Profiles of the Potato Particles (1/8 open rate, 0-5 cm, diameter <75 microns)

Figure 46 shows the test result under condition of flow rate control gate at 1/8 open rate using the potato particles (sizing less than 75 microns). The image range was 0 to 5cm from the flow rate control gate. Figure 46 shows that the velocity range of particles was between -26.5204 cm/sec and 25.7178 cm/sec. From 700 to 500 of Y pixel, most of the particles have positive high velocity.

Table 19 Summary of Potato Particles (diameter less than 75 microns) Velocity Change under Different Experimental Conditions

| Open Rate of Flow Rate Control Gate | Observation Range | Replication1 | Replication2 | Replication3 | Replication4 | Replication5 | Replication6 |
|---|---|---|---|---|---|---|---|
| **1/16** | 0-5 cm | 23.5485 ~ -25.2168 (cm/s) | 23.4515 ~ -26.8126(cm/s) | 24.7051 ~ -25.5237(cm/s) | 25.709 ~ -26.6757(cm/s) | 24.6155 ~ -26.5592(cm/s) | 25.2544 ~ -25.4284(cm/s) |

| | | | | | | | |
|---|---|---|---|---|---|---|---|
| | 5-10 cm | 25.4627 ~ -26.5766 (cm/s) | 25.274 ~ -26.6733(cm/s) | 24.6679 ~ -26.8168(cm/s) | 25.3959 ~ -26.7716(cm/s) | 25.3706 ~ -26.55(cm/s) | 25.379 ~ -26.3116(cm/s) |
| **1/8** | 0-5 cm | 25.3534 ~ -26.5647(cm/s) | 25.4733 ~ -26.6778(cm/s) | 24.8942 ~ -26.7163(cm/s) | 25.7178 ~ -26.5204(cm/s) | 25.6859 ~ -26.5941(cm/s) | 25.2917 ~ -26.7065(cm/s) |
| | 5-10 cm | 25.7168 ~ -26.6482(cm/s) | 25.6236 ~ -26.751(cm/s) | 25.6312 ~ -26.7558(cm/s) | 25.6386 ~ -26.7307(cm/s) | 25.5087 ~ -26.6547(cm/s) | 25.2916 ~ -26.6019(cm/s) |

Table 19 shows the summary of particles velocity change under different experimental conditions. There were two different groups of flow rate 1/16 open rate and 1/8 open rate. The observation range was 0 ~ 5 cm below the hopper system and 5~10 cm below the hopper system.

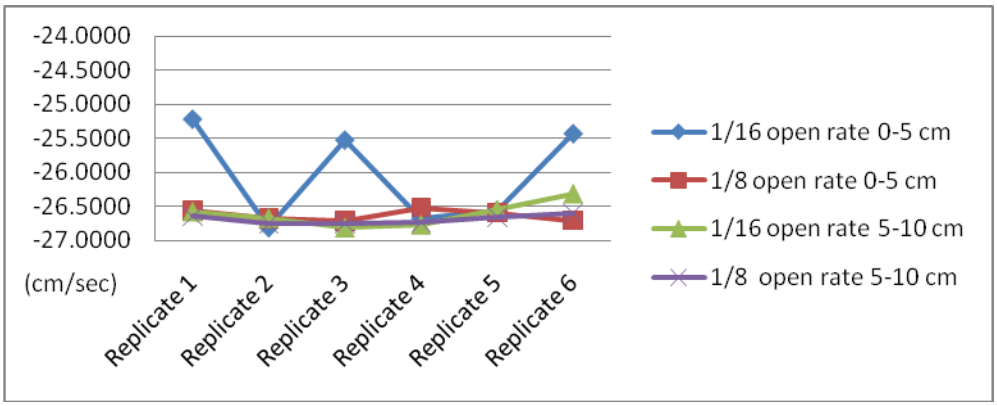


Figure 47 Potato Particles (diameter less than 75 microns) Velocity Change under Different Conditions (Lower Limit)

Figure 47 shows the lower limit of the particles velocity under different experimental conditions. The widest velocity was ranged at 0~5 cm from the flow rate control gate with the 1/16 open rate. The results also shows 1/8 open rate and observation range of 0~5 cm, 1/16 open rate and observation range of 5~10 cm, and 1/8 open rate and observation range of 5~10 cm. They have similar velocity range and more stable in lower limit. The other three cases were not affected by the experiment number and also the velocity range was very small.

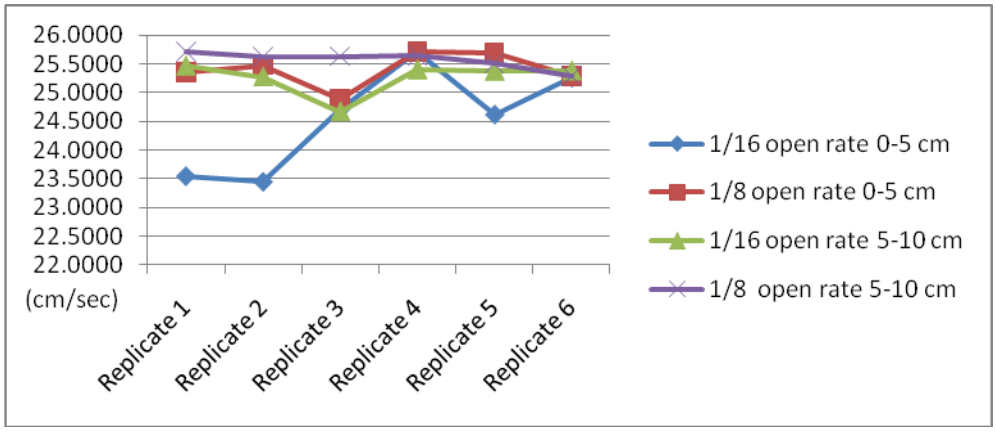


Figure 48 Potato Particles (diameter less than 75 microns) Velocity Change under Different Conditions (Upper Limit)

Figure 48 shows the upper limit of the particles velocity under different experimental conditions. The widest velocity was ranged at 0~ 5 cm from the flow rate control gate with the 1/16 open rate. The results also show the velocity range under the condition of 1/8 open rate and observation range of 5 cm to 10 cm, which had almost no change.

$$SS_{OpenRate} = \frac{[ab + a - b - (1)]^2}{4n}$$

$$SS_{ObserveRange} = \frac{[ab + b - a - (1)]^2}{4n}$$

$$SS_{Interaction} = \frac{[ab + (1) - a - b]^2}{4n}$$

$$SS_{Error} = SS_{Total} - SS_{OpenRatel} - SS_{ObserveRange} - SS_{Interaction}$$

$$SS_{Total} = \sum_{i=1}^{2}\sum_{j=1}^{2}\sum_{k=1}^{n} y_{ijk}^2 - \frac{y_{...}^2}{4n}$$

Table 20 ANOVA Table for the Lower Limit of the Potato Particles (diameter less than 75 microns) Velocity

| ***Source of variation*** | ***Sum of Squares*** | ***Degrees of Freedom*** | ***Mean Square*** | $F_0$ |
|---|---|---|---|---|
| **Open rate** | 0.6686 | 1 | 0.6686 | 4.76 > 4.28 |
| **Observe Range** | 0.6163 | 1 | 0.6163 | 4.39 >4.28 |
| **Interaction** | 0.4059 | 1 | 0.4059 | 2.89 <4.28 |
| **ERROR** | 2.8088 | 20 | 0.1404 | |
| **TOTAL** | 4.4996 | 23 | | |

Table 20 was the analysis of variance (ANOVA) table for the lower limit of the particles velocity.[32] The open rate of flow rate control gate and observation range have significant effect on the lower limit of the particles velocity with 95% of confidence, However the interaction had no significant effect on the lower limit of the particles velocity.

Table 21 ANOVA Table for the Upper Limit of the Potato Particles (diameter less than 75 microns) Velocity

| *Source of variation* | *Sum of Squares* | *Degrees of Freedom* | *Mean Square* | $F_0$ |
|---|---|---|---|---|
| **Open rate** | 2.0374 | 1 | 2.0374 | 8.01 >4.28 |
| **Observe Range** | 1.1529 | 1 | 1.1529 | 4.53 >4.28 |
| **Interaction** | 0.4461 | 1 | 0.4461 | 1.75 <4.28 |
| **ERROR** | 5.0861 | 20 | 0.2543 | |
| **TOTAL** | 8.7225 | 23 | | |

Table 21 was the analysis of variance (ANOVA) table for the lower limit of the particles velocity. The open rate of flow rate control gate and observation range have significant effect on the upper limit of the particles velocity with 95% of confidence, but the interaction had no significant effect on the upper limit of the particles velocity.

## 5.9 Potato Particles (diameter between 63 and 75 microns) and Wheat Particles (diameter between 63 and 75 microns) Test Using PIV in the Open Environment

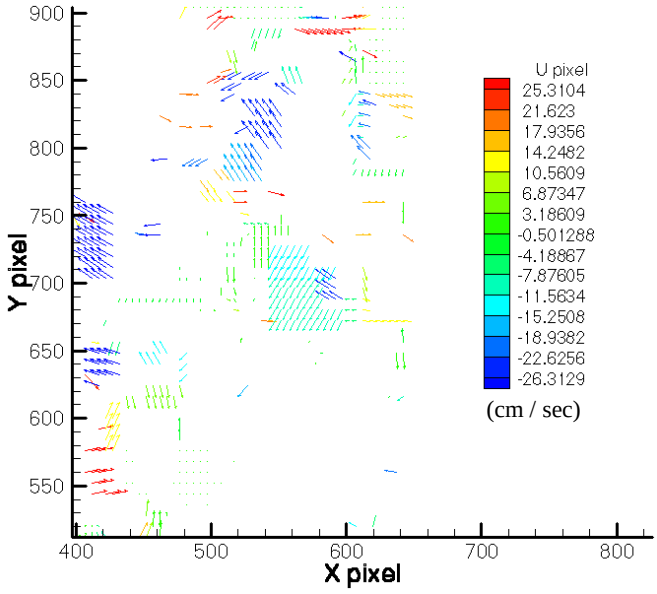


Figure 49 The Particles Velocity Profiles of the Potato Particles (1/8 open rate, 0-5 cm, 63<diameter<75 microns)

Figure 49 shows the test result under condition of flow rate control gate at 1/8 open rate using the potato particles (sizing between 63 microns to 75 microns). The image range was 0 cm to 5cm from the flow rate control gate. Also shows that the velocity range of particles was between -26.3129 cm/sec and 25. 3104 cm/sec. Most of particles have negative velocity.

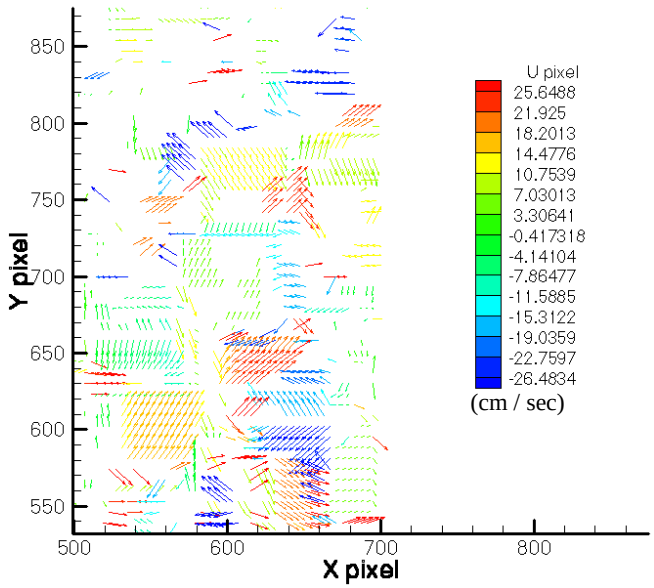


Figure 50 The Particles Velocity Profiles of the Wheat Particles (1/8 open rate, 0-5 cm, 63<diameter<75 microns)

Figure 50 shows the test result under condition of flow rate control gate at 1/8 open rate using the wheat particles (sizing between 63 microns 75 microns). The image range was 0 cm to 5cm from the flow rate control gate. Also shows that the velocity range of particles was between -26.4834 cm/sec and 25.6488 cm/sec. In the middle section from 700 to 650 of Y pixel, most of particles have positive velocity.

Table 22 Summary of Particles Velocity Change under Different Experimental Conditions

| *Particles Type* | *Open Rate of Flow Rate Control Gate* | *Observation Range* | *Replication1* | *Replication2* | *Replication3* | *Replication4* | *Replication5* | *Replication6* |
|---|---|---|---|---|---|---|---|---|
| Potato | **1/16** | 0-5 cm | 25.3741 ~ -26.1528(cm/s) | 25.2562 ~ -26.311 (cm/s) | 24.4326 ~ -26.6394(cm/s) | 25.3141 ~ -26.3077(cm/s) | 25.1886 ~ -26.3487(cm/s) | 25.4196 ~ -26.5567(cm/s) |
| | | 5-10 cm | 25.5846 ~ -26.7431(cm/s) | 25.5947 ~ -26.2417(cm/s) | 25.7304 ~ -26.7465(cm/s) | 25.6799 ~ -26.7133(cm/s) | 25.7186 ~ 26.6281(cm/s) | 25.5164 ~ -25.5144(cm/s) |
| | **1/8** | 0-5 cm | 25.542 ~ -26.1086(cm/s) | 25.4737 ~ -26.3487(cm/s) | 25.3242 ~ -26.3915(cm/s) | 25.4726 ~ -26.624(cm/s) | 25.5347 ~ -26.5569(cm/s) | 25.3104 ~ -26.3129(cm/s) |
| | | 5-10 cm | 25.7237 ~ -26.468(cm/s) | 24.2289 ~ -25.1868(cm/s) | 25.6694 ~ -26.2999(cm/s) | 25.3406 ~ -26.1377(cm/s) | 25.7354 ~ -26.6531(cm/s) | 25.3891 ~ -26.4835(cm/s) |

| | | | | | | | | |
|---|---|---|---|---|---|---|---|---|
| Wheat | **1/16** | 0-5 cm | 25.5421 ~ -26.6268(cm/s) | 25.6471 ~ -26.6906(cm/s) | 25.4527 ~ -26.6914(cm/s) | 25.6897 ~ -26.6896(cm/s) | 25.2867 ~ -26.7419(cm/s) | 25.5393 ~ -26.6529(cm/s) |
| | | 5-10 cm | 25.745 ~ -26.6591(cm/s) | 25.7097 ~ -26.4834(cm/s) | 25.7447 ~ -26.7374(cm/s) | 25.7266 ~ -26.6313(cm/s) | 25.6849 ~ -26.3556(cm/s) | 25.7477 ~ -26.7362(cm/s) |
| | **1/8** | 0-5 cm | 25.746 ~ -26.6591(cm/s) | 25.6488 ~ -26.4834(cm/s) | 25.6428 ~ -26.701(cm/s) | 25.6826 ~ -26.6253(cm/s) | 25.7651 ~ -26.0624(cm/s) | 25.7072 ~ -26.6054(cm/s) |
| | | 5-10 cm | 24.9778 ~ -26.5356(cm/s) | 25.1738 ~ -26.5356(cm/s) | 25.3968 ~ -26.6858(cm/s) | 25.6453 ~ -26.6531(cm/s) | 25.3147 ~ -26.4281(cm/s) | 25.3046 ~ -26.5126(cm/s) |

Table 22 shows the summary of particles velocity change under different experimental conditions. There were two different groups of flow rate 1/16 open rate and 1/8 open rate. The observation range was 0 ~ 5 cm below the hopper system and 5~10 cm below the hopper system.

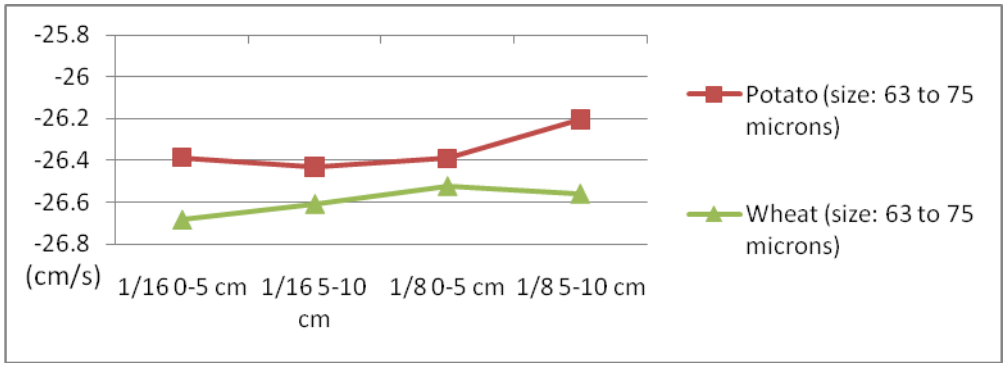


Figure 51 Particles Velocity Change under Different Conditions (Lower Limit)

Figure 51 shows the lower limit of the particles velocity under different experimental conditions. Each point shows the mean velocity of particles under each experimental condition. The widest velocity was ranged at potato particles with diameter between 63 microns to 75 microns in lower limit.

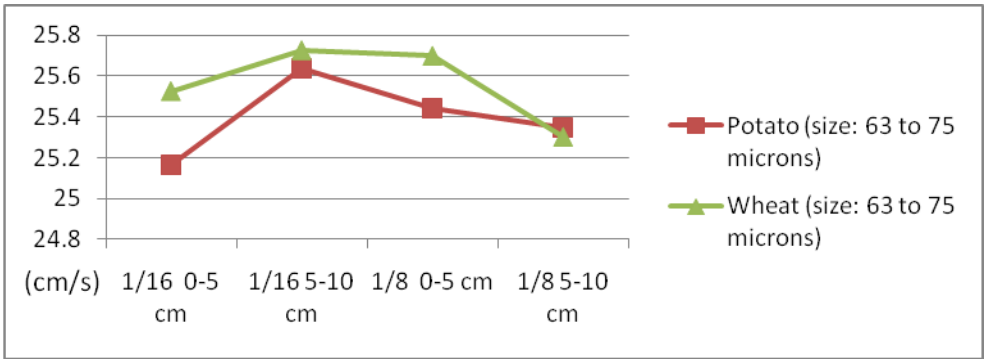


Figure 52 Particles Velocity Change under Different Conditions (Upper Limit)

Figure 52 shows the upper limit of the particles velocity under different experimental conditions.

Each point shows the mean velocity of particles under each experimental condition. The widest velocity was ranged at potato particles with diameter between 63 microns to 75 microns in upper limit.

Table 23 The Analysis of Variance Table for the Three-Factor Fixed Effects Model

| **Source of Variation** | **Sum of Squares** | **Degrees of Freedom** | **Mean Square** | **$F_0$** |
|---|---|---|---|---|
| A | $SS_A$ | a - 1 | $MS_A=SS_A/(a-1)$ | $MS_A/ MS_E$ |
| B | $SS_B$ | b - 1 | $MS_B=SS_B/(b-1)$ | $MS_B/ MS_E$ |
| C | $SS_C$ | c - 1 | $MS_C=SS_C/(c-1)$ | $MS_C/ MS_E$ |
| AB | $SS_{AB}$ | (a -1)(b - 1) | $MS_{AB}=SS_{AB}/((a-1)(b-1))$ | $MS_{AB}/ MS_E$ |
| AC | $SS_{AC}$ | (a -1)(c - 1) | $MS_{AC}=SS_{AC}/((a -1)(c - 1))$ | $MS_{AC}/ MS_E$ |
| BC | $SS_{BC}$ | (b – 1)(c – 1) | $MS_{BC}=SS_{BC}/((b – 1)(c – 1))$ | $MS_{BC}/ MS_E$ |
| ABC | $SS_{ABC}$ | (a - 1)(b - 1)(c - 1) | $MS_{ABC}=SS_{ABC}/((a - 1)(b - 1)(c - 1))$ | $MS_{ABC}/ MS_E$ |
| Error | $SS_E$ | abc(n – 1) | $MS_E=SS_E/(abc(n-1))$ | |
| Total | $SS_T$ | abcn -1 | | |

There were a levels of factor A, b levels of factor B, c levels of factor C, and assuming that A, B, and C were fixed, the analysis of variance table was shown in Table 23. The sum of squares were found from

$$SS_T = \sum_{i=1}^{a}\sum_{j=1}^{b}\sum_{k=1}^{c}\sum_{l=1}^{n} y_{ijkl}^2 - \frac{y_{....}^2}{abcn} \qquad SS_A = \frac{1}{bcn}\sum_{i=1}^{a} y_{i...}^2 - \frac{y_{....}^2}{abcn}$$

$$SS_B = \frac{1}{acn}\sum_{j=1}^{b} y_{.j..}^2 - \frac{y_{....}^2}{abcn} \qquad SS_C = \frac{1}{abn}\sum_{k=1}^{c} y_{..k.}^2 - \frac{y_{....}^2}{abcn}$$

$$SS_{AB} = \frac{1}{cn}\sum_{i=1}^{a}\sum_{j=1}^{b} y_{ij..}^2 - \frac{y_{....}^2}{abcn} - SS_A - SS_B \qquad SS_{AC} = \frac{1}{bn}\sum_{i=1}^{a}\sum_{k=1}^{c} y_{i.k.}^2 - \frac{y_{....}^2}{abcn} - SS_B - SS_C$$

$$SS_{BC} = \frac{1}{an}\sum_{j=1}^{b}\sum_{k=1}^{c} y_{.jk.}^2 - \frac{y_{....}^2}{abcn} - SS_B - SS_C$$

$$SS_{ABC} = \frac{1}{n}\sum_{i=1}^{a}\sum_{j=1}^{b}\sum_{k=1}^{c} y_{ijk}^2 - \frac{y_{...}^2}{abcn} - SS_A - SS_B - SS_C - SS_{AB} - SS_{AC} - SS_{BC}$$

$$SS_E = SS_T - SS_A - SS_B - SS_C - SS_{AB} - SS_{AC} - SS_{BC} - SS_{ABC}$$

Table 24 ANOVA Table for the Lower Limit of the Particles Velocity

| *Source of variation* | *Sum of Squares* | *Degrees of Freedom* | *Mean Square* | $F_0$ | P value |
|---|---|---|---|---|---|
| **Type** | 0.68808 | 1 | 0.68808 | 8.15 > 4.08 | 0.007 |
| **Open rate** | 0.13857 | 1 | 0.13857 | 1.64 < 4.08 | 0.208 |
| **Observation Range** | 0.02432 | 1 | 0.02432 | 0.29 < 4.08 | 0.595 |
| **Type * Open rate** | 0.00015 | 1 | 0.00015 | 0.00 < 4.08 | 0.967 |
| **Type * Observation range** | 0.00763 | 1 | 0.00763 | 0.09 < 4.08 | 0.765 |
| **Open rate * Observation range** | 0.01075 | 1 | 0.01075 | 0.13 < 4.08 | 0.723 |
| **Type * Open rate * Observation range** | 0.08759 | 1 | 0.08759 | 1.04 < 4.08 | 0.315 |
| **ERROR** | 3.37821 | 40 | 0.08446 | | |
| **TOTAL** | 4.33530 | 47 | | | |

Table 24 was the analysis of variance (ANOVA) table for the lower limit of the particles velocity. The particles type had significant effect on the lower limit of the particles velocity with 95% of confidence.

Table 25 ANOVA Table for the Upper Limit of the Particles Velocity

| *Source of variation* | *Sum of Squares* | *Degrees of Freedom* | *Mean Square* | $F_0$ | P value |
|---|---|---|---|---|---|
| **Type** | 0.32789 | 1 | 0.32789 | 4.72 > 4.08 | 0.036 |
| **Open rate** | 0.05173 | 1 | 0.05173 | 0.74 < 4.08 | 0.394 |
| **Observation Range** | 0.02477 | 1 | 0.02477 | 0.36 < 4.08 | 0.554 |
| **Type * Open rate** | 0.04354 | 1 | 0.04354 | 0.63 < 4.08 | 0.433 |
| **Type * Observation range** | 0.24760 | 1 | 0.24760 | 3.56 < 4.08 | 0.066 |
| **Open rate * Observation range** | 1.01804 | 1 | 1.01804 | 14.64<4.08 | 0.000 |
| **Type * Open rate * Observation range** | 0.00061 | 1 | 0.00061 | 0.01 < 4.08 | 0.926 |
| **ERROR** | 2.78155 | 40 | 0.06954 | | |
| **TOTAL** | 4.49572 | 47 | | | |

Table 25 was the analysis of variance (ANOVA) table for the lower limit of the particles velocity. The particles type and interaction of open rate and observation range have significant effect on the upper limit of the particles velocity with 95% of confidence.

## 5.10 Coal Particles (diameter between 63 and 75 microns) and Organic Particles (diameter between 63 and 75 microns) Test Using PIV in the Open Environment

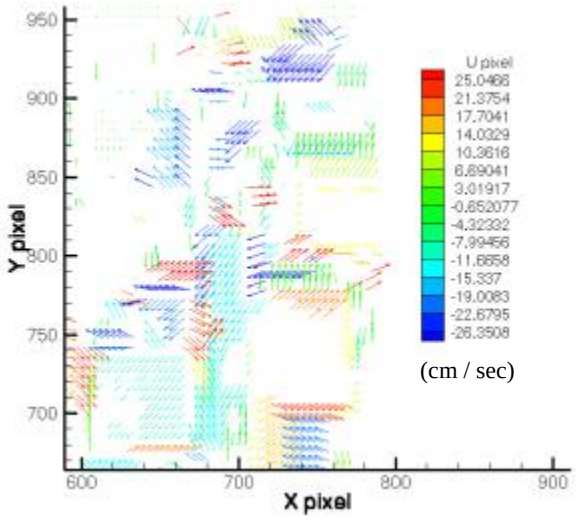


Figure 53 The Particles Velocity Profiles of the Coal Particles (1/8 open rate, 0-5 cm, 63<diameter<75 microns)

Figure 53 shows the test result under the condition of flow rate control gate at 1/8 open rate using the coal particles (sizing between 63 microns and 75 microns). The image range was 0 cm to 5cm from the flow rate control gate. The result also shows that the velocity range of particles was between -26.3508 cm/sec and 25. 0466 cm/sec. Most of particles have negative velocity.

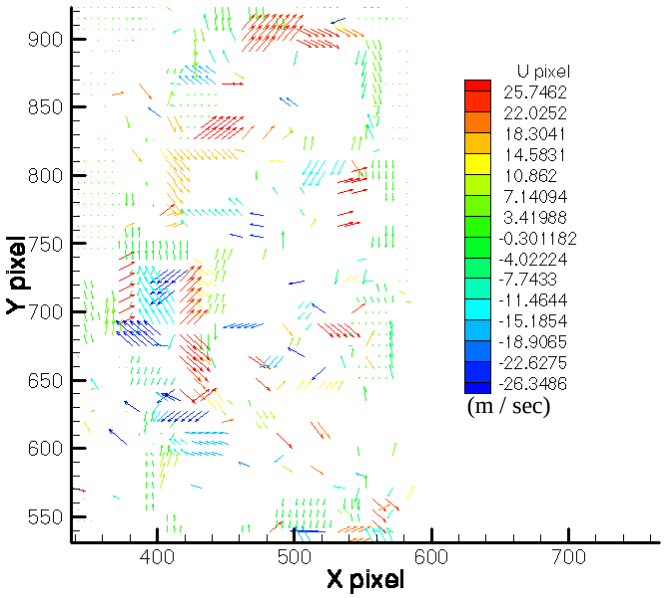


Figure 54 The Particles Velocity Profiles of the Organic Particles (1/8 open rate, 0-5 cm, 63<diameter<75 microns)

Figure 54 shows the test result under the condition of flow rate control gate at 1/8 open rate using the organic particles (sizing between 63 microns and 75 microns). The image range was 0 cm to 5cm from the flow rate control gate. The result also shows that the velocity range of particles was between -26.3486 cm/sec and 25.7462 cm/sec. Most of particles have positive velocity.

Table 26 Summary of Coal Particles (diameter between 63 and 75 microns) and Organic Particles (diameter between 63 and 75 microns) Velocity Changes under Different Experimental Conditions

| *Particles Type* | *Open Rate of Flow Rate Control Gate* | *Observation Range* | *Replication1* | *Replication2* | *Replication3* | *Replication4* | *Replication5* | *Replication6* |
|---|---|---|---|---|---|---|---|---|
| Coal | **1/16** | 0-5 cm | 25.6382 ~ -26.2836(cm/s) | 25.3408 ~ -26.4134(cm/s) | 25.1251 ~ -26.4046(cm/s) | 25.7534 ~ -26.3374(cm/s) | 24.9134 ~ -26.3175(cm/s) | 25.6665 ~ -26.3456(cm/s) |
| | | 5-10 cm | 25.3566 ~ -25.5939(cm/s) | 25.7496 ~ -26.3794(cm/s) | 25.4458 ~ -26.3069(cm/s) | 25.283 ~ -26.4904(cm/s) | 25.2869 ~ -26.5609(cm/s) | 24.5663 ~ -26.3661(cm/s) |
| | **1/8** | 0-5 cm | 25.0466 ~ -26.3508(cm/s) | 25.1845 ~ -26.598(cm/s) | 25.23 ~ -26.6022(cm/s) | 25.4285 ~ -26.2958(cm/s) | 25.5292 ~ -26.7461(cm/s) | 25.7183 ~ -26.714(cm/s) |
| | | 5-10 cm | 25.3333 ~ -26.2901(cm/s) | 25.6692 ~ -26.2991(cm/s) | 24.9942 ~ -26.6038(cm/s) | 24.4018 ~ -26.192(cm/s) | 25.3168 ~ -26.6359(cm/s) | 25.3277 ~ -26.3187(cm/s) |
| Organic | **1/16** | 0-5 cm | 25.5077 ~ -24.5443(cm/s) | 25.3272~ -26.3648(cm/s) | 25.3608 ~ -26.6461(cm/s) | 23.4355 ~ -26.8565(cm/s) | 25.4863 ~ -26.5479(cm/s) | 24.9955 ~ -26.6786(cm/s) |
| | | 5-10 cm | 25.6649 ~ -26.2721(cm/s) | 25.7537 ~ -26.625(cm/s) | 25.5464 ~ -25.613(cm/s) | 25.5437 ~ -26.3963(cm/s) | 25.712 ~ -26.7353(cm/s) | 25.6836 ~ -25.7429(cm/s) |
| | **1/8** | 0-5 cm | 25.6874 ~ -26.4267(cm/s) | 25.3224 ~ -26.6907(cm/s) | 25.4226 ~ -26.6475(cm/s) | 25.7462 ~ -26.3486(cm/s) | 25.7994 ~ -24.6174(cm/s) | 25.3062 ~ -26.6025(cm/s) |
| | | 5-10 cm | 25.6128 ~ -26.2548(cm/s) | 25.4387 ~ -26.7019(cm/s) | 25.5334 ~ -25.8571(cm/s) | 25.5175 ~ -26.6016(cm/s) | 25.5249 ~ 26.4721(cm/s) | 25.5307 ~ -26.6806(cm/s) |

Table 26 shows the summary of particles velocity change under different experimental conditions. There were two different groups of flow rate 1/16 open rate and 1/8 open rate. The observation range was 0 ~ 5 cm below the hopper system and 5~10 cm below the hopper system.

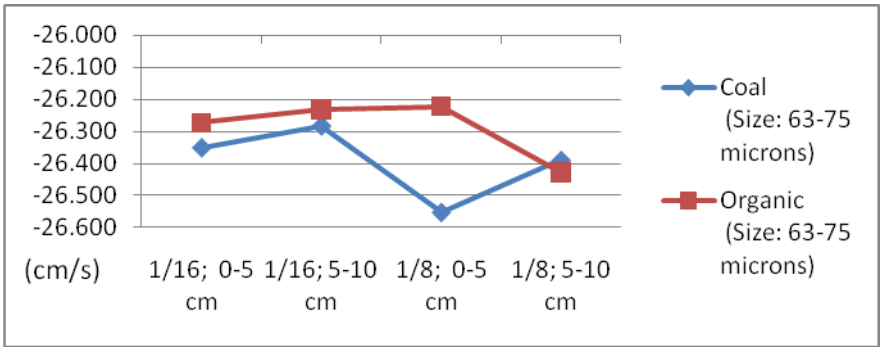


Figure 55 Coal Particles (diameter between 63 and 75 microns) and Organic Particles (diameter between 63 and 75 microns) Velocity Change under Different Conditions (Lower Limit)

Figure 55 shows the lower limit of the particles velocity under different experimental conditions. Each point shows the mean velocity of particles under each experimental condition. The widest velocity was ranged at coal particles with diameter between 63 microns and 75 microns on the lower limit.

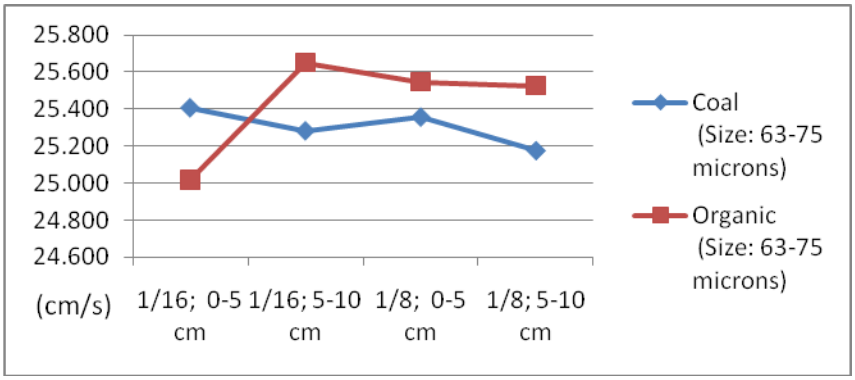


Figure 56 Coal Particles (diameter between 63 and 75 microns) and Organic Particles (diameter between 63 and 75 microns) Velocity Change under Different Conditions (Upper Limit)

Figure 56 shows the upper limit of the particles velocity under different experimental conditions. Each point shows the mean velocity of particles under each experimental condition. The widest velocity was ranged at organic particles with diameter between 63 microns and 75 microns on the upper limit.

Table 27 ANOVA Table for the Lower Limit of the Coal Particles (diameter between 63 and 75 microns) and Organic Particles (diameter between 63 and 75 microns) Velocity

| ***Source of variation*** | ***Sum of Squares*** | ***Degrees of Freedom*** | ***Mean Square*** | ***$F_0$*** | **P value** |
|---|---|---|---|---|---|
| **Type** | 0.1325 | 1 | 0.1325 | 0.56 < 4.08 | 0.458 |
| **Open rate** | 0.1548 | 1 | 0.1548 | 0.66 < 4.08 | 0.423 |
| **Observation Range** | 0.0032 | 1 | 0.0032 | 0.01 < 4.08 | 0.908 |
| **Type * Open rate** | 0.0195 | 1 | 0.0195 | 0.08 < 4.08 | 0.775 |
| **Type * Observation range** | 0.1153 | 1 | 0.1153 | 0.49 < 4.08 | 0.489 |
| **Open rate * Observation range** | 0.0178 | 1 | 0.0178 | 0.08 < 4.08 | 0.785 |
| **Type * Open rate * Observation range** | 0.0876 | 1 | 0.0876 | 0.37 < 4.08 | 0.546 |
| **ERROR** | 9.4482 | 40 | 0.2362 | | |
| **TOTAL** | 9.9790 | 47 | | | |

Table 27 shows the analysis of variance (ANOVA) table for the lower limit of the particles velocity. There was no significant effect on the lower limit of the particles velocity for the source of variation with 95% of confidence.

Table 28 ANOVA Table for the Upper Limit of the Coal Particles (diameter between 63 and 75 microns) and Organic Particles (diameter between 63 and 75 microns) Velocity

| *Source of variation* | *Sum of Squares* | *Degrees of Freedom* | *Mean Square* | $F_0$ | P value |
|---|---|---|---|---|---|
| **Type** | 0.2072 | 1 | 0.2072 | 1.37 < 4.08 | 0.249 |
| **Open rate** | 0.0456 | 1 | 0.0456 | 0.30 < 4.08 | 0.586 |
| **Observation Range** | 0.0691 | 1 | 0.0691 | 0.46 < 4.08 | 0.503 |
| **Type * Open rate** | 0.2367 | 1 | 0.2367 | 1.56 < 4.08 | 0.219 |
| **Type * Observation range** | 0.6321 | 1 | 0.6321 | 4.17 > 4.08 | 0.048 |
| **Open rate * Observation range** | 0.3785 | 1 | 0.3785 | 2.50 < 4.08 | 0.122 |
| **Type * Open rate * Observation range** | 0.2659 | 1 | 0.2659 | 1.76 < 4.08 | 0.193 |
| **ERROR** | 6.0597 | 40 | 0.1515 | | |
| **TOTAL** | 7.8948 | 47 | | | |

Table 28 shows the analysis of variance (ANOVA) table for the lower limit of the particles velocity. The interaction of type of particles and observation range had a significant effect on the upper limit of the particles velocity with 95% of confidence.

## 5.11 Organic Particles (diameter between 63 and 75 microns) and Wheat Particles (diameter between 63 and 75 microns) Test Using PIV in the Closed Environment

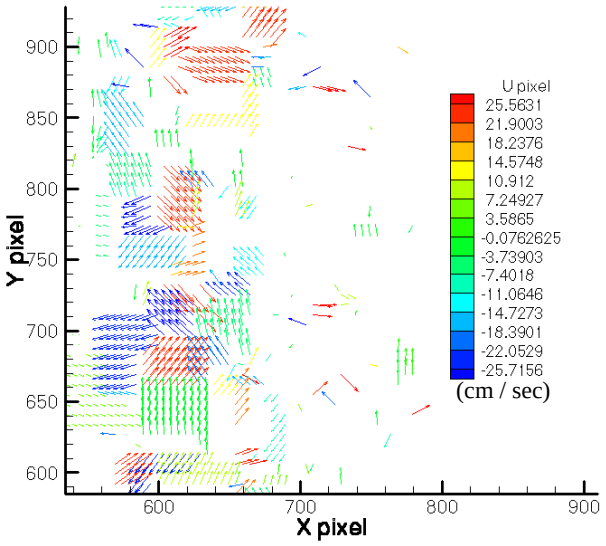


Figure 57 The Particles Velocity Profiles of the Organic Particles in the Closed Environment (1/8 open rate, 0-5 cm, 63<diameter<75 microns)

Figure 57 shows the test result under condition of flow rate control gate at 1/8 open rate using the organic particles (sizing between 63 microns and 75 microns) in the closed environment. The image range was 0 cm to 5cm from the flow rate control gate. The result also shows that the velocity range of particles was between -25.7156 cm/sec and 25.5631 cm/sec. In the middle section from 700 to 650 of Y pixel, most of particles have negative velocity.

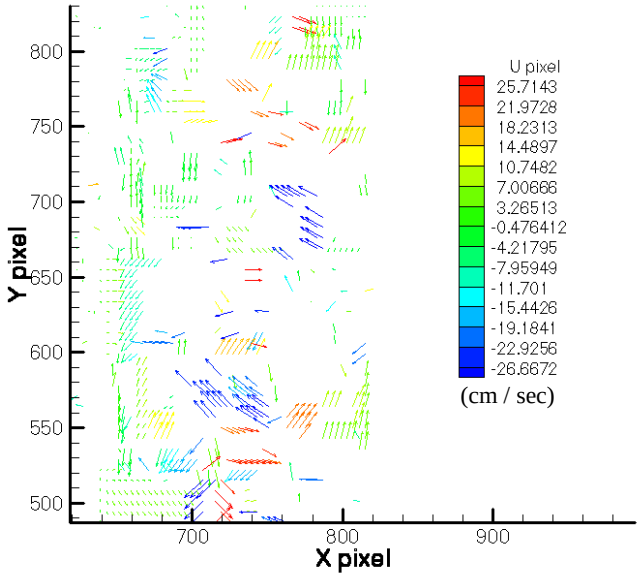


Figure 58 The Particles Velocity Profiles of the Wheat Particles in the Closed Environment (1/8 open rate, 0-5 cm, 63<diameter<75 microns)

Figure 58 shows the test result under the condition of flow rate control gate at 1/8 open rate using the wheat particles (sizing between 63 microns and 75 microns). The image range was 0 cm to 5cm from the flow rate control gate. The result also shows that the velocity range of particles was between -26.6672 cm/sec and 25.7143 cm/sec. Most of particles have negative velocity.

Table 29 Summary of Organic Particles (diameter between 63 and 75 microns) and Wheat Particles (diameter between 63 and 75 microns) Velocity Changes under Different Experimental Conditions

| *Particles Type* | *Open Rate of Flow Rate Control Gate* | *Observation Range* | *Replication1* | *Replication2* | *Replication3* | *Replication4* | *Replication5* | *Replication6* |
|---|---|---|---|---|---|---|---|---|
| Open Environment Organic | **1/16** | 0-5 cm | 25.5077 ~ -24.5443(cm/s) | 25.3272~ -26.3648(cm/s) | 25.3608 ~ -26.6461(cm/s) | 23.4355 ~ -26.8565(cm/s) | 25.4863 ~ -26.5479(cm/s) | 24.9955 ~ -26.6786(cm/s) |
| | | 5-10 cm | 25.2623 ~ -25.4744(cm/s) | 25.7537 ~ -26.625(cm/s) | 25.5464 ~ -25.613(cm/s) | 25.5437 ~ -26.3963(cm/s) | 25.712 ~ -26.7353(cm/s) | 25.4059 ~ -26.6516(cm/s) |
| | **1/8** | 0-5 cm | 25.6874 ~ -26.4267(cm/s) | 25.3224 ~ -26.6907(cm/s) | 25.4226 ~ -26.6475(cm/s) | 25.7462 ~ -26.3486(cm/s) | 25.7994 ~ -24.6174(cm/s) | 24.9098 ~ -26.4644(cm/s) |

| | | | | | | | | |
|---|---|---|---|---|---|---|---|---|
| | | 5-10 cm | 25.244 ~ -26.7185(cm/s) | 25.4387 ~ -26.7019(cm/s) | 25.5334 ~ -25.8571(cm/s) | 25.5175 ~ -26.6016(cm/s) | 25.5249 ~ 26.4721(cm/s) | 25.5307 ~ -26.6806(cm/s) |
| Closed Environment Organic | **1/16** | 0-5 cm | 25.6589 ~ -26.3427(cm/s) | 25.471 ~ -26.3196(cm/s) | 25.7605 ~ -26.5268(cm/s) | 25.4336 ~ -26.3269(cm/s) | 25.6753 ~ -26.6079(cm/s) | 25.6777 ~ -26.687(cm/s) |
| | | 5-10 cm | 25.8081 ~ -25.4563(cm/s) | 25.5031 ~ -26.7628(cm/s) | 25.389 ~ -26.4196(cm/s) | 25.6249 ~ -26.6092(cm/s) | 25.7614 ~ -26.403(cm/s) | 25.3243 ~ -26.4699(cm/s) |
| | **1/8** | 0-5 cm | 23.8018 ~ -26.5323(cm/s) | 24.5662 ~ -26.7762(cm/s) | 25.5631 ~ -25.7156(cm/s) | 25.4205 ~ -26.6263(cm/s) | 25.3009 ~ -26.5283(cm/s) | 25.2689 ~ -26.5286(cm/s) |
| | | 5-10 cm | 25.5908 ~ -26.6967(cm/s) | 25.6658 ~ -26.6977(cm/s) | 25.5371 ~ -26.5399(cm/s) | 25.7527 ~ -26.5887(cm/s) | 25.6876 ~ -26.726(cm/s) | 25.5289 ~ -26.7539(cm/s) |
| Open Environment Wheat | **1/16** | 0-5 cm | 25.5421 ~ -26.6268(cm/s) | 25.6471 ~ -26.6906(cm/s) | 25.4527 ~ -26.6914(cm/s) | 25.6897 ~ -26.6896(cm/s) | 25.2867 ~ -26.7419(cm/s) | 25.5393 ~ -26.6529(cm/s) |
| | | 5-10 cm | 25.745 ~ -26.6591(cm/s) | 25.7097 ~ -26.4834(cm/s) | 25.7447 ~ -26.7374(cm/s) | 25.7266 ~ -26.6313(cm/s) | 25.6849 ~ -26.3556(cm/s) | 25.7477 ~ -26.7362(cm/s) |
| | **1/8** | 0-5 cm | 25.746 ~ -26.6591(cm/s) | 25.6488 ~ -26.4834(cm/s) | 25.6428 ~ -26.701(cm/s) | 25.6826 ~ -26.6253(cm/s) | 25.7651 ~ -26.0624(cm/s) | 25.7072 ~ -26.6054(cm/s) |
| | | 5-10 cm | 24.9778 ~ -26.5356(cm/s) | 25.1738 ~ -26.5356(cm/s) | 25.3968 ~ -26.6858(cm/s) | 25.6453 ~ -26.6531(cm/s) | 25.3147 ~ -26.4281(cm/s) | 25.3046 ~ -26.5126(cm/s) |
| Closed Environment Wheat | **1/16** | 0-5 cm | 25.0099 ~ -26.5669(cm/s) | 24.5433 ~ -- 26.7017(cm/s) | 24.9911 ~ -26.3675(cm/s) | 25.4602 ~ -26.7558(cm/s) | 25.7333 ~ -- 26.7262(cm/s) | 24.287 ~ -26.8211(cm/s) |
| | | 5-10 cm | 25.7339 ~ -26.7241(cm/s) | 25.6652 ~ -26.727(cm/s) | 25.7435 ~ -26.6723(cm/s) | 25.7698 ~ -26.4013(cm/s) | 25.7018 ~ -26.7495(cm/s) | 25.6482 ~ -26.6315(cm/s) |
| | **1/8** | 0-5 cm | 25.2577 ~ -26.4146(cm/s) | 24.7867 ~ -25.9819(cm/s) | 25.7345 ~ -26.7125(cm/s) | 25.7143 ~ -26.6672(cm/s) | 25.6656 ~ -26.3144(cm/s) | 25.336 ~ -26.7269(cm/s) |
| | | 5-10 cm | 25.6451 ~ -26.5537(cm/s) | 25.7567 ~ -25.9419(cm/s) | 25.7039 ~ -26.4547(cm/s) | 25.6565 ~ -26.5306(cm/s) | 25.585 ~ -26.2315(cm/s) | 25.5876 ~ -26.5204(cm/s) |

Table 29 shows the summary of particles velocity change under different experimental conditions. There were two different groups of flow rate 1/16 open rate and 1/8 open rate. The observation range was 0 ~ 5 cm below the hopper system and 5~10 cm below the hopper system.

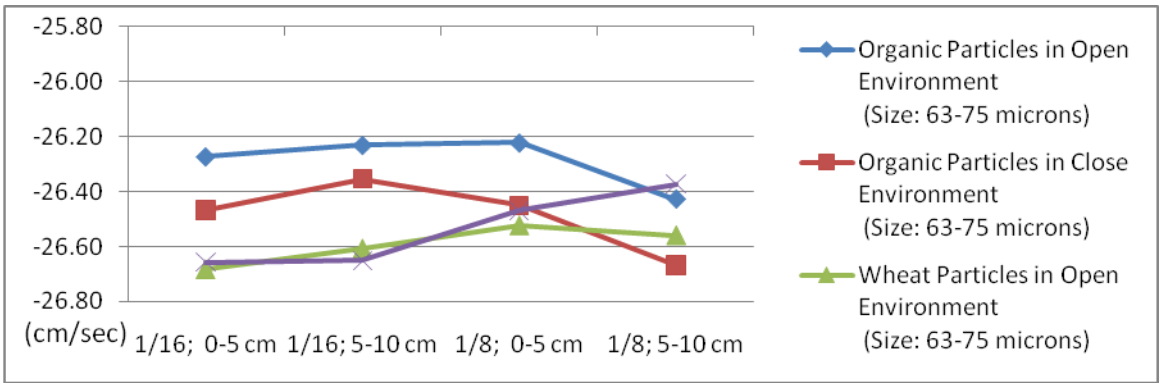


Figure 59 Organic Particles (diameter between 63 and 75 microns) and Wheat Particles (diameter between 63 and 75 microns) Velocity Change under Different Conditions (Lower Limit)

Figure 59 shows the lower limit of the particles velocity under different experimental conditions. Each point shows the mean velocity of particles under each experimental condition.

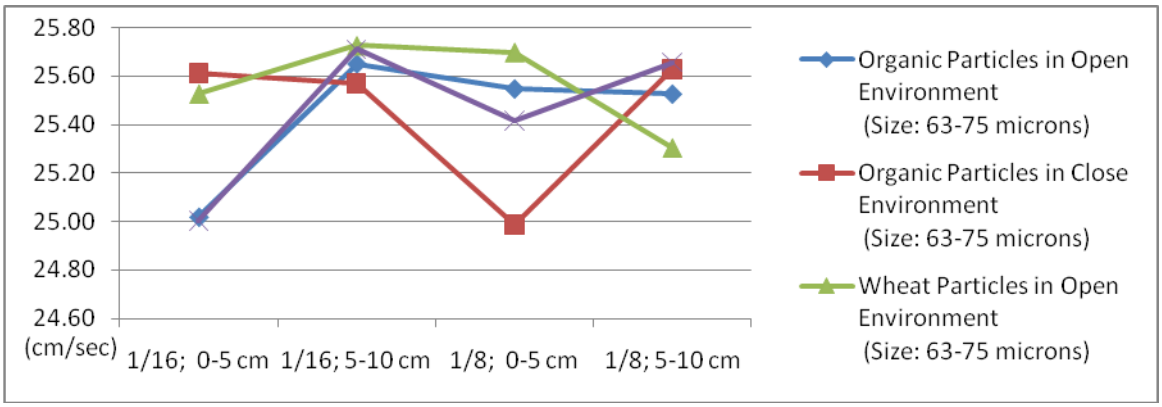


Figure 60 Organic Particles (diameter between 63 and 75 microns) and Wheat Particles (diameter between 63 and 75 microns) Velocity Change under Different Conditions (Upper Limit)

Figure 60 shows the upper limit of the particles velocity under different experimental conditions. Each point shows the mean velocity of particles under each experimental condition.

Table 30 The Analysis of Variance Table for Four-Factor Fixed Effects Model

| **Source of Variation** | **Sum of Squares** | **Degrees of Freedom** | **Mean Square** | **$F_0$** |
|---|---|---|---|---|
| A | $SS_A$ | a - 1 | $MS_A=SS_A/(a-1)$ | $MS_A/ MS_E$ |
| B | $SS_B$ | b - 1 | $MS_B=SS_B/(b-1)$ | $MS_B/ MS_E$ |
| C | $SS_C$ | c - 1 | $MS_C=SS_C/(c-1)$ | $MS_C/ MS_E$ |
| D | $SS_D$ | d - 1 | $MS_D=SS_D/(d-1)$ | $MS_D/ MS_E$ |
| AB | $SS_{AB}$ | (a -1)(b - 1) | $MS_{AB}=SS_{AB}/((a-1)(b-1))$ | $MS_{AB}/ MS_E$ |
| AC | $SS_{AC}$ | (a -1)(c - 1) | $MS_{AC}=SS_{AC}/((a -1)(c - 1))$ | $MS_{AC}/ MS_E$ |
| AD | $SS_{AD}$ | (a -1)(d - 1) | $MS_{AD}=SS_{AD}/((a -1)(d - 1))$ | $MS_{AD}/ MS_E$ |
| BC | $SS_{BC}$ | (b – 1)(c – 1) | $MS_{BC}=SS_{BC}/((b – 1)(c – 1))$ | $MS_{BC}/ MS_E$ |
| BD | $SS_{BD}$ | (b – 1)(d – 1) | $MS_{BD}=SS_{BD}/((b – 1)(d – 1))$ | $MS_{BD}/ MS_E$ |
| CD | $SS_{CD}$ | (c – 1)(d – 1) | $MS_{CD}=SS_{CD}/((c – 1)(d – 1))$ | $MS_{CD}/ MS_E$ |
| ABC | $SS_{ABC}$ | (a - 1)(b - 1)(c - 1) | $MS_{ABC}=SS_{ABC}/((a - 1)(b - 1)(c - 1))$ | $MS_{ABC}/ MS_E$ |
| ABD | $SS_{ABD}$ | (a - 1)(b - 1)(d - 1) | $MS_{ABD}=SS_{ABD}/((a - 1)(b - 1)(d - 1))$ | $MS_{ABD}/ MS_E$ |
| ACD | $SS_{ACD}$ | (a - 1)(c - 1)(d - 1) | $MS_{ACD}=SS_{ACD}/((a - 1)(c - 1)(d - 1))$ | $MS_{ACD}/ MS_E$ |
| BCD | $SS_{BCD}$ | (b - 1)(c - 1)(d - 1) | $MS_{BCD}=SS_{BCD}/((b - 1)(c - 1)(d - 1))$ | $MS_{BCD}/ MS_E$ |
| ABCD | $SS_{ABCD}$ | (a - 1)(b - 1)(c - 1)(d - 1) | $MS_{ABCD}=SS_{ABCD}/((a – 1)(b - 1)(c - 1)(d - 1))$ | $MS_{ABCD}/ MS_E$ |
| Error | $SS_E$ | abcd(n – 1) | $MS_E=SS_E/(abcd(n-1))$ | |
| Total | $SS_T$ | abcdn -1 | | |

There were four different factor's levels including a levels of factor A, b levels of factor B, c levels of factor C, d levels of factor D, and assuming that A, B, C, and D were fixed, the analysis of variance table was shown in Table 30. The sums of squares were found from the following equations.

$$SS_T = \sum_{i=1}^{a}\sum_{j=1}^{b}\sum_{k=1}^{c}\sum_{p=1}^{d}\sum_{l=1}^{n} y_{ijkpl}^2 - \frac{y_{.....}^2}{abcdn} \qquad SS_A = \frac{1}{bcdn}\sum_{i=1}^{a} y_{i....}^2 - \frac{y_{.....}^2}{abcdn}$$

$$SS_B = \frac{1}{acdn}\sum_{j=1}^{b} y_{.j...}^2 - \frac{y_{.....}^2}{abcdn} \qquad SS_C = \frac{1}{abdn}\sum_{k=1}^{c} y_{..k..}^2 - \frac{y_{.....}^2}{abcdn}$$

$$SS_D = \frac{1}{abcn}\sum_{p=1}^{d} y_{...p.}^2 - \frac{y_{.....}^2}{abcdn} \qquad SS_{AB} = \frac{1}{cdn}\sum_{i=1}^{a}\sum_{j=1}^{b} y_{ij...}^2 - \frac{y_{.....}^2}{abcdn} - SS_A - SS_B$$

$$SS_{AC} = \frac{1}{bdn}\sum_{i=1}^{a}\sum_{k=1}^{c} y_{i.k..}^2 - \frac{y_{.....}^2}{abcdn} - SS_B - SS_C \qquad SS_{AD} = \frac{1}{bcn}\sum_{i=1}^{a}\sum_{k=1}^{d} y_{i..p.}^2 - \frac{y_{.....}^2}{abcdn} - SS_A - SS_D$$

$$SS_{BC} = \frac{1}{adn}\sum_{j=1}^{b}\sum_{k=1}^{c} y_{.jk..}^2 - \frac{y_{.....}^2}{abcdn} - SS_B - SS_C \qquad SS_{BD} = \frac{1}{acn}\sum_{j=1}^{b}\sum_{p=1}^{d} y_{.j.p.}^2 - \frac{y_{.....}^2}{abcdn} - SS_B - SS_D$$

$$SS_{CD} = \frac{1}{abn}\sum_{k=1}^{c}\sum_{p=1}^{d} y_{..kp.}^2 - \frac{y_{.....}^2}{abcdn} - SS_C - SS_D$$

$$SS_{ABC} = \frac{1}{n}\sum_{i=1}^{a}\sum_{j=1}^{b}\sum_{k=1}^{c} y_{ijk..}^2 - \frac{y_{.....}^2}{abcdn} - SS_A - SS_B - SS_C - SS_{AB} - SS_{AC} - SS_{BC}$$

$$SS_{ABD} = \frac{1}{n}\sum_{i=1}^{a}\sum_{j=1}^{b}\sum_{p=1}^{d} y_{ij.p.}^2 - \frac{y_{.....}^2}{abcdn} - SS_A - SS_B - SS_D - SS_{AB} - SS_{AD} - SS_{BD}$$

$$SS_{ACD} = \frac{1}{n}\sum_{i=1}^{a}\sum_{k=1}^{c}\sum_{p=1}^{d} y_{i.kp.}^2 - \frac{y_{.....}^2}{abcdn} - SS_A - SS_C - SS_D - SS_{AC} - SS_{AD} - SS_{CD}$$

$$SS_{BCD} = \frac{1}{n}\sum_{i=1}^{b}\sum_{k=1}^{c}\sum_{p=1}^{d} y_{.jkp.}^2 - \frac{y_{.....}^2}{abcdn} - SS_B - SS_C - SS_D - SS_{BC} - SS_{BD} - SS_{CD}$$

$$SS_{ABCD} = \frac{1}{n}\sum_{i=1}^{a}\sum_{j=1}^{b}\sum_{k=1}^{c}\sum_{p=1}^{d} y_{ijkp.}^2 - \frac{y_{....}^2}{abcdn} - SS_A - SS_B - SS_C - SS_D - SS_{AB} - SS_{AC} - SS_{BC} - SS_{ABC} - SS_{ABD} - SS_{ACD} - SS_{BCD}$$

$$SS_E = SS_T - SS_A - SS_B - SS_C - SS_D - SS_{AB} - SS_{AC} - SS_{BC} - SS_{ABC} - SS_{ABD} - SS_{ABCD}$$

In this experiment, four factors were considered as the affecting factors. They were particles type, open rate, observation range, and environment condition. Organic particles and wheat particles were two types of particles used in the experiments. For the open rate 1/16 and 1/8 were compared. The experiments were observed 5cm and 10cm from the nozzle. The open environment means the experiments were conducted in the open air. The closed environment means the experiments were conducted in the enclosure testing model.

Table 31 ANOVA Table for the Lower Limit of the Particles Velocity

| *Source of variation* | *Degrees of Freedom* | *Sum of Squares* | *Mean Square* | $F_0$ | P value |
|---|---|---|---|---|---|
| ***Type*** | 1 | 0.762 | 0.762 | 5.170 > 3.96 | 0.026 |
| ***Open Rate*** | 1 | 0.020 | 0.020 | 0.140 < 3.96 | 0.714 |
| ***Observation*** | 1 | 0.006 | 0.006 | 0.040 < 3.96 | 0.846 |
| ***Env*** | 1 | 0.120 | 0.120 | 0.810 < 3.96 | 0.370 |
| ***Type*Open Rate*** | 1 | 0.468 | 0.468 | 3.170 < 3.96 | 0.079 |
| ***Type*Observation*** | 1 | 0.062 | 0.062 | 0.420 < 3.96 | 0.518 |
| ***Type*Env*** | 1 | 0.381 | 0.381 | 2.580 < 3.96 | 0.112 |
| ***Open Rate*Observation*** | 1 | 0.134 | 0.134 | 0.910 < 3.96 | 0.343 |
| ***Open Rate*Env*** | 1 | 0.004 | 0.004 | 0.030 < 3.96 | 0.864 |
| ***Observation*Env*** | 1 | 0.006 | 0.006 | 0.040 < 3.96 | 0.841 |
| ***Type*Open Rate*Observation*** | 1 | 0.118 | 0.118 | 0.800 < 3.96 | 0.375 |
| ***Type*Open Rate*Env*** | 1 | 0.062 | 0.062 | 0.420 < 3.96 | 0.517 |
| ***Type*Observation*Env*** | 1 | 0.000 | 0.000 | 0.000 < 3.96 | 0.999 |
| ***Open Rate*Observation*Env*** | 1 | 0.005 | 0.005 | 0.040 < 3.96 | 0.849 |
| ***Type*Open Rate*Observation*Env*** | 1 | 0.031 | 0.031 | 0.210 < 3.96 | 0.650 |
| ***Error*** | 80 | 11.797 | 0.148 | | |
| ***Total*** | 95 | 13.975 | | | |

Table 31 shows the analysis of variance (ANOVA) table for the lower limit of the particles velocity. If $\alpha = 0.05$. Because $F_{0.05,1,80} = 3.96$, we conclude that the type of particles had a

significant effect on the lower limit of the particles velocity for the source of variation with 95% of confidence.

Table 32 ANOVA Table for the Upper Limit of the Particles Velocity

| *Source of variation* | *Sum of Squares* | *Degrees of Freedom* | *Mean Square* | $F_0$ | P value |
|---|---|---|---|---|---|
| ***Type*** | 1 | 0.094 | 0.094 | 0.870 < 3.96 | 0.353 |
| ***Open Rate*** | 1 | 0.001 | 0.001 | 0.010 < 3.96 | 0.914 |
| ***Observation*** | 1 | 1.436 | 1.436 | 13.320 > 3.96 | 0.000 |
| ***Env*** | 1 | 0.065 | 0.065 | 0.600 < 3.96 | 0.441 |
| ***Type*Open Rate*** | 1 | 0.027 | 0.027 | 0.250 < 3.96 | 0.618 |
| ***Type*Observation*** | 1 | 0.078 | 0.078 | 0.730 < 3.96 | 0.397 |
| ***Type*Env*** | 1 | 0.101 | 0.101 | 0.940 < 3.96 | 0.335 |
| ***Open Rate*Observation*** | 1 | 0.399 | 0.399 | 3.700 < 3.96 | 0.058 |
| ***Open Rate*Env*** | 1 | 0.049 | 0.049 | 0.460 < 3.96 | 0.501 |
| ***Observation*Env*** | 1 | 0.477 | 0.477 | 4.420 > 3.96 | 0.039 |
| ***Type*Open Rate*Observation*** | 1 | 0.449 | 0.449 | 4.170 > 3.96 | 0.044 |
| ***Type*Open Rate*Env*** | 1 | 0.936 | 0.936 | 8.690 > 3.96 | 0.004 |
| ***Type*Observation*Env*** | 1 | 0.503 | 0.503 | 4.660 > 3.96 | 0.034 |
| ***Open Rate*Observation*Env*** | 1 | 0.808 | 0.808 | 7.500 > 3.96 | 0.008 |
| ***Type*Open Rate*Observation*Env*** | 1 | 0.546 | 0.546 | 5.070 > 3.96 | 0.027 |
| ***Error*** | 80 | 8.624 | 0.108 | | |
| ***Total*** | 95 | 14.594 | | | |

Table 32 shows the analysis of variance (ANOVA) table for the upper limit of the particles velocity. The observation range had a significant effect on the upper limit of the particles velocity with 95% of confidence. And the interaction of observation range and environment condition had a significant effect. The interaction of type of particles, open rate and observation had a significant effect. The interaction of type of particles, open rate and environment condition had a significant effect. The interaction of type of particles, observation range and environment condition had a significant effect. The open rate and observation range and environment condition had a significant effect. The interaction of type of particles, open rate, observation range and environment condition had a significant effect.

## 5.12 Potato Particles (diameter between 63 and 75 microns) Test in the Closed Environment

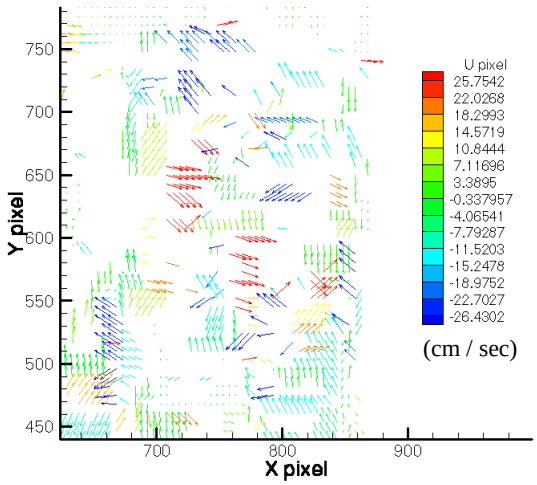


Figure 61 The Particles Velocity Profiles of the Potato Particles in the Closed Environment (1/8 open rate, 0-5 cm, 63<diameter<75 microns)

Figure 61 shows the test result under condition of flow rate control gate at 1/8 of open rate using the potato particles (sizing between 63 microns and 75 microns) in the closed environment. The image range was 0 cm to 5cm from the flow rate control gate. The result also shows that the velocity range of particles was between -25.7542 cm/sec and 26.4302 cm/sec.

Table 33 Summary of Potato Particles (diameter between 63 and 75 microns) Velocity Changes under Different Experimental Conditions

| *Particles Type* | *Open Rate of Flow Rate Control Gate* | *Observation Range* | *Replication1* | *Replication2* | *Replication3* | *Replication4* | *Replication5* | *Replication6* |
|---|---|---|---|---|---|---|---|---|
| Open Environment Potato | **1/16** | 0-5 cm | 25.3741 ~ -26.1528(cm/s) | 25.2562 ~ -26.311(cm/s) | 24.4326 ~ -26.6394(cm/s) | 25.3141 ~ -26.3077(cm/s) | 25.1886 ~ -26.3487(cm/s) | 25.4196 ~ -26.5567(cm/s) |
| | | 5-10 cm | 25.5846 ~ -26.7431(cm/s) | 25.5947 ~ -26.2417(cm/s) | 25.7304 ~ -26.7465(cm/s) | 25.6799 ~ -26.7133(cm/s) | 25.7186 ~ 26.6281(cm/s) | 25.5164 ~ -25.5144(cm/s) |
| | **1/8** | 0-5 cm | 25.542 ~ -26.1086(cm/s) | 25.4737 ~ -26.3487(cm/s) | 25.3242 ~ -26.3915(cm/s) | 25.4726 ~ -26.624(cm/s) | 25.5347 ~ -26.5569(cm/s) | 25.3104 ~ -26.3129(cm/s) |
| | | 5-10 cm | 25.7237 ~ -26.468(cm/s) | 24.2289 ~ -25.1868(cm/s) | 25.6694 ~ -26.2999(cm/s) | 25.3406 ~ -26.1377(cm/s) | 25.7354 ~ -26.6531(cm/s) | 25.3891 ~ -26.4835(cm/s) |
| Closed Environment Potato | **1/16** | 0-5 cm | 25.1301 ~ -26.5192(cm/s) | 25.7425 ~ -26.4533(cm/s) | 25.3456 ~ -26.6822(cm/s) | 25.7249 ~ -26.7352(cm/s) | 25.728 ~ -26.282(cm/s) | 25.6847 ~ -26.5671(cm/s) |
| | | 5-10 cm | 25.5612 ~ -26.6227(cm/s) | 25.2905 ~ -26.6225(cm/s) | 24.2072 ~ -26.1704(cm/s) | 25.6833 ~ -26.6718(cm/s) | 25.6159 ~ -26.5306(cm/s) | 25.1208 ~ -26.3481(cm/s) |
| | **1/8** | 0-5 cm | 25.4769 ~ -26.3006(cm/s) | 25.7542 ~ -26.4302(cm/s) | 25.6702 ~ -26.581(cm/s) | 25.5796 ~ -26.4798(cm/s) | 25.7132 ~ -26.4035(cm/s) | 24.8076 ~ -26.6189(cm/s) |
| | | 5-10 cm | 25.4763 ~ -26.6652(cm/s) | 25.4412 ~ -26.4621(cm/s) | 25.3384 ~ -26.6534(cm/s) | 25.3836 ~ -26.7374(cm/s) | 25.5345 ~ -26.6721(cm/s) | 25.6625 ~ -26.6978(cm/s) |

Table 33 shows the summary of particles velocity change under different experimental conditions. There were groups of flow rate 1/16 of open rate and 1/8 of open rate. The observation range was 0 ~ 5 cm below the hopper system and 5~10 cm below the hopper system.

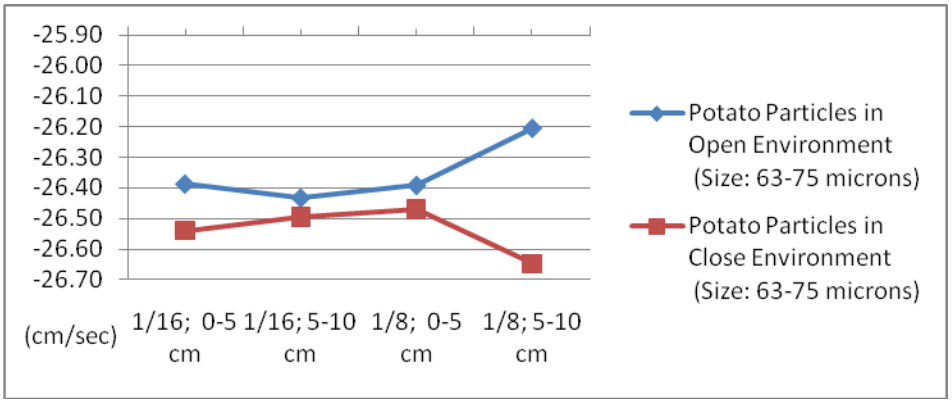


Figure 62 Potato Particles (diameter between 63 and 75 microns) Velocity Change under Different Conditions (Lower Limit)

Figure 62 shows the lower limit of the particles velocity under different experimental conditions. Each point shows the mean velocity of particles under each experimental condition.

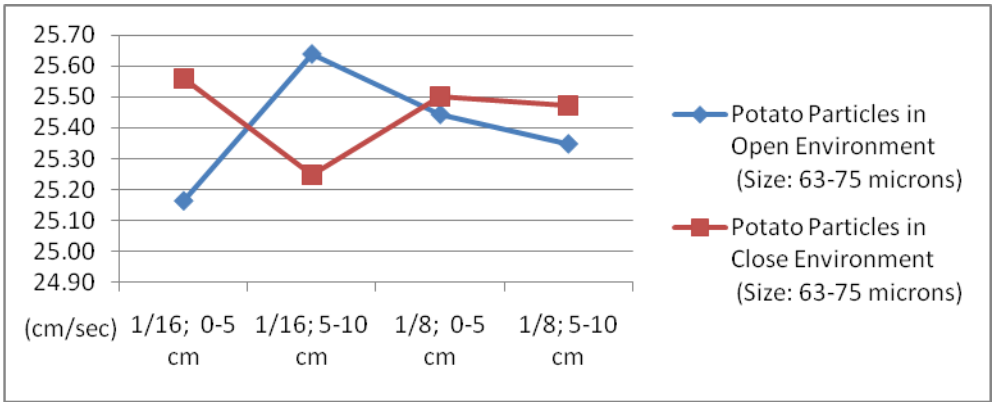


Figure 63 Potato Particles (diameter between 63 and 75 microns) Velocity Change under Different Conditions (Upper Limit)

Figure 63 shows the upper limit of the particles velocity under different experimental conditions. Each point shows the mean velocity of particles under each experimental condition.

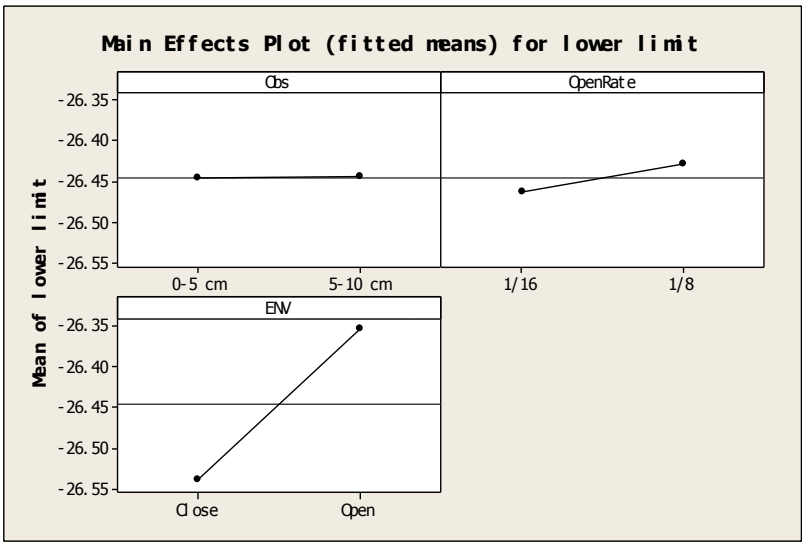


Figure 64 Main Effects Plot (fitted means) for Lower Limit

The effect of a factor was defined as the change in response produced by a change in the level of the factor. It was called a main effect because it refers to the primary factors in the study. Figure 64 shows main effects plot for lower limit. Based on this figure, environment condition was primary factor on the lower limit.

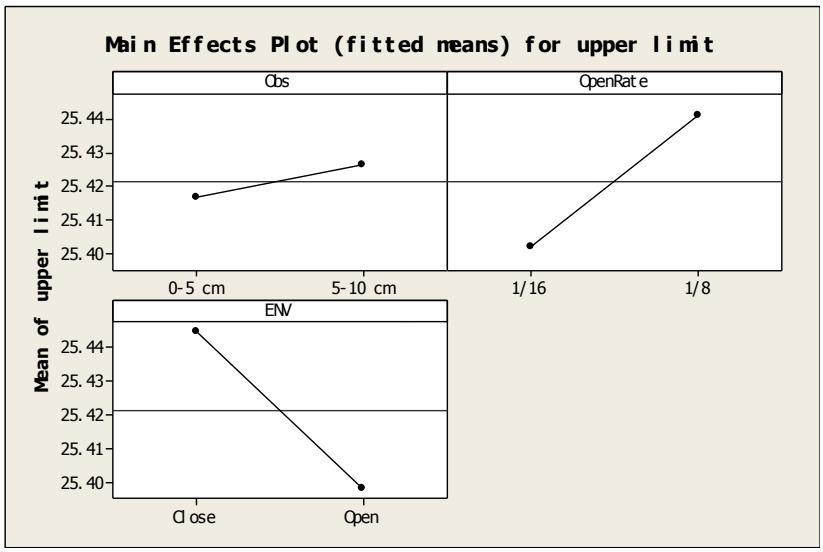


Figure 65 Main Effects Plot (fitted means) for Upper Limit

Figure 65 shows main effects plot for lower limit, based on this figure open rate and environment condition were primary factor in the upper limit.

Table 34 ANOVA Table for the Lower Limit of the Potato Particles (diameter between 63 and 75 microns) Velocity

| *Source of variation* | *Degrees of Freedom* | *Sum of Squares* | *Mean Square* | $F_0$ | *P-value* |
|---|---|---|---|---|---|
| ***Observation*** | 1 | 0.00004 | 0.00004 | 0.00<4.08 | 0.984 |
| ***Open Rate*** | 1 | 0.01452 | 0.01452 | 0.17<4.08 | 0.680 |
| ***Env*** | 1 | 0.40924 | 0.40924 | 4.87>4.08 | 0.033 |
| ***Observation*Open Rate*** | 1 | 0.00003 | 0.00003 | 0.00<4.08 | 0.985 |
| ***Observation*Env*** | 1 | 0.0563 | 0.05630 | 0.67<4.08 | 0.418 |
| ***Open Rate*Env*** | 1 | 0.06967 | 0.06967 | 0.83<4.08 | 0.368 |
| ***Observation*Open Rate*Env*** | 1 | 0.15542 | 0.15542 | 1.85<4.08 | 0.181 |
| ***Error*** | 40 | 3.36042 | 0.08401 | | |
| ***Total*** | 47 | 4.06564 | | | |

Table 34 shows the analysis of variance (ANOVA) for the lower limit of the particles velocity. [32, 33] If $\alpha = 0.05$. Because $F_{0.05,1,40} = 4.08$, we conclude that the environment condition had a significant effect on the lower limit of the particles velocity for the source of variation with 95% of confidence.

Table 35 ANOVA Table for the Upper Limit of the Potato Particles (diameter between 63 and 75 microns) Velocity

| *Source of variation* | *Degrees of Freedom* | *Sum of Squares* | *Mean Square* | $F_0$ | *P-value* |
|---|---|---|---|---|---|
| ***Observation*** | 1 | 0.0011 | 0.0011 | 0.01<4.08 | 0.926 |
| ***Open Rate*** | 1 | 0.0183 | 0.0183 | 0.15<4.08 | 0.703 |
| ***Env*** | 1 | 0.0261 | 0.0261 | 0.21<4.08 | 0.649 |
| ***Observation*Open Rate*** | 1 | 0.0601 | 0.0601 | 0.48<4.08 | 0.491 |
| ***Observation*Env*** | 1 | 0.3872 | 0.3872 | 3.12<4.08 | 0.085 |
| ***Open Rate*Env*** | 1 | 0.0238 | 0.0238 | 0.19<4.08 | 0.664 |
| ***Observation*Open Rate*Env*** | 1 | 0.5465 | 0.5465 | 4.40>4.08 | 0.042 |
| ***Error*** | 40 | 4.9641 | 0.1241 | 0.01<4.08 | |
| ***Total*** | 47 | 6.0271 | | | |

Table 35 shows the analysis of variance (ANOVA) for the upper limit of the particles velocity. The interaction of observation range, open rate and environment condition had a significant effect on the upper limit of the particles velocity for the source of variation with 95% of confidence.

### 5.13 Coal Particles (diameter between 63 and 75 microns) Test in the Closed Environment

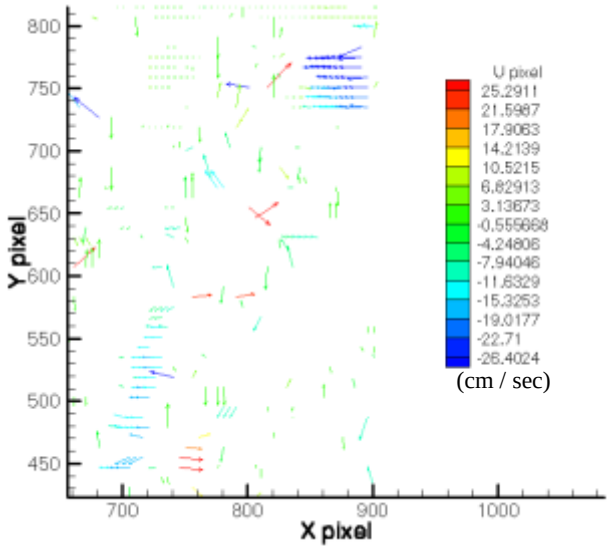


Figure 66 The Particles Velocity Profiles of the Coal Particles in the Closed Environment (1/8 open rate, 0-5 cm, 63<diameter<75 microns)

Figure 66 shows the test result under the condition of flow rate control gate at 1/8 of open rate using the coal particles (sizing between 63 microns and 75 microns). The image range was 0 cm to 5cm from the flow rate control gate. The result also shows that the velocity range of particles was between -26.4024 cm/sec and 25.2911 cm/sec.

Table 36 Summary of Coal Particles (diameter between 63 and 75 microns) Velocity Changes under Different Experimental Conditions

| *Particles Type* | *Open Rate of Flow Rate Control Gate* | *Observation Range* | *Replication1* | *Replication2* | *Replication3* | *Replication4* | *Replication5* | *Replication6* |
|---|---|---|---|---|---|---|---|---|
| Open Environment Coal | **1/16** | 0-5 cm | 25.6382 ~ -26.2836(cm/s) | 25.3408 ~ -26.4134(cm/s) | 25.1251 ~ -26.4046(cm/s) | 25.7534 ~ -26.3374(cm/s) | 24.9134 ~ -26.3175(cm/s) | 25.6665 ~ -26.3456(cm/s) |
| | | 5-10 cm | 25.3566 ~ -25.5939(cm/s) | 25.7496 ~ -26.3794(cm/s) | 25.4458 ~ -26.3069(cm/s) | 25.283 ~ -26.4904(cm/s) | 25.2869 ~ -26.5609(cm/s) | 24.5663 ~ -26.3661(cm/s) |
| | **1/8** | 0-5 cm | 25.0466 ~ -26.3508(cm/s) | 25.1845 ~ -26.598(cm/s) | 25.23 ~ -26.6022(cm/s) | 25.4285 ~ -26.2958(cm/s) | 25.5292 ~ -26.7461(cm/s) | 25.7183 ~ -26.714(cm/s) |
| | | 5-10 cm | 25.3333 ~ -26.2901(cm/s) | 25.6692 ~ -26.2991(cm/s) | 24.9942 ~ -26.6038(cm/s) | 24.4018 ~ -26.192(cm/s) | 25.3168 ~ -26.6359(cm/s) | 25.3277 ~ -26.3187(cm/s) |
| Closed Environment Coal | **1/16** | 0-5 cm | 25.6382 ~ -26.2836(cm/s) | 25.3408 ~ -26.4134(cm/s) | 25.1251 ~ -26.4046(cm/s) | 25.7534 ~ -26.3374(cm/s) | 24.9134 ~ -26.3175(cm/s) | 25.6665 ~ -26.3456(cm/s) |
| | | 5-10 cm | 25.3566 ~ -25.5939(cm/s) | 25.7496 ~ -26.3794(cm/s) | 25.4458 ~ -26.3069(cm/s) | 25.283 ~ -26.4904(cm/s) | 25.2869 ~ -26.5609(cm/s) | 24.5663 ~ -26.3661(cm/s) |
| | **1/8** | 0-5 cm | 25.0466 ~ -26.3508(cm/s) | 25.1845 ~ -26.598(cm/s) | 25.23 ~ -26.6022(cm/s) | 25.4285 ~ -26.2958(cm/s) | 25.5292 ~ -26.7461(cm/s) | 25.7183 ~ -26.714(cm/s) |
| | | 5-10 cm | 25.3333 ~ -26.2901(cm/s) | 25.6692 ~ -26.2991(cm/s) | 24.9942 ~ -26.6038(cm/s) | 24.4018 ~ -26.192(cm/s) | 25.3168 ~ -26.6359(cm/s) | 25.3277 ~ -26.3187(cm/s) |

Table 36 shows the summary of particles velocity change under different experimental conditions. There were groups of flow rate 1/16 of open rate and 1/8 of open rate. The observation range was 0 ~ 5 cm below the hopper system and 5~10 cm below the hopper system.

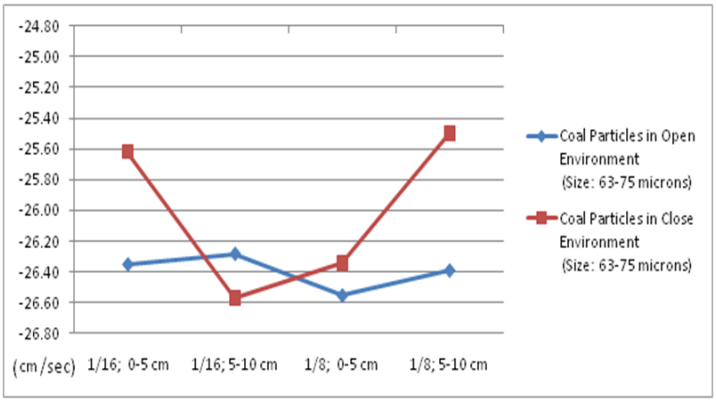


Figure 67 Coal Particles (diameter between 63 and 75 microns) Velocity Change under Different Conditions (Lower Limit) in the Closed Environment

Figure 67 shows the lower limit of the particles velocity under different experimental conditions. Each point shows the mean velocity of particles under each experimental condition.

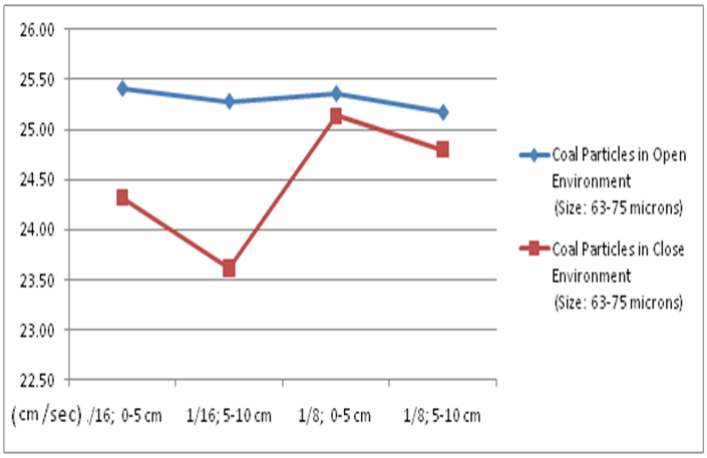


Figure 68 Coal Particles (diameter between 63 and 75 microns) Velocity Change under Different Conditions (Upper Limit) in the Closed Environment

Figure 68 shows the upper limit of the particles velocity under different experimental conditions. Each point shows the mean velocity of particles under each experimental condition.

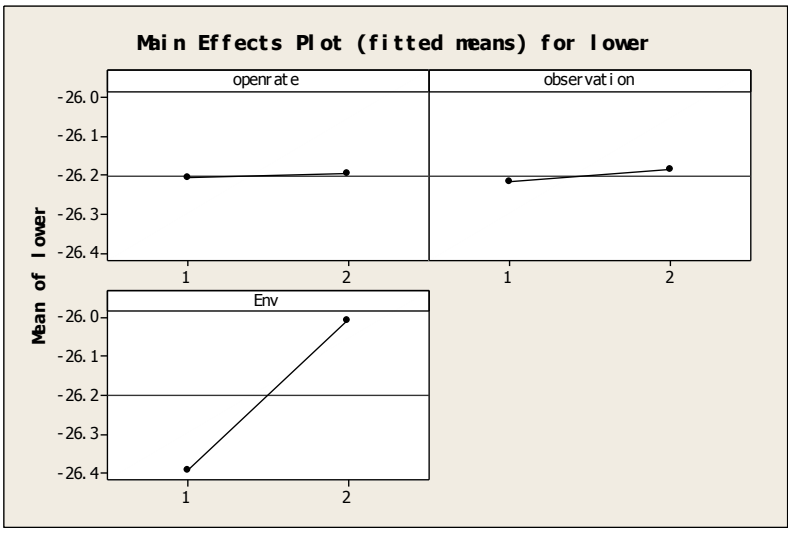


Figure 69 Main Effects Plot (fitted means) for Lower Limit

The effect of a factor was defined as the change in response produced by a change in the level of the factor. It was called a main effect because it refers to the primary factors in the study. Figure 69 shows main effects plot for lower limit. Based on this figure, environment condition was primary factor on the lower limit.

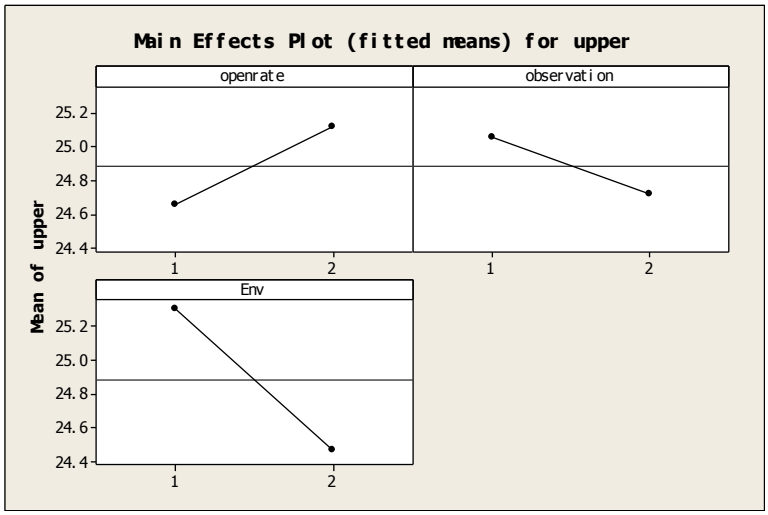


Figure 70 Main Effects Plot (fitted means) for Upper Limit

Figure 70 shows main effects plot for lower limit, based on this figure open rate, observation range and environment condition were primary factor in the upper limit.

Table 37 ANOVA Table for the Lower Limit of the Coal Particles (diameter between 63 and 75 microns) Velocity in the Closed Environment

| *Source of variation* | *Degrees of Freedom* | *Sum of Squares* | *Mean Square* | $F_0$ | *P-value* |
|---|---|---|---|---|---|
| ***Open Rate*** | 1 | 0.0012 | 0.0012 | 0 < 4.08 | 0.965 |
| ***observation*** | 1 | 0.0111 | 0.0111 | 0.02 < 4.08 | 0.895 |
| ***Env*** | 1 | 1.7865 | 1.7865 | 2.85 < 4.08 | 0.099 |
| ***Open Rate*observation*** | 1 | 2.683 | 2.683 | 4.28 > 4.08 | 0.045 |
| ***Open Rate*Env*** | 1 | 0.3228 | 0.3228 | 0.51 < 4.08 | 0.477 |
| ***observation*Env*** | 1 | 0.0845 | 0.0845 | 0.13 < 4.08 | 0.716 |
| ***Open Rate*observation*Env*** | 1 | 2.1771 | 2.1771 | 3.47 < 4.08 | 0.07 |
| ***Error*** | 40 | 25.0975 | 0.6274 | | |
| ***Total*** | 47 | 32.1636 | | | |

Table 37 shows the analysis of variance (ANOVA) for the lower limit of the particles velocity. [32, 33] If $\alpha = 0.05$. Because $F_{0.05,1,40} = 4.08$, we conclude that interaction of open rate and observation range had a significant effect on the lower limit of the particles velocity for the source of variation with 95% of confidence.

Table 38 ANOVA Table for the Upper Limit of the Coal Particles (diameter between 63 and 75 microns) Velocity in the Closed Environment

| *Source of variation* | *Degrees of Freedom* | *Sum of Squares* | *Mean Square* | $F_0$ | *P-value* |
|---|---|---|---|---|---|
| ***Open Rate*** | 1 | 2.5427 | 2.543 | 5.90 > 4.08 | 0.020 |
| ***observation*** | 1 | 1.3503 | 1.350 | 3.14 < 4.08 | 0.084 |
| ***Env*** | 1 | 8.4186 | 8.419 | 19.55 > 4.08 | 0.000 |
| ***Open Rate*observation*** | 1 | 0.0710 | 0.071 | 0.16 < 4.08 | 0.687 |
| ***Open Rate*Env*** | 1 | 3.4877 | 3.488 | 8.10 > 4.08 | 0.007 |
| ***observation*Env*** | 1 | 0.3968 | 0.397 | 0.92 < 4.08 | 0.343 |
| ***Open Rate*observation*Env*** | 1 | 0.1339 | 0.134 | 0.31 < 4.08 | 0.580 |
| ***Error*** | 40 | 17.2279 | 0.431 | | |
| ***Total*** | 47 | 33.6287 | | | |

Table 38 shows the analysis of variance (ANOVA) for the upper limit of the particles velocity. The open rate and environment condition have a significant effect on the upper limit. The interaction of open rate and environment condition had a significant effect on the upper limit of the particles velocity for the source of variation with 95% of confidence.

### 5.14 Coal Particles (diameter between 63 and 75 microns) Test in the Open Environment

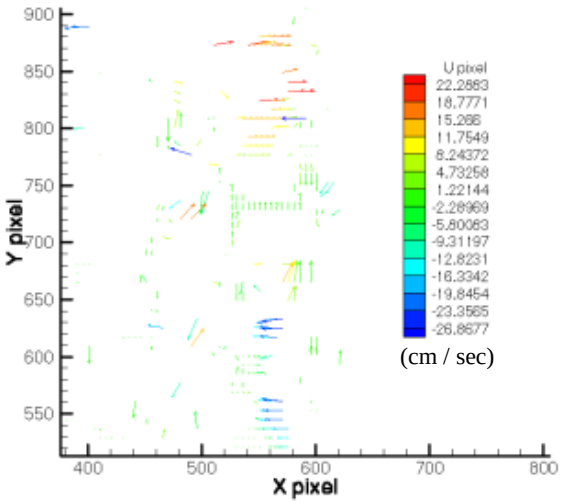


Figure 71 The Particles Velocity Profiles of the Coal Particles in the Open Environment (1/4 open rate, 0-5 cm, 63<diameter<75 microns)

Figure 71 shows the test result under condition of flow rate control gate at 1/4 of open rate using the coal particles (sizing between 63 microns and 75 microns) in the open environment. The image range was 0 cm to 5cm from the flow rate control gate. The result also shows that the velocity range of coal particles was between -26.8677 cm/sec and 22.2883 cm/sec.

Table 39 Summary of Coal Particles (diameter between 63 and 75 microns) Velocity Changes under Different Experimental Conditions

| ***Particles Type*** | ***Open Rate of Flow Rate Control Gate*** | ***Observation Range*** | ***Replication1*** | ***Replication2*** | ***Replication3*** | ***Replication4*** | ***Replication5*** | ***Replication6*** |
|---|---|---|---|---|---|---|---|---|
| **Opened Environment 63<Coal<75** | 1/16 | 0-5 cm | 25.6382 ~ -26.2836(cm/s) | 25.3408 ~ -26.4134(cm/s) | 25.1251 ~ -26.4046(cm/s) | 25.7534 ~ -26.3374(cm/s) | 24.9134 ~ -26.3175(cm/s) | 25.6665 ~ -26.3456(cm/s) |
| | | 5-10 cm | 25.3566 ~ -25.5939(cm/s) | 25.7496 ~ -26.3794(cm/s) | 25.4458 ~ -26.3069(cm/s) | 25.283 ~ -26.4904(cm/s) | 25.2869 ~ -26.5609(cm/s) | 24.5663 ~ -26.3661(cm/s) |
| | | 10-15 cm | 25.3455 ~ -26.241(cm/s) | 25.2705 ~ -24.4689(cm/s) | 24.4532 ~ -26.3644(cm/s) | 25.4304 ~ -26.3144(cm/s) | 25.4324 ~ -23.4512(cm/s) | 24.358 ~ -26.008(cm/s) |
| | 1/8 | 0-5 cm | 25.0466 ~ -26.3508(cm/s) | 25.1845 ~ -26.598(cm/s) | 25.23 ~ -26.6022(cm/s) | 25.4285 ~ -26.2958(cm/s) | 25.5292 ~ -26.7461(cm/s) | 25.7183 ~ -26.714(cm/s) |
| | | 5-10 cm | 25.3333 ~ -26.2901(cm/s) | 25.6692 ~ -26.2991(cm/s) | 24.9942 ~ -26.6038(cm/s) | 24.4018 ~ -26.192(cm/s) | 25.3168 ~ -26.6359(cm/s) | 25.3277 ~ -26.3187(cm/s) |
| | | 10-15 cm | 24.3842 ~ -26.3688(cm/s) | 23.8524 ~ -26.418(cm/s) | 22.6853 ~ -26.4775(cm/s) | 23.116 ~ -26.7839(cm/s) | 24.4427 ~ -25.3738(cm/s) | 25.3199 ~ -26.3059(cm/s) |
| | 1/4 | 0-5 cm | 24.9699 ~ -26.4762(cm/s) | 25.4791 ~ -23.805(cm/s) | 22.2883 ~ -26.8677(cm/s) | 25.7174 ~ -26.6236(cm/s) | 25.3542 ~ -26.3579(cm/s) | 25.6372 ~ -21.3948(cm/s) |
| | | 5-10 cm | 25.2847 ~ -26.2772(cm/s) | 25.2323 ~ -26.6347(cm/s) | 25.7255 ~ -26.281(cm/s) | 24.4415 ~ -25.3836(cm/s) | 24.4304 ~ -26.4687(cm/s) | 24.3688 ~ -26.3982(cm/s) |
| | | 10-15 cm | 24.5892 ~ -23.478(cm/s) | 25.3951 ~ -25.3726(cm/s) | 25.3646 ~ -26.3802(cm/s) | 25.3679 ~ -25.4521(cm/s) | 25.1158 ~ -26.5022(cm/s) | 24.5667 ~ -25.333(cm/s) |

Table 39 shows the summary of coal particles velocity changes under different experimental conditions. There were groups of flow rates: 1/16 of open rate, 1/8 of open rate and 1/4 of open rate. The observation range was 0 ~ 5 cm below the hopper system, 5 ~ 10 cm below the hopper system and 10~15 cm below the hopper system.

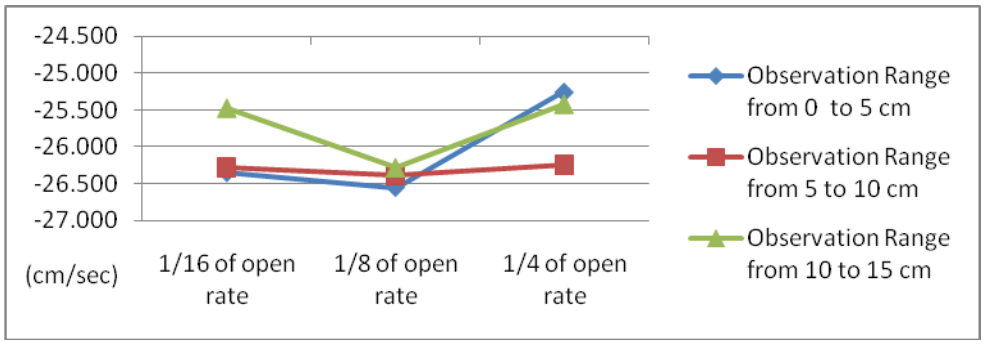


Figure 72 Coal Particles (diameter between 63 and 75 microns) Velocity Changes under Different Conditions (Lower Limit) in the Open Environment

Figure 72 shows the lower limit of the coal particles velocity under different experimental conditions. Each point shows the mean velocity of coal particles under each experimental condition.

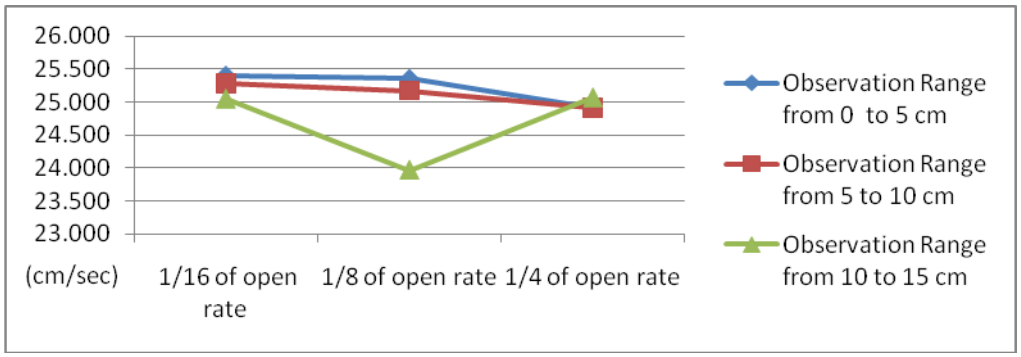


Figure 73 Coal Particles (diameter between 63 and 75 microns) Velocity Changes under Different Conditions (Upper Limit) in the Open Environment

Figure 73 shows the upper limit of the coal particles velocity under different experimental conditions. Each point shows the mean velocity of coal particles under each experimental condition.

Table 40 The Analysis of Variance Table for Two-Factor Fixed Effects Model

| Source of Variation | Sum of Squares | Degrees of Freedom | Mean Square | $F_0$ |
|---|---|---|---|---|

| | | | | |
|---|---|---|---|---|
| A | $SS_A$ | a - 1 | $MS_A=SS_A/(a-1)$ | $MS_A/ MS_E$ |
| B | $SS_B$ | b - 1 | $MS_B=SS_B/(b-1)$ | $MS_B/ MS_E$ |
| AB | $SS_{AB}$ | (a -1)(b - 1) | $MS_{AB}=SS_{AB}/((a-1)(b-1))$ | $MS_{AB}/ MS_E$ |
| Error | $SS_E$ | ab(n – 1) | $MS_E=SS_E/(ab(n-1))$ | |
| Total | $SS_T$ | abn -1 | | |

There were two different factor levels including a levels of factor A, b levels of factor B, and assuming that A and B were fixed, the analysis of variance table was shown in Table 40. The sums of squares were found from the following equations. [32, 33]

$$SS_T = \sum_{i=1}^{a}\sum_{j=1}^{b}\sum_{k=1}^{n} y_{ijk}^2 - \frac{y_{...}^2}{abn} \qquad SS_A = \frac{1}{bn}\sum_{i=1}^{a} y_{i..}^2 - \frac{y_{...}^2}{abn}$$

$$SS_B = \frac{1}{an}\sum_{j=1}^{b} y_{.j.}^2 - \frac{y_{...}^2}{abn}$$

$$SS_{AB} = \frac{1}{n}\sum_{i=1}^{a}\sum_{j=1}^{b} y_{ij.}^2 - \frac{y_{...}^2}{abn} - SS_A - SS_B$$

$$SS_E = SS_T - SS_A - SS_B - SS_{AB}$$

In this experiment, two factors were considered as the affecting factors. They were the open rate, observation ranges. The open rate 1/16, 1/8 and 1/4 were compared. The observed experiments were 0 cm to 5 cm, 5 cm to 10 cm and 10 cm to 15 cm from the nozzle. The open environment means the experiments were conducted in the open air.

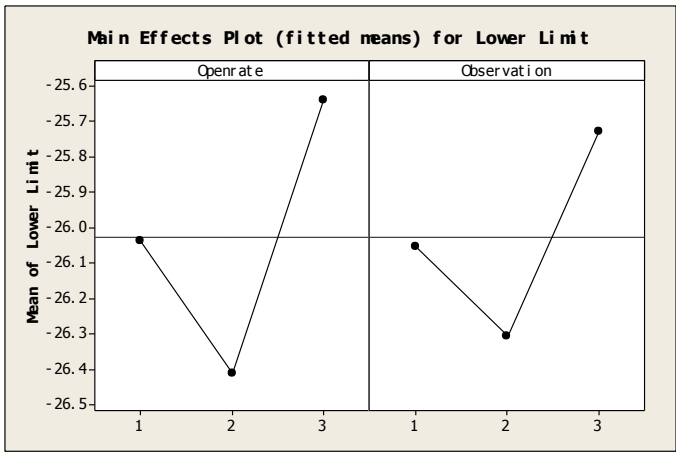


Figure 74 Main Effects Plot (fitted means) for Lower Limit

The effect of a factor was defined as the change in response produced by a change in the level of the factor. It was called a main effect because it refers to the primary factors in the study. Figure 74 shows the main effects plot for lower limit.

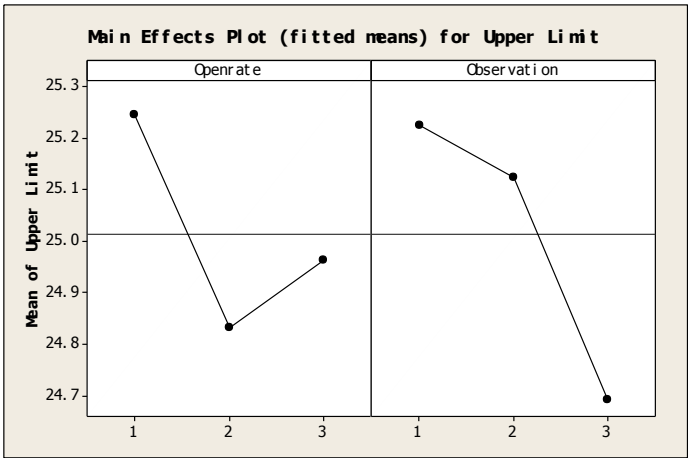


Figure 75 Main Effects Plot (fitted means) for Upper Limit

Figure 75 shows the main effects plot for upper limit, based on this figure both open rate and observation range were primary factor in the upper limit.

Table 41 ANOVA Table for the Lower Limit of the Coal Particles (diameter between 63 and 75 microns) Velocity Changes in the Open Environment

| ***Source of variation*** | ***Degrees of Freedom*** | ***Sum of Squares*** | ***Mean Square*** | $F_0$ | ***P-value*** |
|---|---|---|---|---|---|
| ***Open Rate*** | 2 | 5.3592 | 2.6796 | 2.97 < 3.2 | 0.061 |
| ***observation*** | 2 | 3.0123 | 1.5061 | 1.67 < 3.2 | 0.2 |
| ***Open Rate*observation*** | 4 | 3.3968 | 0.8492 | 0.94 < 2.58 | 0.449 |
| ***Error*** | 45 | 40.6139 | 0.9025 | | |

| | | |
|---|---|---|
| ***Total*** | 53 | 52.3821 |

Table 41 shows the analysis of variance (ANOVA) for the lower limit of the particles velocity. [32, 33] If α = 0.05. Because $F_{0.05,2,45} = 3.20432, F_{0.05,4,45} = 2.57874$, we conclude that there was no significant effect on the lower limit of the particles velocity for the source of variation with 95% of confidence.

Table 42 ANOVA Table for the Upper Limit of the Coal Particles (diameter between 63 and 75 microns) Velocity Changes in the Open Environment

| ***Source of variation*** | ***Degrees of Freedom*** | ***Sum of Squares*** | ***Mean Square*** | ***$F_0$*** | ***P-value*** |
|---|---|---|---|---|---|
| ***Open Rate*** | 2 | 1.605 | 0.8025 | 1.86 < 3.2 | 0.168 |
| ***observation*** | 2 | 2.8476 | 1.4238 | 3.29 > 3.2 | 0.046 |
| ***Open Rate*observation*** | 4 | 4.4873 | 1.1218 | 2.6 > 2.58 | 0.049 |
| ***Error*** | 45 | 19.4531 | 0.4323 | | |
| ***Total*** | 53 | 28.3929 | | | |

Table 42 was the analysis of variance (ANOVA) for the upper limit of the coal particles velocity. The observation range had a significant effect on the upper limit. The interaction of open rate and observation range had a significant effect on the upper limit of the particles velocity for the source of variation with 95% of confidence.

# 6 CONCLUSIONS

The major accomplishments for the preliminary experiments in this period are listed below.

1. The transparent duct model was carefully designed and fabricated for the laser- based-instrumentation of solids-flow monitoring (LISM).
2. The mean diameter of humid particles was between 6.1703 microns and 6.6947 microns when the humidifier was set low flow rate. The mean diameter of humid particles was between 6.7628 microns and 7.1872 microns when the humidifier was set high flow rate. The mean velocity of humid particles was between 1.3394 m/sec and 1.5556 m/sec when the humidifier was set low flow rate. The mean velocity of humid particles was between 1.5694 m/sec and 1.7856 m/sec when the humidifier was set high flow rate.
3. When the humid particles flow rate was low, the maximum number of particles appeared when the mean diameter was 8.43 microns and 17.9 microns. When the humid particles flow rate was high, the maximum number of particles appeared when the mean diameter of was 8.43 microns, 17.94 microns and 19.21 microns. When the humidifier was set low flow rate, at the diameter of 18.1 microns, the maximum velocity of 2.8 m/s appeared. When the humidifier was set to a high flow rate, at the diameter of 5.34 microns, the maximum velocity appeared.
4. The oil type did not have a significant effect on the fog particles mean diameter.
5. The oil type had a significant effect on the fog particles mean velocity.
6. The organic particles (diameter between 150 and 250 microns, between 355 and 425 microns) tested using PIV under the open environment condition, had two factors that were considered as the affecting factors including particles diameter and open rate. In this experiment, the particles diameter and open rate did not have significant effect for the source of variation with 95% of confidence based on analysis of variance (ANOVA) results.

7. The organic particles (diameter between 425 and 500 microns) test using PIV under the open environment condition had two factors that were considered as the affecting factors including open rate and observation range. In this experiment, the particles diameter and interaction of particles diameter and open rate had a significant effect on the lower limit. On the upper limit, none of the parameters had a significant effect on the source of variation with 95% of confidence based on analysis of variance (ANOVA) results.
8. The potato particles (diameter less than 75 microns) tested using PIV under the open environment condition, had two factors that were considered as the affecting factors including open rate and observation range. In this experiment, the open rate and observation range had a significant effect on lower limit. On the upper limit, the open rate of flow rate control gate and observation range also had significant effect on the source of variation with 95% of confidence based on analysis of variance (ANOVA) results.
9. The potato particles (diameter between 63 and 75 microns) and wheat particles (diameter between 63 and 75 microns) tested using PIV under the open environment condition, had three factors were considered as the affecting factors including open rate, observation range, and particle types. In this experiment, the particles type had significant effect on the lower limit. On the upper limit, the particles type and interaction of open rate and observation range had a significant effect on the source of variation with 95% of confidence based on analysis of variance (ANOVA) results.
10. The coal particles (diameter between 63 and 75 microns) and organic particles (diameter between 63 and 75 microns) tested using PIV under the open environment condition, had three factors that were considered as the affecting factors including open rate, observation range, and particle types. In this experiment, there was no significant effect on the lower limit. On the upper limit, the interaction of type of particles and observation range had a significant effect on the source of variation with 95% of confidence based on analysis of variance (ANOVA) results.

11. The organic particles (diameter between 63 and 75 microns) and wheat particles (diameter between 63 and 75 microns) tested using PIV under the closed environment condition, four factors that were considered as the affecting factors including particle type, open rate, observation range, and environment conditions. In this experiment, the type of particles had a significant effect on the lower limit. On the upper limit, the observation range had a significant effect on the source of variation with 95% of confidence based on analysis of variance (ANOVA) results.
12. The potato particles (diameter between 63 and 75 microns) tested under the closed environment condition, three factors that were considered as the affecting factors including open rate, observation range, and environment conditions. In this experiment, the environment conditions had a significant effect on the lower limit. On the upper limit, the interaction of observation range, open rate and environment condition had a significant effect on the source of variation with 95% of confidence based on analysis of variance (ANOVA) results.
13. The coal particles (diameter between 63 and 75 microns) tested under the closed environment condition, three factors that were considered as the affecting factors including open rate, observation range, and environment conditions. In this experiment, the interaction of open rate and observation range had a significant effect on the lower limit. On the upper limit, the open rate and environment condition had a significant effect. In addition, the interaction of open rate and environment condition had a significant effect on the source of variation with 95% of confidence based on analysis of variance (ANOVA) results.
14. The coal particles tested (diameter between 63 and 75 microns) under open environment condition, two factors that were considered as the affecting factors including the open rate, observation ranges. In this experiment, there was no significant effect on the lower limit. On the upper limit, the observation range had a significant effect. In addition, the interaction of

open rate and observation range had a significant effect on the source of variation with 95% of confidence based on analysis of variance (ANOVA) results.

15. The PDPA/PIV can be used to measure coal flow. However there are some limitations like particle size and the object particles need to be in a transparent container.

## REFERENCES


1. *Particle Image Velocimetry User Manual*. 1999: TSI Inc.
2. Albrecht, H., *Laser Doppler and Phase Doppler Measurement Techniques.* Springer-Verlag Publishing, December, 2002.
3. Masutani, S.M., *LABORATORY EXPERIMENTS TO SIMULATE CO2 OCEAN DISPOSAL*. First Joint Power & Fuel Systems Contractors Conference, U.S. Dept. of Energy, Pittsburgh, PA, 1996.
4. Chukwulebe, B.Q. and S. Lee, *Laser-Based Investigation of Liquid Spray Atomization.* 6th Annual Undergraduate/ Graduate Science Research Symposium, pp. 30, April 22, 1999.
5. *Trust. Science. Innovation. (TSI)*. [cited; Available from: http://www.tsi.com/.
6. *Phase Doppler particle analyzer (PDPA)*. [cited; Available from: http://www.ul.com/fire/pdpa.html.
7. Lee, S. and Y. Liu, *The Unique Phase Doppler Particle Analyzer Application/Analysis of Solid Particle Flow in the FBC Cold Model.* Particulate Science and Technology Volume 22, Number 1, pp. 65-73(9), 2004.
8. Lee, S. and S. Zhu, *Factorial Modeling for Transient Solid Particle Velocity in FBC Cold Model.* International Journal of Particulate Science and Technology Vol. 23, pp.205-214, 2005.
9. Lee, S., H.J. Cui, and Y. Huang, *The Particle Characteristics and Analysis using the Laser-based Phase Doppler Particle Analyzer (PDPA) and Statistical Methods.* Intl' Journal of Particulate Science and Technology, Vol 27(3), pp. 263-270, 2009.
10. *Research Directions and Projects of Dean Enrique J. Lavernia -Dean for the College of Engineering at UC Davis.*
11. *Dantecdynamics*. [cited; Available from: http://www.dantecdynamics.com.
12. Lee, S., *Investigation of Gas/Particle Flows in a Gaseous Fluidized Bed Using Particle Image Velocimetry*. Proceedings of The Third International Workshop on PIV 99, pp-689-694, September 1999.
13. Huang, Y. and S. Lee, *Fuel Flow Simulation and Fuel Characteristic Analysis in the Combustion System Using Statistical Method.* Proceedings of the American Society of Engineering Education (ASEE) Mid-Atlantic Section Fall 2007 Conference, November 2007.
14. Jensen, K.D., *Flow Measurements.* Journal of the Brazilian Society of Mechanical Sciences and Engineering, October-December 2004.
15. Pudasaini, S.P., et al., *Velocity measurements in dry granular avalanches using Particle Image Velocimetry-Technique and comparison with theoretical predictions,Physics of Fluids.* American Institute of Physics, 2005.
16. Pudasaini, S.P., et al., *Rapid Flow of Dry Granular Materials down Inclined Chutes Impinging on Rigid Walls,Physics of Fluids.* American Institute of Physics, 2007.
17. Willert, C.E. and M. Gharib, *Digital Particle Image Velocimetry*. Experiments in Fluids 10, p 181-193, 1991.
18. Adrian, R.J., *Particle Imaging Techniques for Experimental Fluid Mechanics.* Annual Review of Fluid Mechanics, vol 23, p 261-304, 1991.
19. Raffel, M., et al., *Particle Image Velocimetry A Practical Guide*. 2nd ed. 1998: Springer.
20. Bendat, J.S. and A.G. Piersol, *Random Data: Analysis and Measurement Procedures*. 2000: Wiley-Interscience, New York.
21. Bracewell, R.N., *The Fourier transform and its applications*. 3nd ed. 1999: McGraw-Hill Science.

22. Brigham, E.O., *The fast Fourier transform*. 1974: Prentice-Hall, Englewood Cliffs, New Jersey.
23. Ndakwah, W., Y. Liu, and S. Lee, *Development of the Advanced Laser-based Instrumentation and Data Acquisition System.* 7th Annual Undergraduate and Graduate Science Research Symposium, pp.35, April 2000.
24. Bachalo, W.D. and M.J. Houser, *Phase/Doppler Spray Analyzer for Simultaneous Measurement of Drop Size and Velocity Distributions.* Opt. Engng 23 1984.
25. Aerometrics, I., *Phase Doppler Particle Analyzer User Manual.* 1998.
26. Ndakwah, W., Y. Liu, and S. Lee, *Development of the Advanced Laser-based Instrumentation and Data Acquisition System.* Published in the Proceedings of 7th Annual Undergraduate and Graduate Science Research Symposium, pp.35, April 2000.
27. *AF10A-AF17 Air Flow Bench and Apparatus User Manual.* TecQuipment Limited, 1999.
28. Lee, S., *Advanced CFD Analysis/Experimental Validation and Transient Model Development for the Flow in SSME Exhaust Duct CFD Analysis /Transient Model for the SSME Exhaust Duct Flow*. 2006, NASA.
29. Jin, W.X. and S.C. Low, *Investigation of Single-phase Flow Patterns in a Model Flash Evaporation Chamber using PIV Measurement and Numerical Simulation.* Journal of Science Direct, 2002.
30. Lee, S., *Advanced CFD Analysis/Experimental Validation and Transient Model Development for the Flow in SSME Exhaust Duct CFD Analysis /Transient Model for the SSME Exhaust Duct Flow.* Final Technical Report to NASA, Feb, 2006.
31. Lee, S., *Innovative Coal Solids-Flow Monitoring and Measurement Using Phase-Doppler and Mie Scattering Techniques.* Technical Progress Report to US. DOE, NETL, April, 2007.
32. Myers, R.H. and D.C. Montgomery, *Response Surface Methodology: Process and Product Optimization using Designed Experiments*. 2nd ed. 2004: John Willey and Sons, Inc.
33. Montgomery, D.C., *Design and analysis of Experiments*. 6th ed. 2005: John Willey and Sons, Inc.